# THE MECHANOBIOLOGY OF DIAPHYSEAL SECONDARY BONE HEALING

vorgelegt von
Devakara Rao Epari B.E., M.Biomed.E
aus Australien

Von der Fakultät V – Verkehrs- und Maschinensysteme
der Technischen Universität Berlin
zur Erlangung des akademischen Grades

Doktor der Ingenieurwissenschaften
– Dr.-Ing. –

genehmigte Dissertation

Promotionsausschuss:
Vorsitzender: Prof. Dr. med. Wolfgang Friesdorf
Berichter: Prof. Dr.-Ing. Georg N. Duda
Berichter: Prof. Dr.-Ing. Marc Kraft

Tag der wissenschaftlichen Aussprache: 28. März 2006

Berlin 2006
D83

*To my beloved and devoted parents, Margaret and Sankararao*

"Live as if you were to die tomorrow. Learn as if you were to live forever."

Mohandas K. Gandhi (1869 - 1948)

# Preface

The present thesis arose from my activities as a research assistant at the Musculoskeletal Research Centre Berlin – Centre for Musculoskeletal Surgery (Director: Prof. Dr. med. N. P. Haas), Charité - Universitätsmedizin Berlin, which is a joint institution of the Free University and the Humboldt-University of Berlin.

This work would not have been possible without the support and vision of Prof. Dr. Ing. Georg N. Duda. His advice has been invaluable to me and his perpetual drive for perfection has encouraged me to continually set higher standards for myself which has added considerably to the quality of this thesis.

I would like thank Prof. Dr. Ing. Marc Kraft for reviewing and supporting my thesis, his comments were most helpful in focusing the work.

My thanks must also go to my first mentor, A/Prof. William Walsh, for passing on his enthusiasm for orthopaedic research and for giving me my first research opportunities in his laboratory in Sydney, Australia.

I gratefully acknowledge the contributions of our lab veterinarian Dr. Hanna Schell who was responsible for surgery and care of the animals. In addition, our discussions on the biology of healing were most stimulating. Also, my thanks go to Dr. Jean-Pierre Kassi and Mr Jan-Eric Hoffmann for their work in developing and testing the external fixation devices. I am grateful to my engineering colleagues Dr. Markus Heller and Dr. Mark Thompson for providing critical review and constructive discussion. I would also like to thank my fellow lab colleagues who have contributed to creating a pleasant and friendly working atmosphere.

Thanks must go to the AO Foundation (Switzerland) for their financial support.

To my close friend and colleague Dr. William Taylor, I am particularly grateful for all his assistance, since the day I arrived in Berlin. His mateship has made an at times daunting relocation overseas so much easier.

Finally, words can not express my gratitude to my parents. For their hard work and sacrifice that has given me this opportunity I am deeply indebted. They believed in and encouraged me always and have in no small way contributed to who I am today. In spite of the huge distance separating us, my family remains very close to my heart.

# Table of Contents

## Summary

The main treatment for fractures in the diaphysis of the long bones is a fixation procedure known as splinting. The degree of fixation stability is known to influence the healing outcome. Bone healing typically occurs with the formation of bony callus. Callus formation is initiated by signalling molecules released during inflammation which leads to pooling and differentiation of pluripotent mesenchymal cells. Later bone is formed by a combination of intramembranous and endochondral ossification. However, it is still unclear how tissue regeneration within the callus is influenced by the fixation stability and in particular the local mechanical conditions. The aim of this thesis is to further the understanding of the mechano-biology of bone healing. In particular, the tissue response to different mechanical stimuli and levels of stimulation is of interest.

The tissue responses to mechanical stimulation were studied in an ovine osteotomy model of bone healing under defined conditions of fixation stability. Histological and histomorphometric techniques were used to characterize the changes in callus composition and morphology over the course of healing. In addition, a novel technique for quantifying bone quality by calculation of the moment of inertia was introduced. The mechanical competence of the healing callus was examined by tests to determine its strength and stiffness. Numerical analyses were then used to estimate the local mechanical stimuli in the callus during hard callus development. The tissue distribution described histologically was then correlated with the local mechanical conditions.

Osteosynthesis with semi-rigid fixation, characterised by larger interfragmentary movements, led to inferior torsional stiffness at 6 weeks. At 9 weeks no difference in the mechanical competence could be determined. In the group rigidly fixed, fibrous tissue content reduced earlier, while in semi-rigidly treated animals cartilage persisted longer. Regardless of the fixation stability the initial bone formation by intramembranous ossification was the same. The calculation of the moment of inertia confirmed in the semi-rigidly treated animals a larger callus at six and nine weeks.

Analysis of the mechanical conditions during healing found that only moderate axial interfragmentary movements were needed to produce mechanical stimuli of the same magnitude produced by larger interfragmentary shear and torsional movements

believed to be critical to healing. Interfragmentary shear and torsion produced only deviatoric strains, whilst axial movements produced additionally a hydrostatic stress signal and fluid flow. In vivo determined movements applied to the finite element model resulted in little difference in the mechanical stimuli in the region of active bone formation for the two healing stabilities initially. For the semi-rigid group, large tensile strains on the surface of the periosteal hard callus were estimated at a time corresponding to the onset of endochondral ossification.

In this study of bone healing, intramembranous ossification was determined to be relative insensitive to the fixation stability and mainly dependant upon biological factors. The delay in healing was related to a retarded endochondral ossification. Large tensile strains appearing in regions corresponding to sites of endochondral ossification suggest a link between the local mechanical conditions and the process of endochondral ossification. Finally, a number of relationships between local mechanical stimuli and processes of callus development are presented in a revised theory of the mechano-biology of secondary bone healing.

# Zusammenfassung

Die Hauptbehandlungsmethode bei diaphysären Frakturen langer Knochen stellt eins als Schienung bekanntes Verfahren dar. Das Ausmaß der Fixationsstabilität beeinflusst bekanntlich das Heilungsergebnis. Knochenheilung erfolgt in der Regel durch Bildung von Knochenkallus. Die Kallusbildung wird durch Signalmoleküle initiiert, die in der Inflammationsphase freigegeben werden. Startpunkt dabei ist die Vereinigung und Differenzierung pluripotenter Mesenchymalzellen. Danach bildet sich Knochen durch eine kombinierte intramembranöse und endochondrale Ossifikation. Unklar bleibt jedoch, wie die Fixationstabilität und speziell die lokalen mechanischen Bedingungen die Geweberegeneration innerhalb des Kallus beeinflussen. Das Ziel dieser Arbeit ist daher, das Verständnis der Mechano-Biologie der Knochenheilung zu verbessern. Insbesondere soll die Gewebeantwort auf verschiedenen mechanischen Stimuli und Stimulationsamplituden analysiert werden.

Die Gewebereaktionen auf mechanische Stimulation wurden in einem Osteotomiemodell zur Analyse der Frakturheilung unter definierten Bedingungen am Schaf untersucht. Histologische und histomorphometrische Techniken wurden verwendet, um die Änderungen in Kalluszusammensetzung und –Morphologie im Verlauf der Heilung zu charakterisieren. Zusätzlich wurde eine neue Technik zur Quantifizierung der Knochenqualität durch Ermittlung des Flächenträgheitsmomentes eingesetzt. Die mechanische Kompetenz des heilenden Kallus wurde durch in vitro Bestimmung deren Festigkeit und Steifigkeit evaluiert. Weiterhin wurden numerische Analysen durchgeführt, um die lokalen mechanischen Stimuli im Kallus während dessen Ausreifung abzuschätzen. Die histologisch beschriebene Gewebeverteilung wurde anschließend mit den lokalen mechanischen Bedingungen korreliert.

Nach einer Osteosynthese mittels semi-rigider Fixation, gekennzeichnet durch größere interfragmentäre Bewegungen, führte zu einer niedrigen Steifigkeit nach sechs Wochen. Nach neun Wochen konnte keinen Unterschied in der mechanischen Kompetenz ermittelt werden. In der Gruppe mit rigider Fixation nahm der Gehalt fibrösen Gewebes früher ab, während länger anhaltende Knorpelanteile bei Tieren mit semi-rigider Fixationsversorgung beobachtet wurden. Unabhängig von der Fixationsstabilität war die Ausprägung des initial durch intramembranöse Ossifikation gebildeten Knochens vergleichbar. Die berechneten Flächenträgheitsmomente

bestätigten die ausgeprägtere Kallusformation bei den Tieren mit semi-rigider Fixation nach sechs und neun Wochen.

Die Analyse der mechanischen Bedingungen der Frakturheilung zeigte, dass nur mäßige axiale interfragmentäre Bewegungen erforderlich waren, um mechanische Stimuli vergleichbarer Größenordnung wie beim Vorliegen höherer, für die Heilung als kritisch angesehenen interfragmentären Scher- und Torsionsbewegungen hervorzurufen. Letztere Bewegungskomponenten verursachten lediglich deviatorische Dehnungen, während axiale Bewegungskomponenten zusätzlich ein hydrostatisches Spannungssignal sowie einen Flüssigkeitsstrom hervorriefen. Die Simulation in vivo ermittelter Bewegungen im Finite-Elemente-Modell führte bei beiden Osteosynthesevarianten in Regionen aktiver Knochenbildung initial zu geringen Unterschieden bezüglich mechanischen Stimuli. In der semi-rigiden Gruppe wurden im festen periostalen Kallus große Oberflächendehnungen zu einem Zeitpunkt ermittelt, der mit dem Begin der endochondralen Ossifikation gleichgestellt wird.

In dieser Studie zur Knochenheilung zeigte sich die intramembranöse Ossifikation als in erster Linie abhängig von biologischen Faktoren und relativ unempfindlich gegenüber Fixationsstabilität. Eine verzögerte endochondrale Ossifikation ging mit einer verspäteten Heilung einher. Die beobachteten größeren Dehnungen in Regionen endochondraler Ossifikation legen eine Verknüpfung zwischen lokalen mechanischen Bedingungen und endochondraler Ossifikation nahe. Zum Abschluss wird eine Reihe von Zusammenhängen zwischen lokalen mechanischen Stimuli und Phasen der Kallusentwicklung in Form einer überarbeiteten Theorie zur Mechano-Biologie der sekundären Knochenheilung präsentiert.

# 1 Introduction

---

This chapter introduces the problem that fractures pose now and in the future to managers of public health care and the means by which knowledge of the mechanics may assist. The specific goals of this thesis are then outlined and the overall hypothesis is presented. Finally, it is described how the various elements of the thesis are brought together to tackle this multi-disciplinary task.

---

## 1.1 Background

The bony skeleton's potential for regeneration is astounding. In contrast to other adult tissues that heal with the production of scar tissue, new bone is formed and continuously remodelled until the original site of injury is barely recognisable. During fracture healing bone is formed by a combination of processes seen in both adult growth and embryonic development. The mechanisms controlling these processes are however not easily elucidated. Among many factors, the blood supply and the fixation stability are seen as being critical for successful healing.

Despite all the recent developments in fracture treatment, cases of delayed healing and non union are still encountered. The ageing of the population in developed nations is expected to increase the prevalence of such cases with every second woman and every eighth man over the age of 50 likely to suffer a fracture due to osteoporosis. Aside from the staggering cost of primary fracture treatments ($13.8 billion in the U.S.A. in 1995), follow up operations on account of delayed healing or non-union require additional hundreds of millions of dollars per year, not too mention the costs of lost employment (The Medical and Healthcare Marketplace Guide 2000-2001, Knowledge Enterprises, Inc., 2000).

Mechanics is a field that has been identified that could be used to enhance bone healing. In particular, knowledge of the mechano-biology appears especially promising. An understanding of these principles may have far reaching uses beyond fracture fixation, with applications in such fields as tissue engineering and tissue regeneration.

## 1.2 Problem

Even though the influence of mechanics on bone healing is well recognised, the mechanism by which mechanical stimuli are transferred to a biological response remains unknown. The interfragmentary movements, or the relative movements of the fracture fragments, are related to the type of fracture fixation. Moderate axial interfragmentary movements have been shown to enhance bone healing, while in some studies delayed healing has been observed in the presence of interfragmentary shear. However, it is not well understood how axial movements stimulate and why interfragmentary shear is detrimental. In addition, recent studies have also suggested that the initial mechanical conditions may be particularly important for the healing outcome. However, it has not been well described just how the initial mechanics influences the path of healing.

## 1.3 Goals

The goal of this project is to extend the knowledge on the role of mechanical factors during fracture healing. Findings from this study will be used to improve the clinical treatment of long bone fractures.

The individual aims are to,

- determine the influence of mechanical stability on the healing path and define boundaries of interfragmentary shear for optimal healing.
- determine the influence of the different modes of interfragmentary movement of the bio-physical stimuli within the callus.
- correlate experimental and numerical findings to further the understanding of the mechano-biology of bone healing.

## 1.4 Hypothesis

The overall hypothesis of this study was that the formation of the tissues comprising the fracture callus is regulated by the mechanical stability of fixation and in particular the local mechanical conditions.

## 1.5 Outline of Thesis

Mechanobiology is the study of the influence of mechanics on biological processes. This thesis brings together knowledge of the histology of healing in a well characterised model of bone healing with numerical analyses to estimate the local mechanical conditions. How these aspects are presented in this thesis and then interlinked is shown in the chart below.

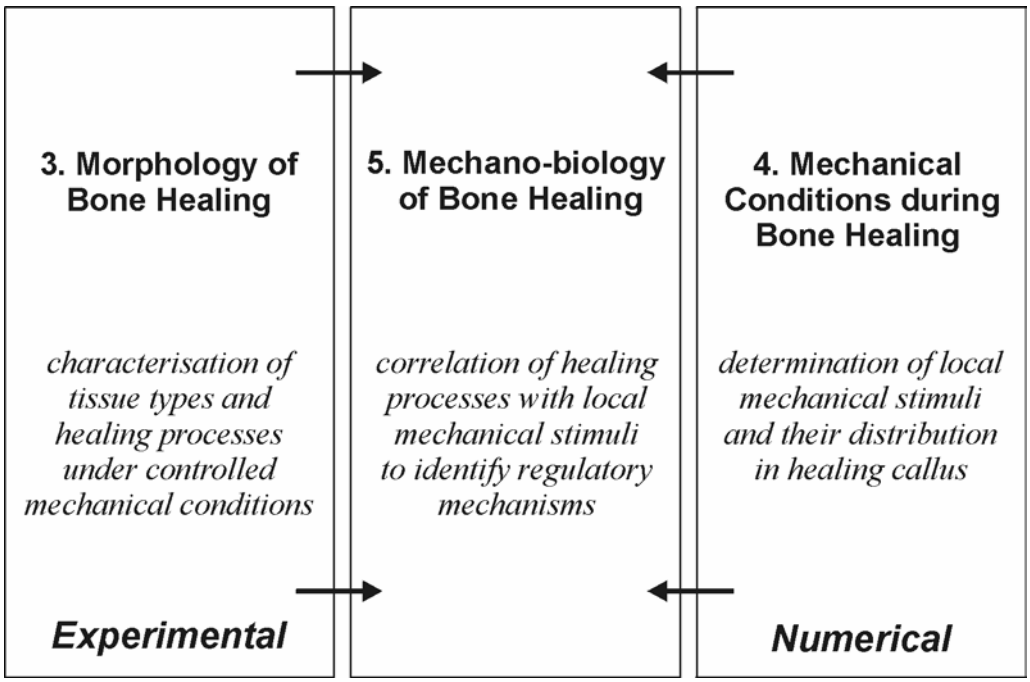

# 2 Healing of Diaphyseal Fractures

---

This chapter provides a comprehensive review of the literature. First a description of the basic anatomy of diaphyseal bone is given including the prominent cell types. This is followed by an overview of the types of bone healing and an in depth description of the phases of secondary healing. The current treatments for bone fractures are presented and the types of complications that can result are discussed. Finally, the influence of mechanics on bone healing is reviewed and the current understanding of mechano-biology is summarised.

---

## 2.1 Basic Anatomy of Diaphyseal Bone

Fractures in the diaphyseal region typically affect a type of bone known as cortical or compact bone. This contrasts to fractures in the metaphyseal region where the predominant bone type is cancellous bone (Figure 2-1). This project deals with bone healing in the diaphyseal region of the long bones, with the tibia taken as an example.

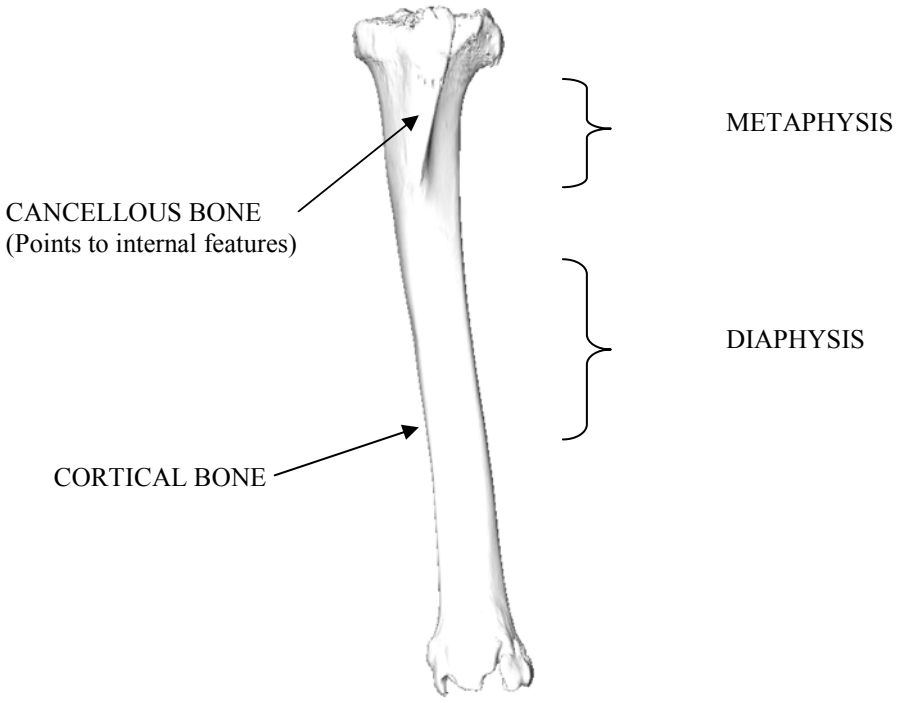


**Figure 2-1 shows the surface of an ovine tibia (Frontal view) reconstructed from a computer tomography scan using AMIRA software (Indeed – Visual Concepts GmbH, Berlin, Germany).**

The outer surface of diaphyseal bone is covered by the periosteum. The periosteum consists of a sheet of fibrous connective tissue and an inner cambium layer of undifferentiated cells. The periosteum is involved in bone formation during both growth and repair. The marrow cavity of the diaphysis is also lined with a thin cellular layer called the endosteum. The endosteum (an internal periosteum) is also a membrane containing bone surface cells (osteoblasts, osteoclasts and bone-lining cells) (Jee, 2001).

The cortical bone itself is composed of both cellular and non-cellular elements. The cells are derived from several stem cell lines and include osteoblasts, osteocytes, osteoclasts and mesenchymal osteoprogenitor cells. Osteoblasts are bone forming cells. Osteoblasts secrete glycoproteins and mucopolysaccharides to form the

uncalcified ground substance of bone called osteoid. Osteoblasts may be found on the internal surface and externally under the periosteum. When not in the process of forming bone their appearance is flattened and they are known as bone-lining cells. Osteocytes are osteoblasts that have been surrounded with matrix and lie in lacunae. The osteocytes maintain appropriate concentrations and arrangements of various molecules that compose the matrix. If blood supply to a portion of bone stops, the osteocytes die and the entire bony substance supported by them is resorbed and eventually replaced by new osteoblasts and new matrix. Osteoclasts are multi-nucleated giant cells found in cavities on bone surfaces where they are involved in bone resorption. (Jee, 2001)

The extra-cellular bone substance is called matrix and is similar to other forms of connective tissue in that it is formed from collagen fibres. However, in bone the fibres are arranged in highly ordered lamellae, reinforced with mineral. The characteristic hardness of bone comes from hydroxyapatite, a crystalline form of calcium phosphate. The collagen base of bone allows for some flexibility.

## 2.2 Fracture Healing

### 2.2.1 General

Bone, when injured, has the capability to regenerate itself. Unlike the processes employed by other tissues that produce scar tissue, bone has the ability to repair itself with bone. Once a healed fracture has undergone remodelling the structure will have returned to the pre-injury state.

A fracture occurs when the upper limit of bone strain is exceeded. Fracture initially disrupts the local blood supply, causing haemorrhage, anoxia, death of cells, and an aseptic inflammatory response (Simmons, 1985).

A fracture results in a series of tissue responses that are designed to remove tissue debris, re-establish the vascular supply, and produce new skeletal matrices (Simmons, 1985). Two types of fracture healing have been described based on classic histological observations, primary and secondary.

Primary fracture healing, also known as direct or osteonal healing, involves intramembranous bone formation and direct cortical remodelling without external callus (Willenegger et al., 1971). Primary healing occurs when there is a combination

of anatomical reduction, stabilisation and compression of the fracture. In contrast, secondary healing occurs in the presence of interfragmentary movement and is the process by which the majority of fractures heal. It involves a sequence of tissue regeneration processes by which the bone fragments are first stabilised by means of an external callus (Willenegger et al., 1971).

### 2.2.2 Secondary Bone Healing

The process of bone repair by secondary healing can be divided into four overlapping stages. Healing begins with inflammation which is followed by the formation of hard callus by intramembranous ossification, bridging is achieved by endochondral ossification of the soft callus and finally the callus is resorbed during callus remodelling (Cruess and Dumont, 1975, Brighton, 1984, Frost, 1989, Owen, 1970).

**a) Inflammatory Phase**

Healing begins with bleeding from the trauma which disrupts the fracture surfaces, the periosteum and the surrounding soft tissues and results in the formation of the fracture haematoma. Simultaneously lifting of the periosteum occurs (Figure 2-2). The haematoma forms an important source of haematopoietic cells and platelets that initiate the inflammatory process. The haematoma releases a large number of signalling molecules, including cytokines and growth factors (Bolander, 1992).

The disruption of the blood supply leads to the development of hypoxic areas. Low oxygen tensions are thought to invoke the release of cytokines that stimulate the healing process. Many of the cytokines have an angiogenic function to restore the blood supply. Angiogenesis involves the sprouting of capillary buds from undamaged vessels. It has been shown that the periosteal circulatory system is the most active in the early stages of healing (Rhinelander, 1968).

Cell division is first seen in the periosteum and to begin with extends the length of the injured bone. Within a few days this activity is confined to the immediate area adjacent to the fracture where it remains above normal levels for several weeks (McKibbin, 1978).

Mesenchymal cells, originating from the periosteum, endosteum, bone marrow and the vascular endothelium, are seen among the myofibrils migrating towards the fracture region. No cells are arriving from the fracture gap which is covered in haematoma. Mesenchymal cells and inflammatory cells form granulation tissue.

Mesenchymal cells condense against the fracture ends that have been deprived of periosteum. In these condensations the first formation of cartilage occurs. Mesenchymal cells stop their locomotion when they become anchored on the relatively stable bone ends or fibrous capsule of the periosteal callus. Mesenchymal cells differentiate to become chondrocytes or osteocytes, which proliferate and generate the regenerative callus (Bostrom, 1998).

The ends of the broken bones themselves appear not to participate in the initial reaction, and are in fact dead as evidenced by the empty osteocyte lacunae which extend for a variable distance from the fracture (McKibbin, 1978).

Brighton and Hunt (1991) described a loss of normal architecture in the medullary canal and a loss of blood vessels in regions adjacent to the fracture clot (Brighton and Hunt, 1991). Endothelial cells appear to undergo a transformation to become polymorphic cells which go on to express an osteogenic phenotype and form bone.

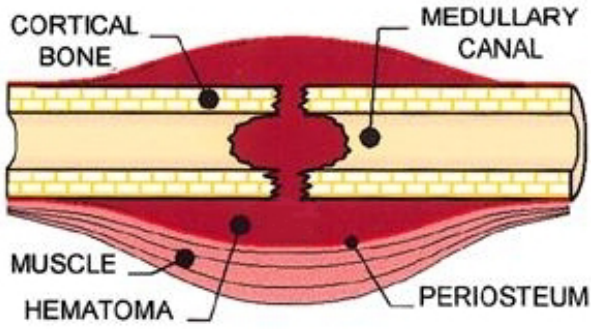


**Figure 2-2 demonstrates the lifting of the periosteum around the fracture haematoma (Modified from (Li et al., 2001)).**

### b) Hard Callus (Intramembranous Ossification)

Once the blood supply is re-established and mesenchymal cells have pooled from the inflammatory response, callus formation begins. The first process is the production of woven bone beneath the periosteum (Figure 2-3) several millimetres away from the fracture gap (Brighton, 1984, Einhorn, 1998). This bone is produced by committed osteoprogenitor cells present in the cambium layer of the periosteum via intramembranous ossification (Owen, 1970). It occurs within connective tissue when a group of mesenchymal cells (presumably osteoblasts but not yet differentiable) begin to produce osteoid at a nidus or ossification centre. Ossification extends progressively into surrounding tissue as lamellar bone replaces the osteoid.

Maturation and growth occur through remodelling. As neighbouring ossification centres expand, they eventually fuse producing the final form of the bone. The formation of this hard callus is related to motion and appears to be inhibited in rigid fixation. The bone formation proceeds in the direction of the fracture gap (Brighton, 1984, McKibbin, 1978).

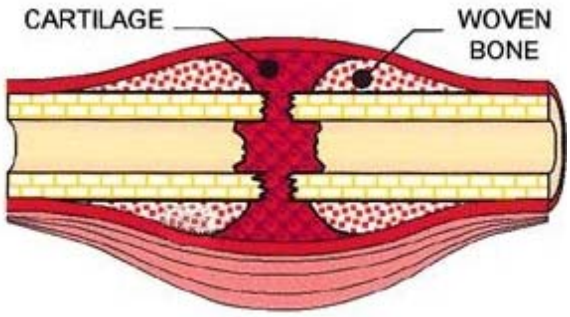


**Figure 2-3 shows woven bone formation beneath the periosteum during the hard callus phase (Modified from (Li et al., 2001)).**

### c) Soft Callus (Endochondral Ossification)

The second area of callus formation occurs by endochondral ossification at and overlying the fracture area. The soft callus consists of a cartilage intermediate. During the repair stage chondrocytes within the matrix proliferate becoming the dominant cell type in soft callus. As the cells hypertrophy, matrix vessels release their contents (proteases, phosphates and calcium) into the extra-cellular space allowing cartilage to calcify (Figure 2-4). The calcified cartilage acts as a stimulus for angiogenesis and new blood vessels bring chondrocytes and osteoblasts to the site replacing the cartilage with woven bone (Webb and Tricker, 2000). The amount of cartilage is variable, occurring prominently in lower animals and where excessive movement is permitted (McKibbin, 1978). The formation of cartilage begins on the relatively stable points at the bone ends and widens outward. The bone formation occurs step by step toward the central line through the fracture gap, where the most movement occurs for the longest time.

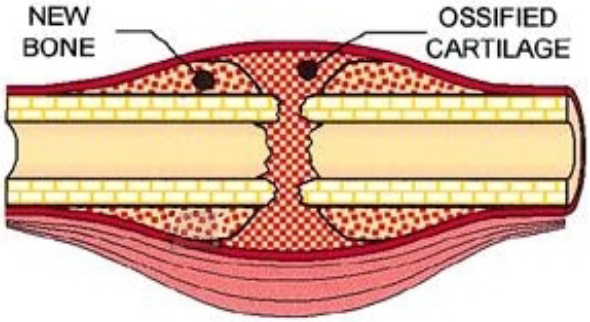


**Figure 2-4 showing regions of cartilage ossification during the soft callus phase of healing (Modified from (Li et al., 2001)).**

The endochondral bone formation occurs via capillaries that originate from the periosteal callus. The new capillaries are deemed to be indispensable for the deposition of bone. The process bears strong resemblance to the embryonic development of long bones (Hulth, 1989). Angiogenesis occurs in parallel with endochondral ossification, leading to erosion of the mineralized cartilage and deposition of bone (Mark et al., 2004b).

**d) Remodelling**

Upon bridging of the callus and reunion of the fracture ends, the processes of remodelling and resorption become the dominant activities in the callus. The woven bone laid down in converted to lamellar bone (Marsh and Li, 1999). It is thought that fluid shear stresses in bone modulate the remodelling activities, with disuse leading to osteocyte apoptosis and osteoclast recruitment (Bakker et al., 2004). Eventually, osteonal remodelling of the newly formed bone tissue and of the fracture ends restores the original shape and lamellar structure of the bone (Brighton, 1984, Owen, 1970, Willenegger et al., 1971). Resorption of the endosteal callus coincides with re-establishment of the original blood supply (Rhinelander, 1968).

## 2.3 Fracture Treatments

### 2.3.1 Splinting

The most basic and least invasive method to treat a fracture is with a plaster cast. Casting allows simple anatomical alignment of the fragments, but a relatively large interfragmentary movement is permitted.

When a fracture is accompanied by an open soft tissue wound, external stabilization by an external fixator is often preferred (Runkel and Klepsch, 1999). The external

fixator is composed of screws or pins that are inserted percutaneously into the bone and fixed to one another using connecting rods or rings (Höntzsch, 1997). The advantage of external fixation is the flexibility of mounting which allows a conservation of blood supply and major muscle groups (Claes, 1990). However, due to the location of the fixator external to the body, this method of fixation is susceptible to infection (Krischak et al., 2002). Pin infections are painful, require extensive antibiotic treatment and can lead to pin loosening and require a change of treatment (Anderson and St Jean, 1996). The stability of the fixation is determined by the stiffness of the fixator and in particular by the diameter of the bone screws, the number of screws and the distance between fixator connecting rod and fracture (Claes, 1990, Palmer et al., 1992).

Intramedullary nailing is an internal fixation splinting method that involves insertion of a nail into the medullary canal of a long bone (Tarr and Wiss, 1986). Torsional stability of the implant is achieved by placing additional screws (called locking screws) perpendicular to the axis of the nail through the nail and anchoring in the bone (Vecsei and Hertz, 1977). Intramedullary nailing is advantageous in that is offers greater patient comfort and a reduced risk of infection (Krettek et al., 1994, Runkel and Klepsch, 1999). However, a reduced stability (Blachut et al., 1997) and a disruption of the endosteal canal which limits the biological capacity for healing (Stürmer and Schuchardt, 1980) are the disadvantages of intramedullary nailing. Fracture stability is determined by the material properties of the nail, the fit of the nail in the canal and the mechanical properties of the locking screws (Claes and Ito, 2005).

Plate fixation is a further method of internal fixation that is similar to external fixation in resemblance but takes place under the skin and close to the bone. The plate of an internal fixation device is different to conventional plating in that contact between plate and bone does not occur and hence the periosteal blood supply and callus formation is not inhibited by the fixation device (Rüedi and Murphy, 2000).

### 2.3.2 Interfragmentary Compression

The goal of interfragmentary compression techniques is to create absolute stability. A number of devices, lag screws, compression plates, and tension bands, can be used to achieve interfragmentary compression. When absolute stability is achieved healing can occur by direct osteonal bridging (2.2.1) with little or no callus formation. In

contrast to callus healing, the diameter of the bone is not increased and therefore the load bearing capacity of the healing bone is limited, requiring a longer period of protection by the implant (Rüedi and Murphy, 2000).

## 2.4 Complications in Fracture Healing

Despite the body's methods for repair, not all fractures are able to heal. Delayed union occurs when periosteal callus formation ceases prior to complete union, leaving union dependent upon the late endosteal healing. Non-union occurs when both the endosteal and periosteal callus formation fails. Sclerosis, a stiffening and hardening of the tissues, of the medullary canal occurs and the fracture remains open or becomes filled with scar tissue, usually fibrous in nature but occasionally a fibrocartilaginous pseudarthrosis or `false' joint is formed.

Non-union may be associated with patient factors, characteristics of the fracture, type of treatment and pharmacological factors. The nutritional status of the patient is important; deficiencies of calcium, phosphate, vitamins C and D are all associated with delayed callus formation. Protein malnutrition, anaemia, diabetes and growth hormone deficiency have been shown to play a role, while local factors such as pre-injury vascular status and muscle quality are also important (Babhulkar and Pande, 2005).

Injury sites and high energy injuries that lead to extensive soft tissue damage are associated with higher rates of non-union. Additionally fractures may be complicated by compartment syndrome, infection and nerve injury. Treatment techniques can impede fracture healing, with inadequate immobilisation or mobilisation, fracture distraction, periosteal stripping and repeated manipulations being common examples. Because of the vasoconstrictive effects of nicotine, smoking is related to an increase rate of delayed union. Corticosteroids, anti-inflammatory drugs, anticoagulants, and certain antibiotics have been related to fracture healing complications (Babhulkar and Pande, 2005).

## 2.5 Mechanics and Bone Healing

### 2.5.1 Influence of Mechanics on Bone Healing

Splinting techniques, such as internal and external fixation, often allow a certain degree of interfragmentary motion. In such cases, healing with formation of an

external callus is observed. The type of fixation device and the nature of the musculoskeletal loading determine the mechanical environment within the regenerating tissue which in turn has been shown to influence the callus size, ossification rate and the strength of the healing bone.

Goodship et al (1993) conducted experiments to demonstrate the importance of mechanical environment for fracture healing. It was concluded that, "More flexible fixation may lead to excessive interfragmentary motion … whereas more rigid fixation may impair callus formation contributing to … non-union. (Goodship et al., 1993)"

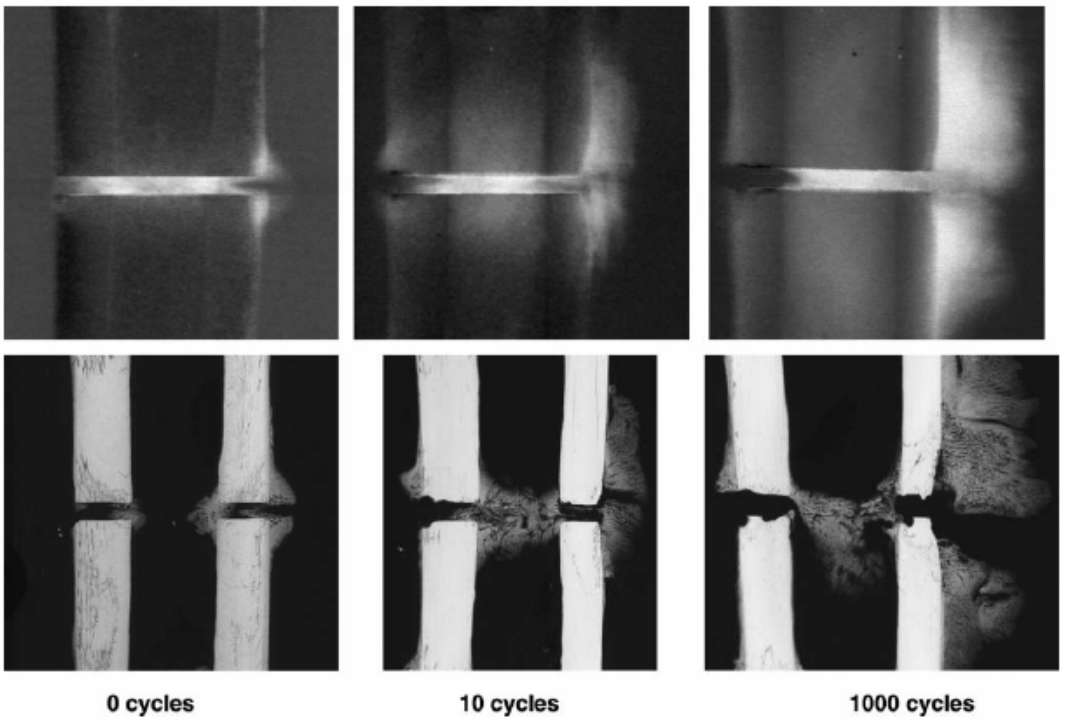


**Figure 2-5 Typical radiographs from digital subtraction analysis and corresponding central micro-radiographic section of the tibiae. In all groups periosteal callus formation is significantly increased on the far side of the external fixator (right side of the bone), where compressive displacement was induced. Only a small amount of periosteal callus formation was observed on the distraction side. With a higher number of applied cycles, the amount of periosteal callus formation is increased (Reproduced from (Hente et al., 2004)).**

Healing has been shown to be more rapid if the loading is reduced as healing progresses (Gardner et al., 1998). But if stimulation is delayed until after the initiation of ossification the benefits of cyclical loading are eliminated (Goodship et al., 1998). The rate of strain has also been shown to influence healing, with fractures subjected to a moderate strain rate (40 $mms^{-1}$) quicker to reach peak mineral content and stiffness compared to fractures subjected to slower (2 $mms^{-1}$) and faster (400 $mms^{-1}$) strain rates.

In addition to the timing of mechanical stimulation, the magnitude and direction are also important for the healing outcome. The interfragmentary movements can be broken down into three translational and three rotational components. Animal experiments have shown that an axial interfragmentary movement within the range of 0.2 - 1.0 mm seems to be optimal for healing for gap sizes of 3 mm (Claes et al., 1998). In vivo measurements and analytical studies report that bones are mainly axially loaded with only moderate bending. However, musculoskeletal analyses have shown that despite the predominant axial loading in the tibia for example, asymmetries in fracture fixation devices may induce considerable interfragmentary shear (Duda et al., 1998), which is confirmed by measurement of the interfragmentary movements in clinical and experiments situations (Klein et al., 2003, Klein et al., 2004, Duda et al., 2003, Duda et al., 2002, Gardner et al., 1998). Whilst the benefit of moderate axial interfragmentary movements has been clearly demonstrated, it remains unclear how fracture healing is related to other movement components (Klein et al., 2003, Augat et al., 2003, Yamagishi and Yoshimura, 1955, Park et al., 1998).

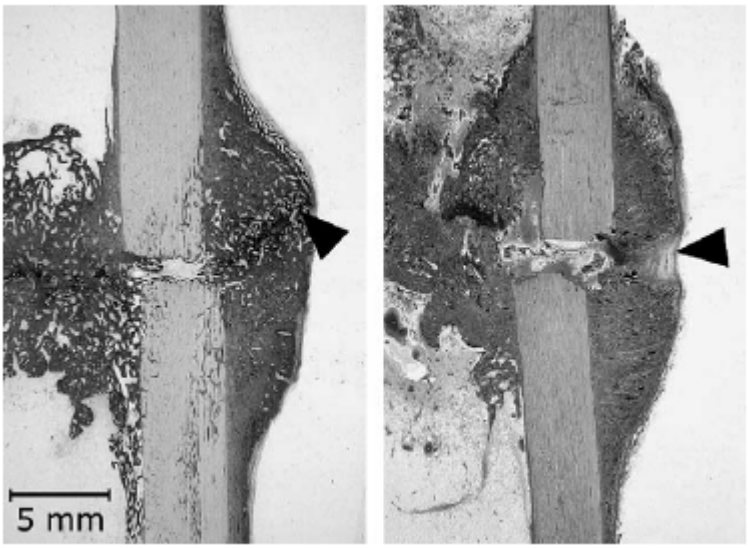


**Figure 2-6 Characteristic histologic appearance of healing under axial compression (left) and interfragmentary shear (right). Differences were most pronounced in the healing zone (arrows) and in the osteotomy gap. While in the AXIAL group these areas were dominated by bone, in the SHEAR group fibrous tissue was seen (Reproduced from (Augat et al., 2003)).**

### 2.5.2 Mechano-biology of Bone Healing

The course of healing is related to the stability of the fracture fragments, which in turn influences the local mechanical conditions. The local mechanical conditions in the regenerating tissues can be described in terms of the stresses and strains.

The concept that biological processes at the cellular level can be regulated by mechanical loading can be traced backed to the late 1800s when Roux introduced his theory of functional adaptation (Roux, 1895). Building on these initial works, Pauwels suggested cell or extracellular matrix deformation associated with distortional stress (pure shear) is a stimulus for mesenchymal cell differentiation into fibroblasts (fibrous tissue) and hydrostatic compression, which causes a volume change, stimulates mesenchymal cell differentiation into chondrocytes (cartilage) (Pauwels, 1980). Combinations of shear and hydrostatic pressure stimulates the differentiation to form fibrocartilage (Figure 2-7), whilst primary bone formation requires a stable low strain mechanical environment so endochondral bone formation will proceed only if the soft tissues create this low strain environment.

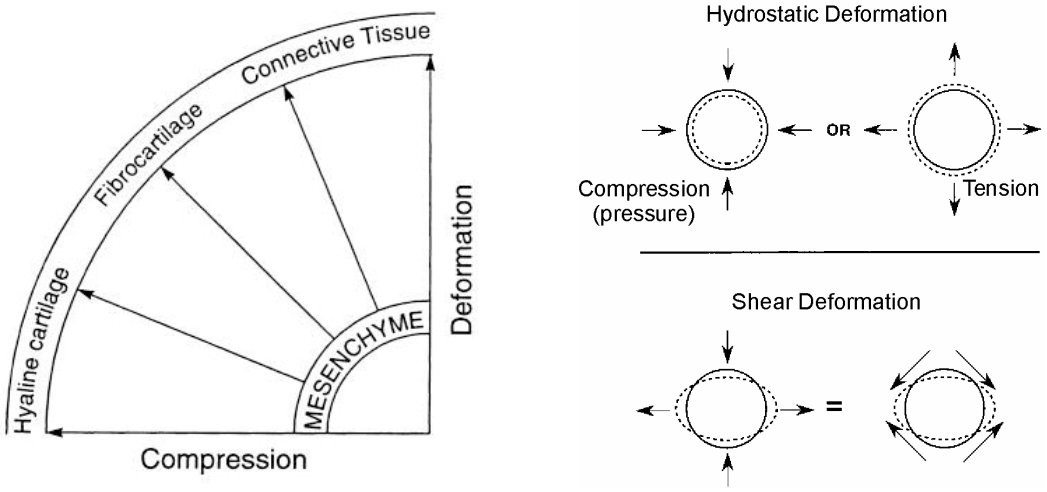


**Figure 2-7 Pauwels' view of the role played by tissue mechanical stimuli in tissue differentiation (left). Schematic representations of the deformation caused by hydrostatic stress and deviatoric stress (right) (Reproduced from (Carter et al., 1998)).**

Perren's observations of healing under differing mechanical conditions led him to propose the "Interfragmentary Strain Theory" (Perren and Cordey, 1980). The interfragmentary strain is determined by taking the longitudinal fracture gap movement and dividing by the size of the gap. The theory states that only a tissue that can withstand the interfragmentary strain can occupy the gap. As a tissue in the fracture gap stiffens, the interfragmentary strain is reduced allowing healing by a

progressive tissue differentiation from the initial granulation tissue, to fibrous tissue, cartilaginous tissue and finally bony tissue. However the hypothesis that interfragmentary strain controls the morphological patterns of fracture healing developed by Perren only considered longitudinal or axial strains associated with deformation of the interfragmentary region. In doing so, contributions to the strain environment from radial and circumferential strains were ignored. While Perren's "Interfragmentary Strain Theory" provided a means to understand the consequence of tissue differentiation on interfragmentary strain, it could not account for changes in the different regions of the callus.


**Figure 2-8 Representation of boundaries for tissue formation according to Perren's Interfragmentary Strain Theory (Perren and Cordey, 1980).**

DiGioia et al investigated the three-dimensional strain fields in a uniform osteotomy gap subjected to known levels of interfragmentary strain (DiGioia et al., 1986). Using the finite element method, the calculation of the three dimensional strain patterns showed variations in strain through the thickness of the gap as well as radial variations. The complexities led DiGioia to conclude that the maximum longitudinal strain, or interfragmentary strain, alone in not a sufficient basis to determine tissue yielding as the resulting principal strains were significantly greater than the applied longitudinal strains.

Continuing the work of DiGioia, Cheal analysed a model consisting of geometry based on photographs taken of sheep tibia cross-sections (Cheal et al., 1991). An elastic material was used while accounting for kinematic non-linearity with an incremental solution strategy. Cheal attempted to relate bone resorption to various stress criteria. However no such relationship was supported, although the spatial distribution of bone fragment resorption corresponded to areas of elevated strain. Cheal found however that the variations in hydrostatic and octahedral shear stress were parralled with the variations in principal strain (Cheal et al., 1991).

Following on from initial attempts to relate the mechanical conditions in the regenerating tissues of the callus and the ideas of Pauwels, Carter (1988) proposed that local stress or strain history could be used to explain tissue differentiation over

time. Compressive hydrostatic stress history was postulated to guide formation of cartilage, whereas a tensile strain history favoured the formation of fibrous tissue and bone formation is formed in lowly stressed regions (Figure 2-9). Additionally, Carter added that in regions of low oxygen tension cells are diverted down a cartilaginous pathway.

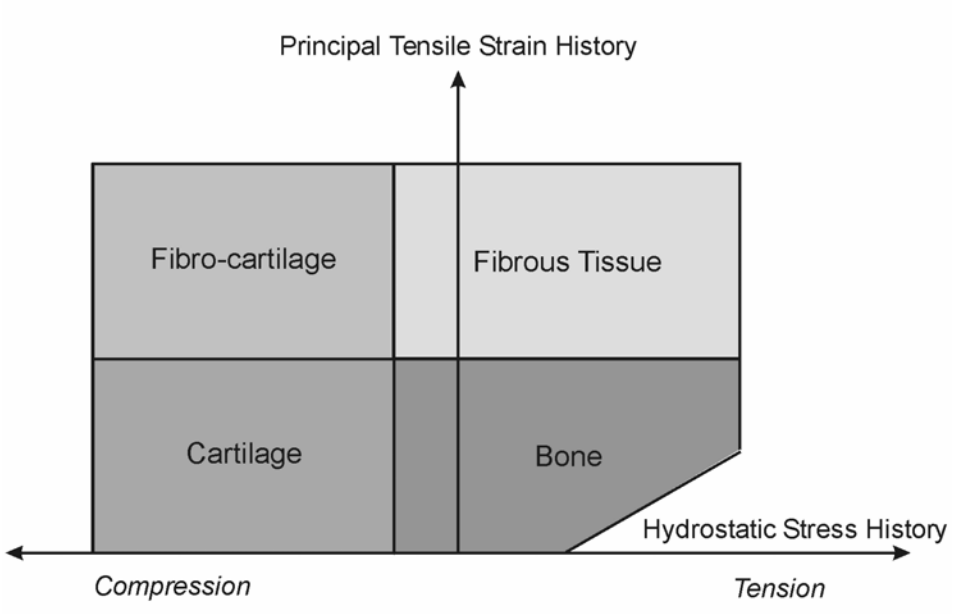


**Figure 2-9 shows the role of tissue mechanical loading history on skeletal tissue regeneration (Carter et al., 1998).**

Claes performed an interdisciplinary study comparing data from animal experiment, finite element analyses and cell culture to assess the influence of gap size and interfragmentary strain on bone healing. Drawing on their histological observation, Claes and Heigele (1999) formulated a mechano-regulation theory (Figure 2-10) similar to that of Carter and co-workers (Figure 2-9), but in quantitative terms. Further, their theory was based on observations that bone formation occurs mainly near calcified surfaces and that both intramembranous and endochondral ossification exist. The comparison of the histology with the mathematical analyses of stress and strain allowed attribution of intramembranous bone formations to local strain of less than 5%. Compressive hydrostatic pressures greater than –0.15 MPa and strains smaller than 15% appeared to stimulate endochondral ossification, with all other conditions corresponding to areas of connective tissue or fibrous cartilage (Claes and Heigele, 1999).

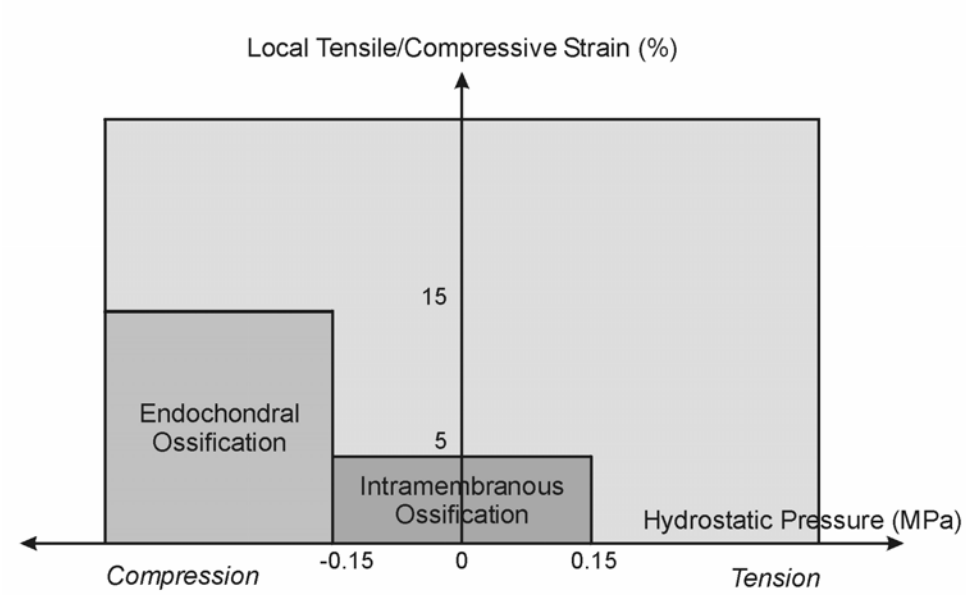


**Figure 2-10 shows correlations between the mechanical conditions and types of tissue formed in a fracture callus as described by Claes and Heigele (1999).**

Following on from previous work of Prendergast and co-workers (1997) in which mechano-regulation of tissue differentiation was controlled by two biophysical stimuli: tissue shear strain and interstitial fluid flow, at the bone implant interface, Lacroix (2002) applied the same theory to investigate fracture healing (Figure 2-11). Lacroix used a 2D axisymmetric biphasic finite element model with tissues represented by soil elements, shown to be comparable to the poroelastic theory as developed by Mow (1980). The dynamic model created by Lacroix was able to simulate intramembranous bone formation far from the fracture site, endochondral ossification in the external callus, stabilisation when bridging of the external callus occurs, and resorption of the external callus (Lacroix et al., 2002). The model was able to predict slower healing with increasing gap size and increased connective tissue production with increased interfragmentary strain.

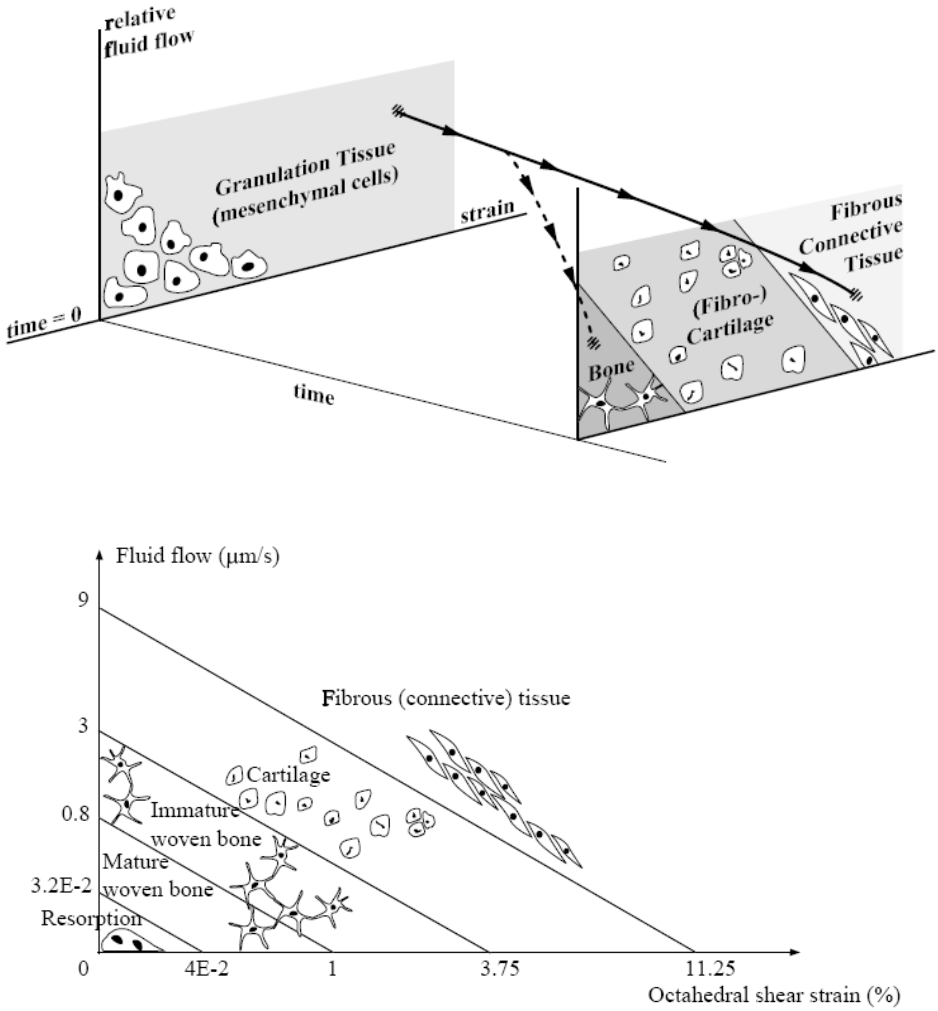


**Figure 2-11 Top: Mechano-regulation pathway for tissue differentiation based on strain and fluid flow (Reproduced from Prendergast (1997). Bottom: Mechano-regulation pathway applied to fracture healing (Reproduced from Lacroix (2002)).**

Taking a more biological approach, Bailon-Plaza and van der Meulen (2001) developed a mathematical framework to study the effects of growth factor influences on fracture healing. In their model cell differentiation was controlled by the presence of osteogenic and chondrogenic growth factors (Bailon-Plaza and van der Meulen, 2001). The model was later further developed (Figure 2-12) to include the influences of the mechanical environment (Bailon-Plaza and van der Meulen, 2003). Deviatoric strains were assumed to stimulate and dilatational strains to inhibit osteogenesis (Carter et al., 1988). Ranges of stimulatory and inhibitory strains in agreement with in vitro studies and a study by Claes and Heigele (1999) were examined.

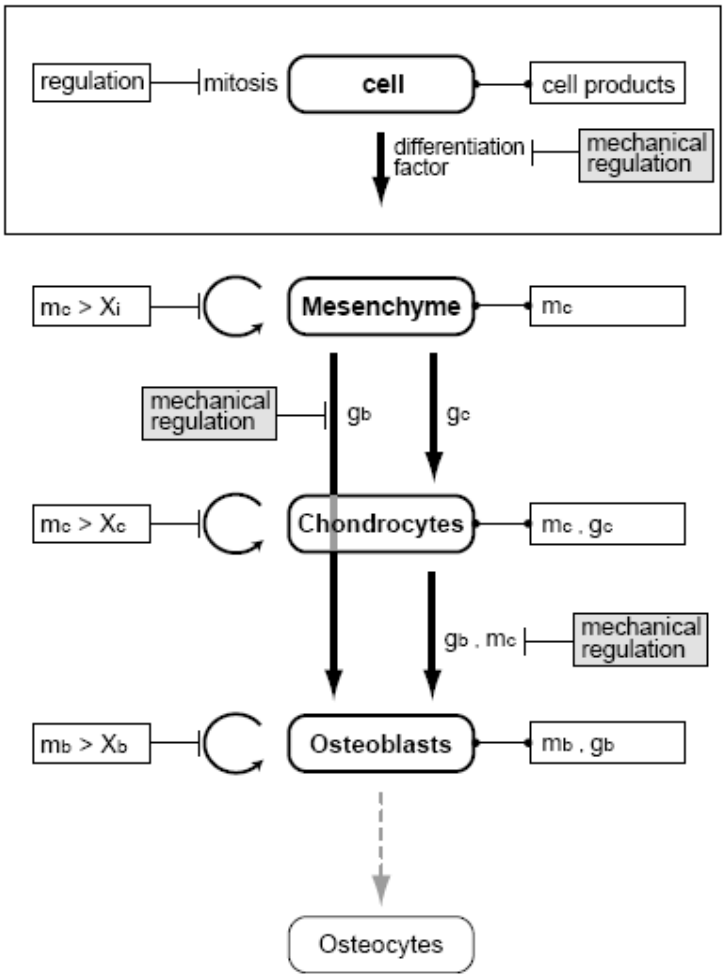


**Figure 2-12 Cell differentiation pathway: osteogenic and chondrogenic growth factors ($g_b$ and $g_c$), drive the differentiation of mesenchymal cells into osteoblasts and chondrocytes, and, depending on the connective/cartilage matrix density, the replacement of chondrocytes into osteoblasts. In this work, mechanical stimulus further regulates cell differentiation (shaded boxes). All the cells undergo mitosis, which is inhibited at high ECM density, and synthesize ECM matrix. Chondrocytes and osteoblasts synthesize the chondrogenic and osteogenic growth factors, respectively. Finally, osteoblasts undergo apoptosis or become osteocytes (Reproduced from (Bailon-Plaza and van der Meulen, 2003)).**

# 3 Morphology of Bone Healing

In this chapter, an experimental animal model to investigate the influence of fixation stability on the course of bone healing is presented. The mechanical fixation stability was altered in order to observe the biological response to a tibial osteotomy under rigid and semi-rigid conditions. Radiological, histological and mechanical techniques were used to document the spatial and temporal changes in tissue composition during callus development. Comparison of healing under these different fixation stabilities was then performed to identify healing processes that may be under the influence of the local mechanical conditions.

## 3.1 Introduction

Bone can show a remarkable capacity for self repair following trauma. Contrary to other musculoskeletal tissues that heal with the formation of a scar, healing of bone restores not only function but also the original anatomical configuration. Under flexible fixation conditions fracture healing in the diaphysis of long bones, such as the tibia, occurs with the formation of a callus in what is known as secondary healing. Secondary healing can be divided into a number of stages: inflammation, granulation tissue formation, callus formation, and remodelling (Brighton, 1984, Cruess and Dumont, 1975, Frost, 1989, Owen, 1970). Initially, bleeding leads to the formation of the fracture haematoma. Subsequent new bone formation occurs by either intramembranous or endochondral ossification pathways (Einhorn, 1998). Intramembranous bone is produced directly on the periosteal and endosteal cortical surfaces (Claes et al., 1998, Mark et al., 2004a). Other regions of the haematoma undergo a process of differentiation through granulation tissue, fibrous tissue, fibrocartilage and hyaline cartilage which mineralizes to form woven bone by the process of endochondral ossification.

The fixation stability and the resulting mechanical conditions in the gap have been shown in numerous studies to influence callus formation during bone healing (Yamagishi and Yoshimura, 1955, Stürmer, 1988, Sarmiento et al., 1996, Claes et al., 1998, Park et al., 1998, Webb and Tricker, 2000, Perren, 2002, Augat et al., 2003, Lill et al., 2003, Klein et al., 2004, Wu et al., 1984, Goodship et al., 1993, Hente et al., 2004, Claes et al., 1997). The size of the external callus produced has been related to both the magnitude and frequency of the interfragmentary movements (Goodship et al., 1993, Goodship et al., 1998, Le et al., 2001, Hente et al., 2004). Whilst some interfragmentary movement has been shown to be important to stimulate callus formation and healing, a large callus does not necessarily provide the best stability (Augat et al., 1997). Just how movements at the fracture site influence the proliferation and differentiation of the healing tissue over the course of healing is unclear.

Recent studies have suggested that the initial mechanical conditions are especially important for the repair process (Klein et al., 2003). This is supported by the observation that the differentiation of mesenchymal cells towards either an osteogenic

or chondrogenic cell line is not only dependent on the mechanical stability but is also determined within days of a fracture incident (Thompson et al., 2002, Le et al., 2001). Although the influence of mechanics on the healing outcome is well documented, its role during the early phase and over the course of fracture healing has not been well described.

As mechanical conditions, determined by fixation stability, have been shown to influence fracture healing, efforts have been made not only to determine the magnitude of the mechanical stimulus necessary to ensure bone healing free of complication, but also if possible the magnitude of the stimulus necessary to accelerate the healing process (Wallace et al., 1991, Wentzensen, 1999). This stimulus is often expressed in terms of the amount of interfragmentary movement. The range of optimal interfragmentary movement has only been partially described. Initial axial interfragmentary movement of 0.2 - 1 mm for gap sizes of 3 mm are believed to give the best healing results (Stürmer, 1996, Claes et al., 1997, Wolf et al., 1998). However, animal experiments and measurements on human patients have shown that interfragmentary movements are multidirectional (Duda et al., 2003). Furthermore, significant shear movements may be present and are sometimes a factor of two greater than those in the axial direction (Duda et al., 2003). Limits of acceptable shear movement have as yet not been defined and the effect of shear movement on fracture healing is controversial (Yamagishi and Yoshimura, 1955, Park et al., 1998, Augat et al., 2003).

The purpose of this experimental study was to characterise the influence of fixation stability on callus formation at the different stages of bone healing. It was hypothesised that mechanical conditions influence not only the longer term healing outcome, but also callus formation in the early phase of fracture healing. Furthermore, it was hypothesised that mechanical conditions characterised by an increased shear interfragmentary movement component would result in a delay in healing relative to a fixation characterised by comparatively moderate shear movements. Thereby, it was the aim of this study to determine an upper boundary for an acceptable amount of shear interfragmentary movement. To test these hypotheses, an external fixator was modified from its standard form so as to increase the magnitude of the shear interfragmentary movement component. The course of healing was then characterised

mechanically and histologically in a sheep osteotomy model for rigid and semi-rigid fixation stabilities.

## 3.2 Materials and Methods

### 3.2.1 External Fixators

The standard (rigid) monolateral external fixator (Figure 3-1) consisted of six Ø5 mm Schanz screws and two Ø10 mm steel rods (Synthes, Germany). In addition, a semi-rigid external fixator was constructed by cutting through the inner bar and reconnecting it by means of a custom made sliding joint. The distance between skin and inner rod was 15 mm for the rigid and 10 mm for the semi-rigid fixator.

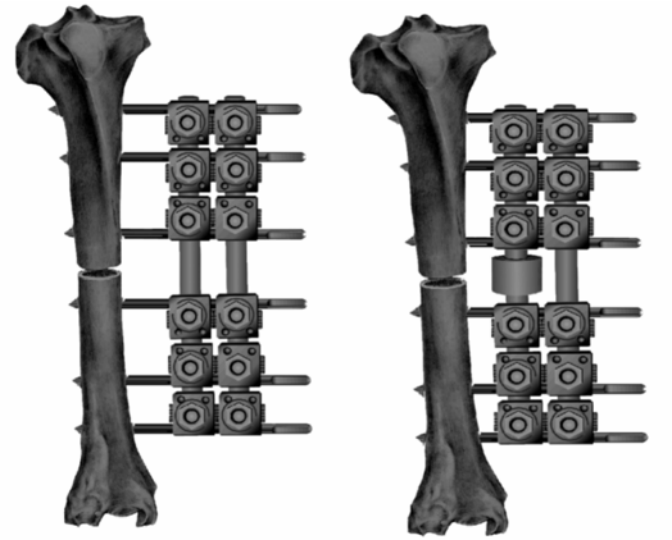

**Figure 3-1 Rigid (left) and semi-rigid (right) external fixator attached to the medial aspect of the right ovine tibia. Note the custom-made sliding joint bisecting the inner bar of the semi-rigid fixator.**

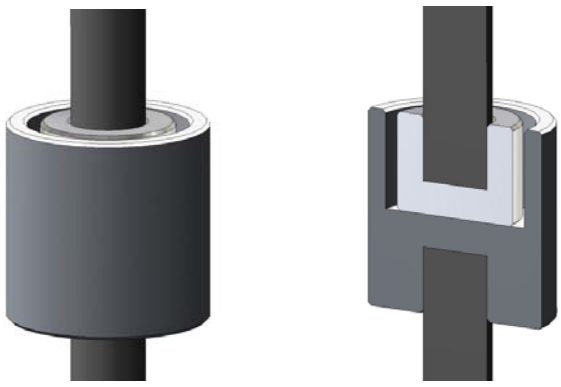

**Figure 3-2 provides a detailed schematic of the sliding joint used to create semi-rigid fixation stability. The joint is designed to maintain the axial stability while increasing the amount of interfragmentary movement in vivo.**

The sliding joint, used to rejoin the inner bar, consists of two bodies in axial contact but able to slide laterally with respect to one another. The surfaces in contact are highly polished to minimise frictional resistance. The degree to which one bar can move relative the other is defined by the difference in diameters of the two joint bodies. The sliding joint was constructed so as to increase the interfragmentary shear movement, whilst producing similar axial movements to the standard rigid fixator.

In order to confirm the effect of the sliding joint, the stiffness of the fixators was characterised by means of in vitro mechanical testing prior to use in this study. Following assembly of the fixator on cadaveric ovine tibiae (n = 6, each), the proximal and the distal ends of the tibia were potted in PMMA and mounted using a custom-made jig in a material testing machine (Zwick 1445, Germany). Six independent load cases (axial compression, torsion, cranial-caudal bending and shear, medial-lateral bending and shear) were then tested (Figure 3-3). Interfragmentary movements were recorded using an optical measurement system (PCReflex, Qualisys, Sweden; accuracy of measurements: ± 0.1 mm) and correlated to the applied loads to determine the stiffness of the fixation (Kassi et al., 2001).

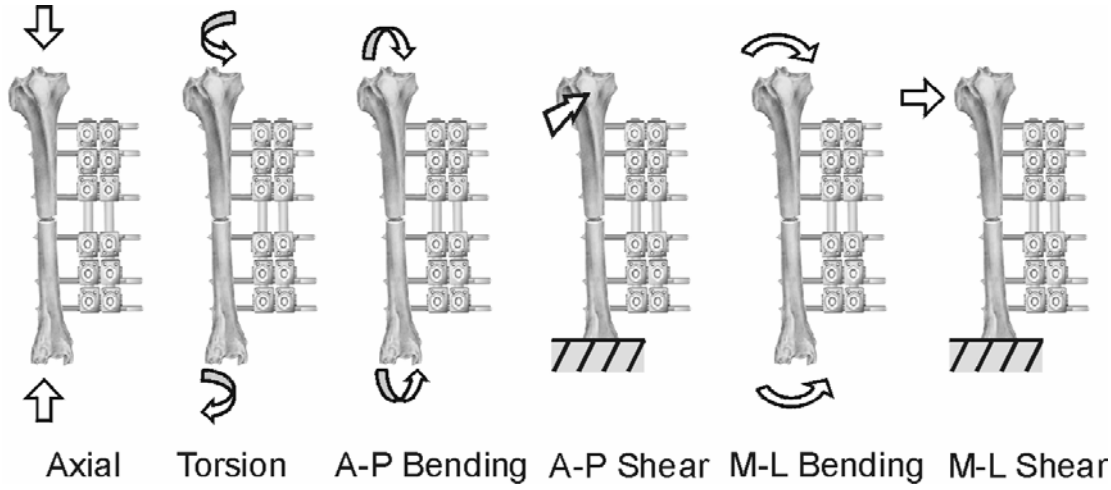


**Figure 3-3 demonstrates the loads applied in the six different load cases.**

A similar stiffness in axial compression, shear and torsion was determined for both fixators in vitro (Table 3-1). The bending stiffness of the semi-rigid fixator [16.4 ± 5.2 Nm/$^{o}$] in the medial-lateral plane was significantly (p* = 0.029) lower than the rigid fixator [27.1 ± 8.9 Nm/$^{o}$] (Schell et al., 2005).

| group | | A/P shear [N/mm] | M/L shear [N/mm] | A/P bending [Nm/°] | M/L bending [Nm/°] | Compression [N/mm] | Torsion [Nm/°] |
|---|---|---|---|---|---|---|---|
| rigid | 1 | 266.67 | 210.53 | 133.33 | 28.57 | 1333.33 | 4.17 |
| | 2 | 500.00 | 333.33 | 200.00 | 13.79 | 1666.67 | 3.91 |
| | 3 | 235.29 | 210.53 | 100.00 | 28.57 | 1250.00 | 3.45 |
| | 4 | 363.64 | 190.48 | 100.00 | 21.05 | 3076.92 | 3.47 |
| | 5 | 400.00 | 173.91 | 57.14 | 30.77 | 2000.00 | 2.99 |
| | 6 | 35.40 | 28.57 | 44.44 | 40.00 | 1379.31 | 3.14 |
| | mean | 300.2 | 191.2 | 105.8 | 27.1* | 1784.4 | 3.5 |
| | stabw | 160.8 | 97.7 | 56.3 | 8.9 | 690.5 | 0.4 |
| semi-rigid | 1 | 285.71 | 210.53 | 10.53 | 16.00 | 975.61 | 3.16 |
| | 2 | 400.00 | 125.00 | 19.05 | 15.38 | 1052.63 | 3.16 |
| | 3 | 210.53 | 444.44 | 26.67 | 16.00 | 2352.94 | 3.47 |
| | 4 | 400.00 | 121.21 | 66.67 | 7.69 | 1290.32 | 2.60 |
| | 5 | 190.48 | 173.91 | 44.44 | 21.05 | 1666.67 | 3.01 |
| | 6 | 285.71 | 444.44 | 133.33 | 22.22 | 2105.26 | 3.33 |
| | mean | 295.4 | 253.3 | 50.1 | 16.4* | 1573.9 | 3.1 |
| | stabw | 89.8 | 151.7 | 45.4 | 5.2 | 567.1 | 0.3 |

**Table 3-1 Results of in vitro testing of rigid and semi-rigid fixators (n = 6, each). The results for medial-lateral bending are significantly (p* = 0.029) different between both groups (Schell et al., 2005).**

### 3.2.2 Animals

Sixty four healthy female Merino sheep (aged between 2.5 – 3.5 years and a mean weight of 63 kg (± 8 kg)) were subdivided into 2 groups. The first group received the rigid fixator, while the second was treated with the semi-rigid fixator. Each fixator group was further divided into 4 subgroups (n = 8, each) based on the prescribed healing time (sacrificed at 2, 3, 6 and 9 weeks postoperatively).

All experiments were carried out according to the policies and principles established by the Animal Welfare Act, the NIH Guide for Care and Use of Laboratory Animals and the National Animal Welfare Guidelines and were approved by the local legal representative[1].

### 3.2.3 Surgical Procedure

Under general anaesthesia, the external fixator was attached to the medial aspect of the right tibia, placing the Schanz screws perpendicular to the skin. The Schanz

[1] Landesamt für Arbeitsschutz, Gesundheitsschutz und technische Sicherheit, Berlin: registration number G 0224/01

screws were reproducibly placed using a drill guide which also avoided pre-bending between the screws. The osteotomy of the tibial diaphysis was performed with an oscillating saw and distracted to 3 mm using a spacer tool. The animals of the 9 week group received two additional Ø4 mm Schanz screws (Synthes, Germany) placed cranially, proximally and distally to the gap. Reflective markers were attached to these additional screws during the measurements of interfragmentary movements, as previously described (Klein et al., 2003). The skin was sutured and the shank was covered with a tube bandage. All animal surgery and postoperative care was performed by an experienced veterinarian.

### 3.2.4 Radiological and Clinical Observations

An analgesic was administered (Meglumin-Flunixin, Finadyne®, Essex, Germany) for seven days postoperatively. Daily animal care involved cleaning the insertion points of the Schanz screws with Ethacridinlactate (Rivanol®, Germany). Cranial-caudal radiographs were taken directly postoperatively and then at weekly intervals.

### 3.2.5 In vivo Monitoring of Fixation Stability

In vivo monitoring of the mechanical stability was performed through measurement of the interfragmentary movements and the ground reaction forces. Measurements began 3 days postoperative and then at weekly intervals. The interfragmentary movements were determined from the recording of reflective markers positions by an optical measurement system (PCReflex, Qualisys, Sweden; accuracy of measurements: ± 0.1 mm) and the intra-operative measurement of the offsets of the markers to the centre of the osteotomy according to a previously described technique (Klein et al., 2003). The movements of the reflective marker sets were then transformed into relative interfragmentary movements at the osteotomy site using matrix algebra. Weight bearing of all limbs was assessed by measuring ground reaction forces using a pressure sensitive platform (Emed SF-4, Novel, Munich, Germany) and the first step method (Rosenbaum and Becker, 1997). The measured interfragmentary movements confirmed that different in vitro fixator stiffness resulted in different mechanical conditions at the site of osteotomy (Schell et al., 2005). A higher shear movement in the cranial-caudal direction was determined initially (3 days) in the semi-rigid group compared to the rigid fixator group [rigid: 0.52 [0.36/0.75] (median [min /max]) vs. semi-rigid: 0.78 [0.47/1.31] mm, $p = 0.043$]. No significant differences in the axial

movements were determined [rigid: 0.32 [0.26/0.61], semi-rigid: 0.46 [0.40/0.72] mm, p = 0.059]. At this initial time point, weight bearing in all sheep was similar to the preoperative value. Within 2 weeks the interfragmentary movements reduced and converged such that no differences were determined during the remainder of the healing process.

### 3.2.6 Biomechanical Testing – Torsional Moment and Stiffness

Following sacrifice and removal of the fixator, the left and right tibiae of the six and nine week groups were tested mechanically (Zwick 1445, Germany). The two and three week groups were excluded from testing due to the immature callus tissue. The proximal and distal ends of each tibia were embedded in acrylate (Beracryl, W. Troller AG, Switzerland) for mounting in the material testing machine (Zwick1445, Germany) (Figure 3-4). Torsional testing was performed until failure at the rate of 10 degrees per minute. Prior to and during mechanical testing the attached muscles were covered with a gauze bandage moistened with 0.9% NaCl. The torsional stiffness and torsional moment to failure of the operated tibia, reported as a percentage of the values from the intact contralateral side, were determined according to a previously reported procedure (Klein et al., 2003).

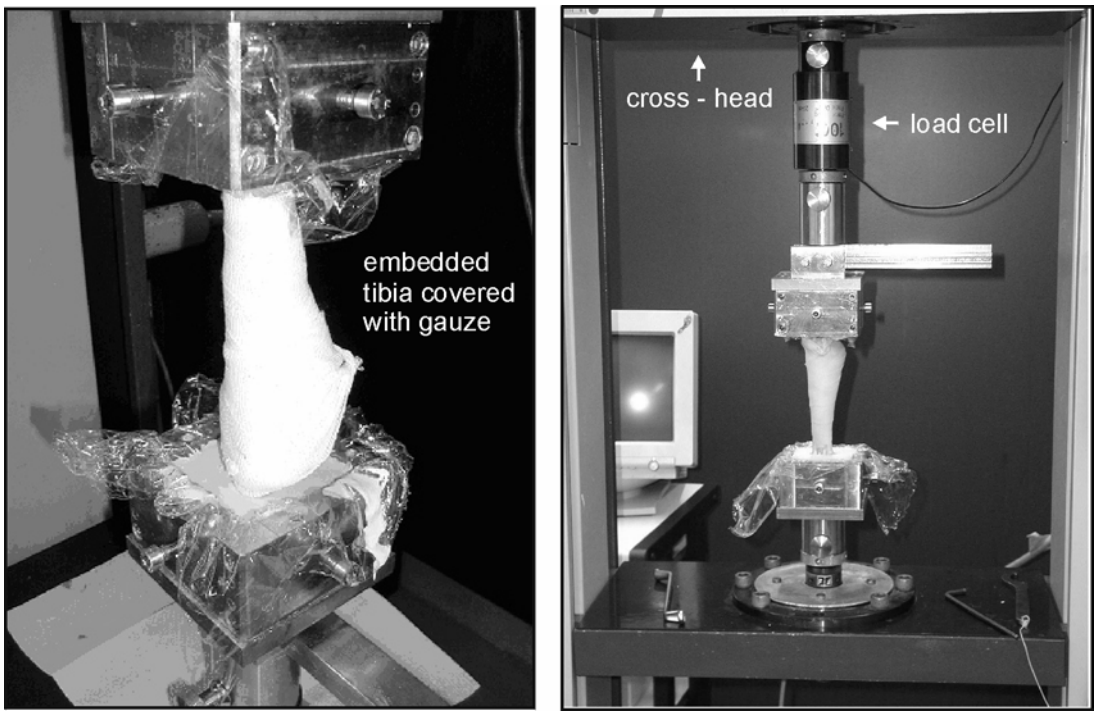


**Figure 3-4 shows the set up for mechanical testing in torsion of explanted tibia.**

### 3.2.7 Moment of Inertia

The moments of inertia (MOI), used to provide a quantification as to the amount, quality and distribution of bone, were determined from sequences reconstructed from computer tomography (CT) scans taken immediately after sacrifice and prior to mechanical testing (Figure 3-5). The intact and fractured tibiae were scanned together with a bone phantom (Model 3 CT Phantom, Mindways Software, USA) enabling later conversion of Hounsfield unit values to mineral density.

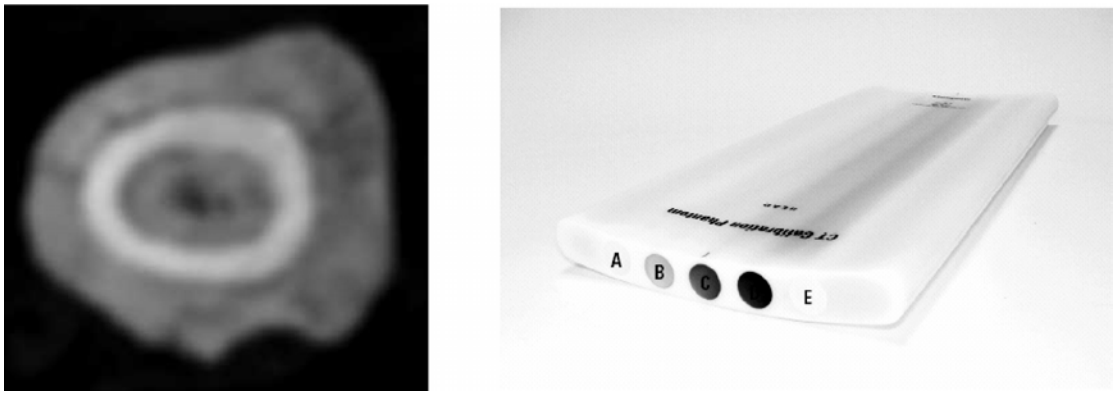


**Figure 3-5 (Left) CT slice through a tibial callus showing high density cortical bone surrounded by less dense newly formed callus (right) CT bone phantom used for conversion of Hounsfield units to bone density**

Using the Amira software (Indeed - Visual Concepts, Germany), mineralised tissue was segmented first automatically using a threshold tool and secondly with conventional graphic tools for mask correction. The principal axes of the mineralised tissue between the two inner screws of the external fixator and also for the corresponding segment of the intact tibia were calculated using the software. Then, the cross-sectional moment of inertia (maximum), taking into account mineral density, was determined about the maximum principal axis. The moment of inertia of the healed tibia was then normalised by expressing it as a percentage of the intact value from the intact contralateral side.

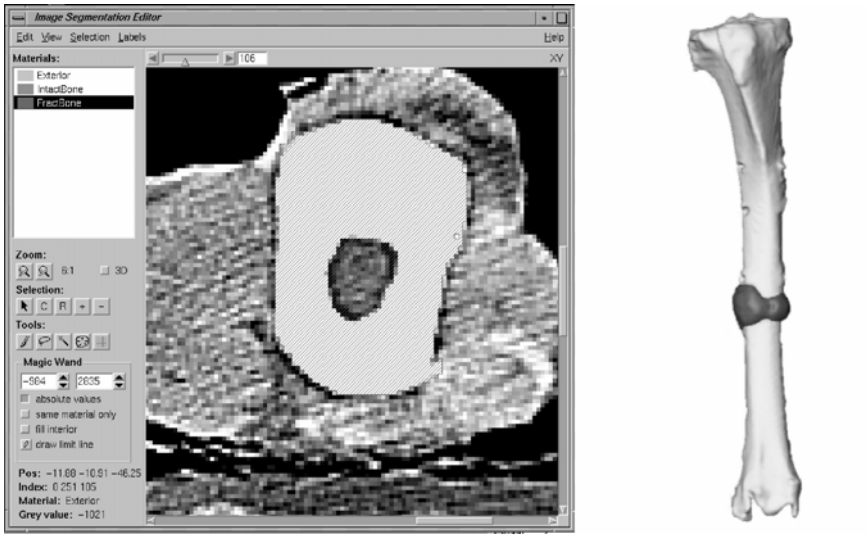


**Figure 3-6 (left) screenshot from Amira program showing segmentation of mineralised tissue (right) tibia reconstructed from CT data showing callus formation (dark grey) at 6 weeks**

### 3.2.8 Histologic and Histomorphometric Analysis

Immediately following biomechanical testing (6 and 9 weeks groups) and post mortem harvesting and CT (2 and 3 weeks groups) histological sections of the callus region stained with either Safranin Orange/von Kossa or Safranin Orange/Fast Green were prepared (Klein et al., 2004). Qualitative morphologic examination of the fractured area was done in the central section from each specimen, by two investigators. The morphologic features of the periosteal, intercortical, and intramedullary zones in each section were described. Histomorphometric analysis was performed with an image analysis system (KS400, Zeiss, Germany). The region of interest (ROI) comprised the gap plus one and a half times the width of the gap in the proximal and distal direction, resulting in a ROI with a height of twelve millimetres. The width of the ROI was defined by the callus-width. The quality and quantity of the callus tissue was examined with respect to bone, cartilage and fibrous tissue composition (Parfitt, 1988b, Parfitt, 1988a).

### 3.2.9 Statistical Analyses

Statistical comparison between the groups was performed using the Mann-Whitney-U-Test for unpaired non-parametric data (SPSS 10.0, SPSS Inc., USA). A p-value of less than 0.05 was taken as a significant difference and was corrected by Bonferroni-Holm-test procedure, if indicated.

## 3.3 Results

### 3.3.1 Radiological and Clinical Results

All animals showed a regular wound and fracture healing without complications. Pin infections, limited to serous discharge, were observed in two animals (one three week animal (1 pin) and one six week animal (2 pins)).

At two weeks, the osteotomy gap is clearly visible in both fixation groups and there were no visible signs of bony callus formation (Figure 3-7, row 1). At three weeks, a similar amount of periosteal bony callus formation was visible for both fixation groups with callus formation appearing considerably larger on the lateral side (Figure 3-7, row 2). At six weeks, bridging of the periosteal callus was apparent on the lateral side of rigidly fixed calluses, with only a small gap remaining on the medial side (Figure 3-7, row 3). In contrast, the osteotomy gap of semi-rigidly treated animals was still clearly visible and a distinct gap remained throughout the periosteal callus. By nine weeks, bridging on both medial and lateral aspects could be seen in rigidly treated animals (Figure 3-7, row 4). The size of the periosteal callus appeared reduced compared to the corresponding six week image. In the semi-rigid group, bridging of the periosteal callus was complete; however the osteotomy gap was still clearly identifiable.

### 3.3.2 Mechanical Testing of Explanted Tibia

The torsional stiffness of the tibiae stabilised with the rigid fixator was higher than that of those tibiae stabilised with the semi-rigid fixator at 6 weeks [73 [68/111] vs. 60 [47/83] %, $p = 0.041$] (Figure 3-8). The torsional moment to failure of the rigid fixator treated tibiae only tended to be larger than that of the tibiae treated with the semi-rigid fixator [43 [31/72] vs. 29 [22/40] %, $p = 0.093$]. The stiffness of the tibiae increased between the 6th and 9th week, more so in the semi-rigid fixator group. After 9 weeks of healing no significant differences between the torsional stiffness [98 [75/115] vs. 91 [53/112] %, $p = 0.383$] or in the maximum moment to failure [71 [57/98] vs. 66 [51/105] %, $p = 0.165$] of the rigid and semi-rigid fixator remained.

Actual values for the torsional stiffness and torsional moment for the intact and fractured tibia are presented in Table 3-2.

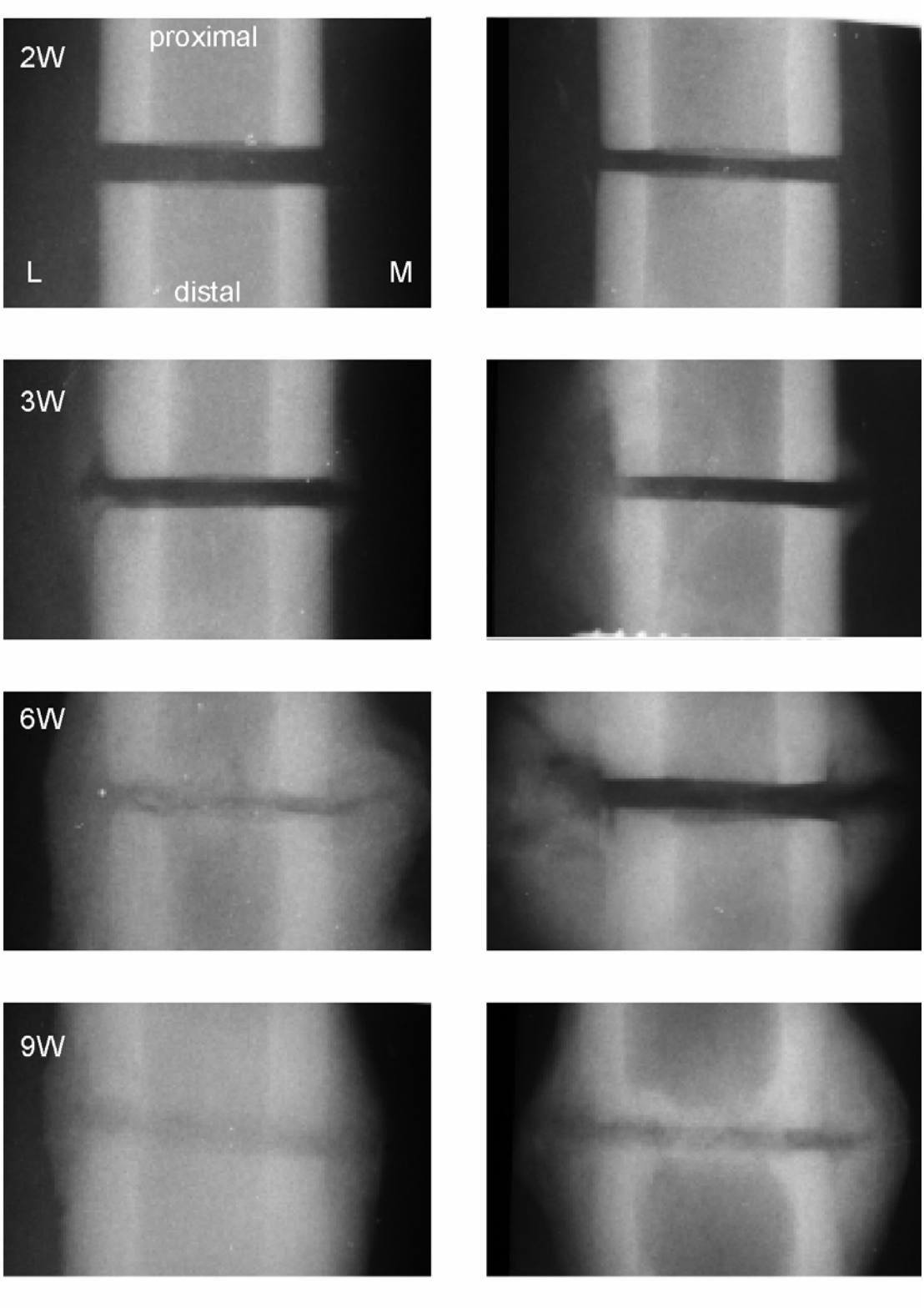


**Figure 3-7 The radiological course of healing shown under rigid (left) and semi-rigid (right) fixation at 2, 3, 6 and 9 week time points.**

| Weeks | Fixator | Intact | | Fractured | |
|---|---|---|---|---|---|
| | | moment [Nm] | stiffness [Nm/°] | moment [Nm] | stiffness [Nm/°] |
| 6 | rigid | 74.9 (66.1/89.3) | 3.7 (3.0/5.1) | 32.0 (20.6/49.4) | 2.9 (2.5/3.7) |
| | semi | 67.5 (57.3/77.8) | 3.5 (2.0/3.9) | 24.1 (15.6/27.9) | 2.1 (1.8/3.0) |
| 9 | rigid | 63.3 (56.0/74.3) | 3.5 (2.5/4.2) | 45.0 (26.1/64.6) | 3.4 (2.3/3.8) |
| | semi | 63.6 (47.1/72.9) | 3.8 (3.3/4.2) | 41.8 (36.7/50.4) | 3.3 (1.9/4.2) |

**Table 3-2 Results of biomechanical testing at 6 and 9 weeks. Actual values [median (min/max)] for the torsional moment to failure and the torsional stiffness for both the fractured and intact contralateral tibia are given.**

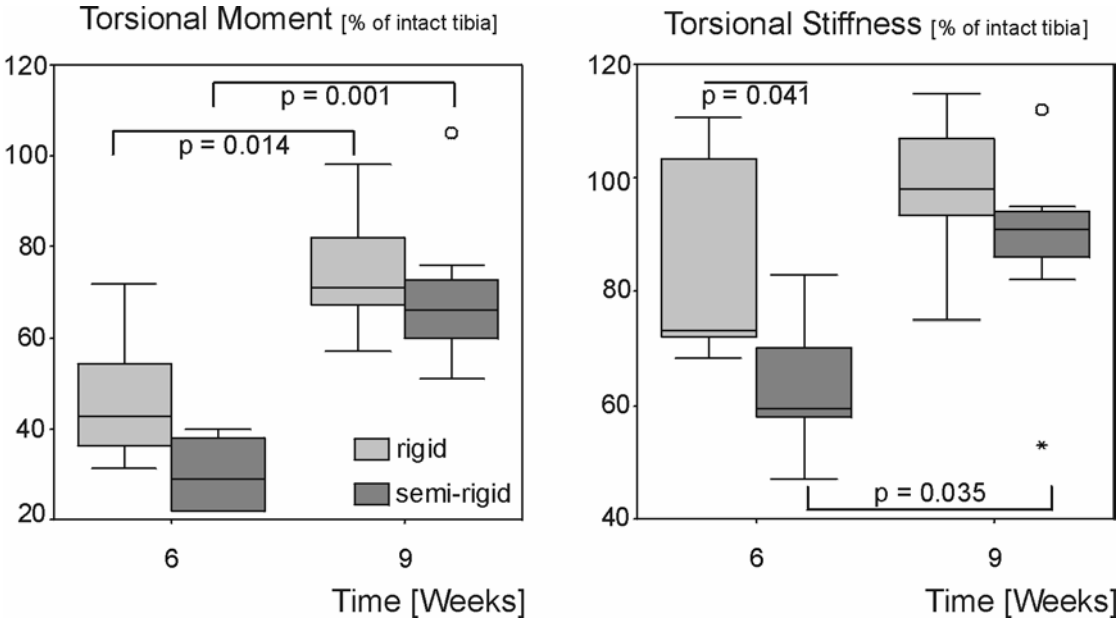


**Figure 3-8 Torsional moment and torsional stiffness of the right tibia as measured during postmortem in vitro biomechanical testing. All results are given as percentage of the intact contralateral side values (circles represent outliers and asterisks are extreme values).**

### 3.3.3 Moment of Inertia

The MOI in both groups increased over the course of the 9 week healing period (Figure 3-9). At 2 weeks, the MOI of rigid fixator treated tibiae was slightly higher than the semi-rigid fixator treated tibiae [94 [77/109] vs. 83 [66/92] %, p = 0.038]. By 3 weeks the MOI of the callus in both groups reached approximately 100 % of the corresponding intact tibiae [rigid: 104 [93/112] vs. semi-rigid: 100 [77/116] %, p = 0.994]. At 6 weeks, the MOI in the rigid fixator group tended to be lower [112 [101/151] vs. 133 [109/140] %, p = 0.336]. This trend was continued at the final investigated time point of 9 weeks [163 [153/210] vs. 179 [128/232] %, p = 0.152].

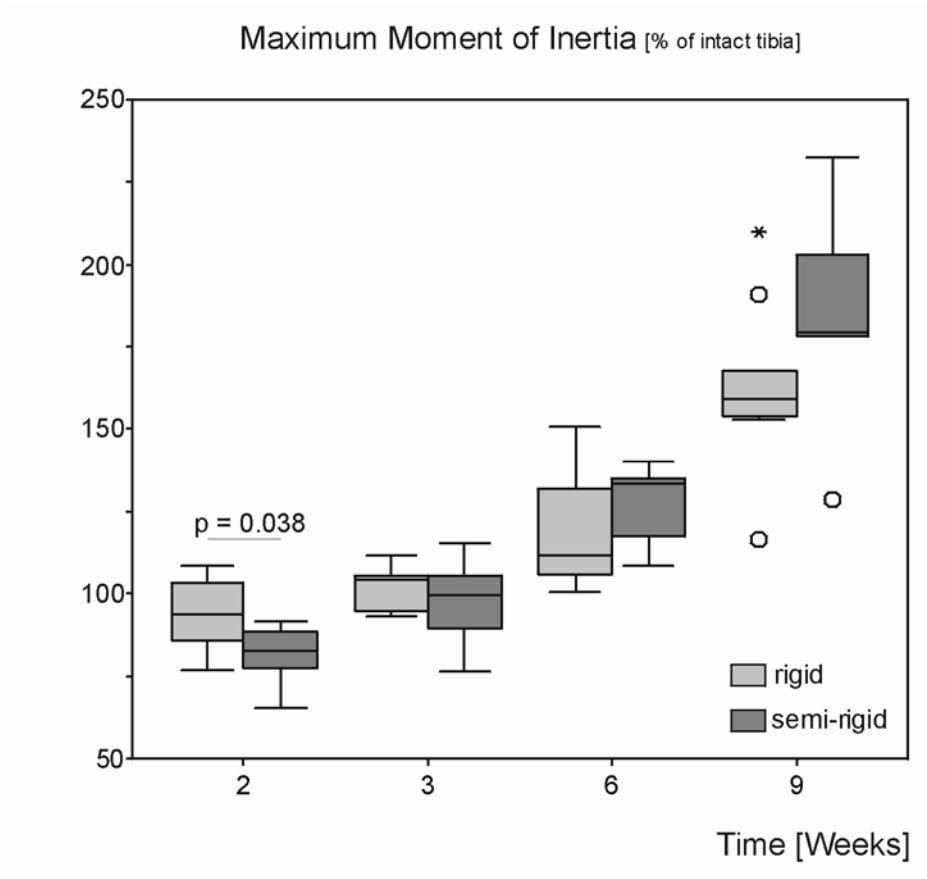


**Figure 3-9 Moment of inertia (maximum) over course of healing, values reported as percentage of the intact contralateral side.**

### 3.3.4 Qualitative Histology

**a) Two Weeks**

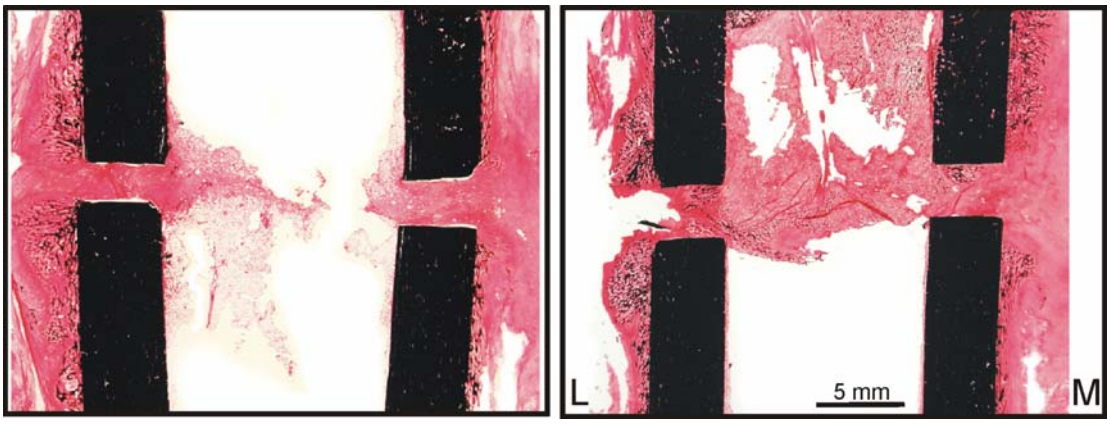


**Figure 3-10 The callus histology (Safranin Orange/von Kossa) after 2 weeks healing shown under rigid (left) and semi-rigid (right) fixation. The medial-lateral orientation is indicated by the M and L respectively with the proximal fragment arranged above.**

After two weeks, woven bone formation was present on the periosteal surface of the cortical bone fragments in both fixation groups (Figure 3-10). Bone formation appeared larger and structurally more organized on the lateral aspect of the tibia

compared to the medial side. The structure of the bone differed not only from medial to lateral, but also with proximity to the gap. In regions adjacent to the gap, the bone appeared to be aligned radially, whilst bone distanced further from the gap showed a longitudinal alignment (Figure 3-14). The thickness of the newly formed periosteal bone on the medial aspect was relatively constant over the length of bone between fracture gap and the innermost pin of the fixator. Adjacent to the gap the bone bulged slightly. Bone formation was rarely observed endosteally or intercortically. The remaining soft callus was composed of fibrous tissues of varying densities; fibrous tissue in the intercortical zone appeared to be transversely aligned. Remnants of the haematoma, fibrin and erythrocytes, were only found intercortically (Figure 3-14) and in only a few of the animals treated with rigid fixation. In contrast, remnants of the haematoma were visible in nearly all specimens of animals treated with semi-rigid fixation.

**b) Three Weeks**

**Figure 3-11 The callus histology (Safranin Orange/von Kossa) after 3 weeks healing shown under rigid (left) and semi-rigid (right) fixation.**

At 3 weeks, many similarities were also seen in histology from animals treated with rigid and semi-rigid fixation (Figure 3-11). Since two weeks, the periosteal callus had increased visibly in size with continued woven bone formation. On the lateral side the periosteal callus had reached a size such that the bony components were opposing one another and beginning to bridge the gap. The surface of the advancing ossification fronts were covered with a layer of chondral tissue bearing a resemblance to hyaline cartilage. In some specimens the chondrocytes were hypertrophic. The space remaining between contained fibrocartilage and extended into the gap becoming a mixture of fibrocartilage and dense fibrous tissue (Figure 3-14). On the medial side,

the ossification was typically less developed with the approaching mineralisation fronts covered with a layer of fibrocartilage. Bone formation on the endosteal side was increasingly observed but the amount of bone varied substantially from sheep to sheep. A number of animals (5/8) belonging to the semi-rigid group still contained some remnants of the fracture haematoma in the intercortical region.

**c) Six Weeks**

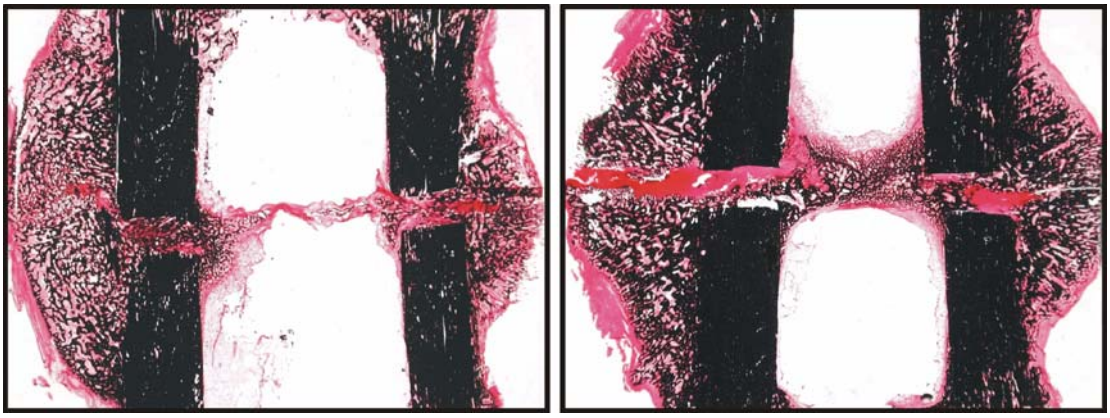

**Figure 3-12 The callus histology (Safranin Orange/von Kossa) after 6 weeks healing shown under rigid (left) and semi-rigid (right) fixation.**

At 6 weeks, bridging of the periosteal callus on the lateral side had occurred in most animals of both groups, although a small region of hyaline cartilage or fibrocartilage typically remained in the middle of the periosteal callus (Figure 3-12). In most cases, bridging of the periosteal callus on the medial side had also occurred and the lateral and medial periosteal calluses had reached similar sizes. On the outermost border of the periosteal callus on the lateral side of most animals, a large presence of osteoclasts was seen indicating resorption of the callus, whilst on the medial side enlarged osteoblasts were suggestive of continued bone formation in the medial periosteal callus. In the majority of animals bridging of the endosteal callus was also complete. In the intercortical zone, only one animal belonging to the rigid group remained not bridged. In contrast five of the animals treated with semi-rigid fixation were not bridged intercortically. The rigid group was also characterized by more extensive remodelling of the cortices, with pores appearing in the bone directly adjacent to the gap.

### d) Nine Weeks

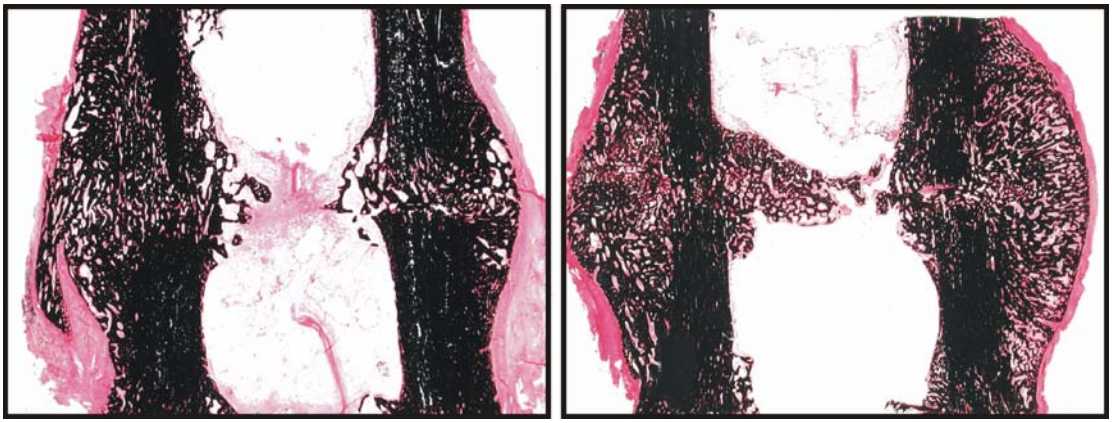

**Figure 3-13 The callus histology (Safranin Orange/von Kossa) after 9 weeks healing shown under rigid (left) and semi-rigid (right) fixation.**

At nine weeks, significant remodelling changes in the cortices as a result of osteoclastic activity were visible in the rigid group (Figure 3-13). The ends of the bone fragments were rounded off and large pores in the cortices could be seen (Figure 3-14). The size of the lateral periosteal callus now seemed to be smaller than that on the medial side. Directly adjacent to the gap, where the last ossification had taken place, the bone appeared the least organized. Large vessels in the endosteal/marrow cavity could be seen and in all animals the continuity of the marrow canal had been restored with on going resorption of the endosteal callus. At nine weeks, bony bridging of the intercortical zone was complete, however some animals of the semi-rigid group still showed evidence of continual expansion of the lateral periosteal callus, indicated by enlarged osteoblasts. In only about half of the animals was evidence of extensive remodelling activity in the gap and in the cortices visible. There was little sign of endosteal resorption and in 6 animals the continuity of the marrow canal had not been re-established.

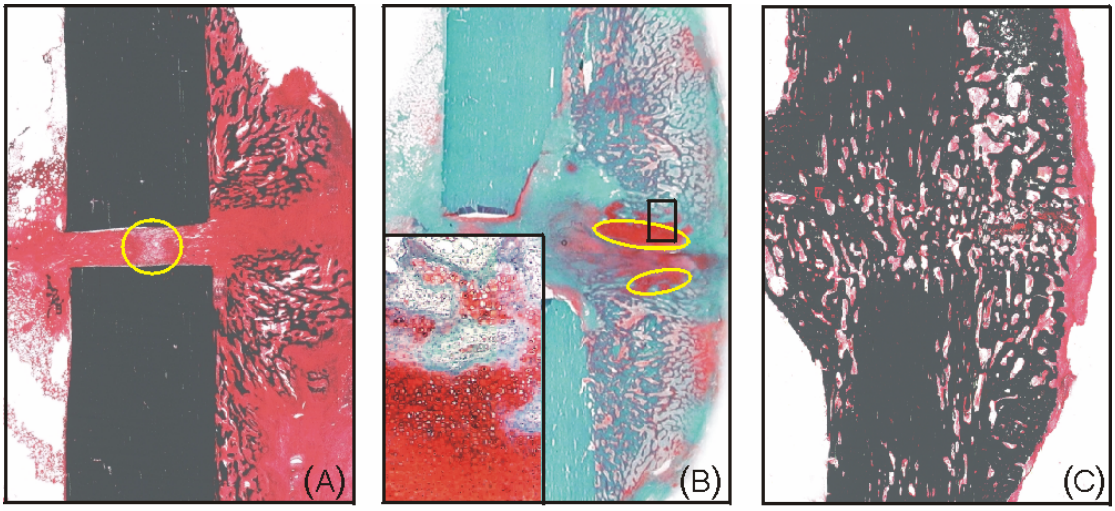


**Figure 3-14 Histology of the periosteal callus at 2, 3 and 9 weeks. (a) At 2 weeks different orientations of the bone trabeculae can be seen distanced from the gap (longitudinal) and adjacent to the gap (radial). Remnants of the haematoma can be seen intercortically, marked in yellow. (Safranin Orange/von Kossa) (b) At 3 weeks cartilage formation on existing bone surfaces is visible, marked in yellow (Safranin Orange/Fast Green) (c) At nine weeks the effects of remodelling on the cortices and the periosteal callus can be seen. (Safranin Orange/von Kossa)**

### 3.3.5 Quantitative Histomorphometry

The maximum callus area (Table 3-3 – histomorphometric results with min/max values) was reached at 3 weeks in the rigid fixator group (298 $mm^2$) and at 6 weeks in the semi-rigid fixator group (320 $mm^2$) ($p = 0.382$). The callus area of the semi-rigid group was significantly ($p = 0.001$) larger than in the rigid fixator group at 6 weeks (188 $mm^2$). Despite a decrease in callus area from 6 to 9 weeks the semi-rigid fixator group had a larger callus area than the rigid fixator group at 9 weeks [rigid: 178 vs. semi-rigid: 239 $mm^2$, $p = 0.015$]. The fibrous tissue areas were similar in both groups at 2 and 3 weeks postoperatively, but then in the rigid fixator group the fibrous tissue content decreased considerably over the next 3 weeks, while in the semi-rigid fixator group it remained high until the 6th week (Table 3-3). At 6 weeks the fibrous tissue area in the callus of the rigid fixator group was lower than in the semi-rigid fixator group [55 vs. 124 $mm^2$, $p = 0.002$]. Mineralized bone area in the rigid fixator group increased steadily up until the 6th week and then remained constant up till the 9th week (Table 3-3). In contrast, the mineralized bone area in the semi-rigid fixator group increased until the final investigated point at 9 weeks. The mineralized bone area in the rigid fixator group was significantly smaller than in the semi-rigid fixator group at both 6 [125 vs. 167 $mm^2$, $p = 0.001$] and 9 weeks [122 vs. 184 $mm^2$, $p = 0.002$]. The cartilage area was similar for both fixations at 2 and 3 weeks (Table 3-3).

The amount of cartilage in the rigid fixator group remained constant till the 6th week and then fell considerably. The semi-rigid fixator group showed a slight increase up to the 6th week, at which time the cartilage area in the rigid group was significantly lower than in the semi-rigid group [16 vs. 25 mm², p = 0.007].

| | Fixator | 2 weeks | 3 weeks | 6 weeks | 9 weeks |
|---|---|---|---|---|---|
| Total callus | rigid | 185.4 [124.5-211.3] | 297.5 [213.6-347.4] | 187.7 [136.5-238.8]a | 177.9 [124.5-213.2]f |
| | semi | 176.4 [122.7-261.3] | 286.5 [187.0-382.8] | 320.0 [233.2-447.1]a | 238.5 [183.4-342.2]f |
| Min. bone | rigid | 83.3 [73.5-99.5] | 103.9 [85.4-127.9] | 124.6 [92.2-157.4]b | 122.3 [109.0-179.8]d |
| | semi | 85.5 [69.1-98.1] | 96.9 [82.5-117.0] | 167.4 [143.6-210.5]b | 183.8 [139.6-241.8]d |
| Fibrous tissue | rigid | 81.4 [39.3-100.3] | 174.8 [114.9-225.6] | 54.7 [24.7-89.2]c | 37.1 [15.3-80.7] |
| | semi | 77.5 [35.1-130.3] | 147.4 [85.0-208.4] | 123.7 [77.2-234.9]c | 23.6 [21.0-24.9] |
| Cartilage | rigid | 19.0 [2.2-27.1] | 21.1 [10.8-68.7] | 16.0 [3.0-20.2]e | 0.4 [0.0-0.8] |
| | semi | 17.1 [6.5-36.3] | 27.4 [11.8-68.9] | 24.9 [10.8-53.3]e | 0.4 [0.0-18.6] |

**Table 3-3 Histomorphometrical analysis of callus size and composition Median values [mm²] [Min-Max], $p^{a,b} = 0.001$, $P^{c} = 0.002$, $p^{d,e} = 0.007$, $p^{f} = 0.015$**

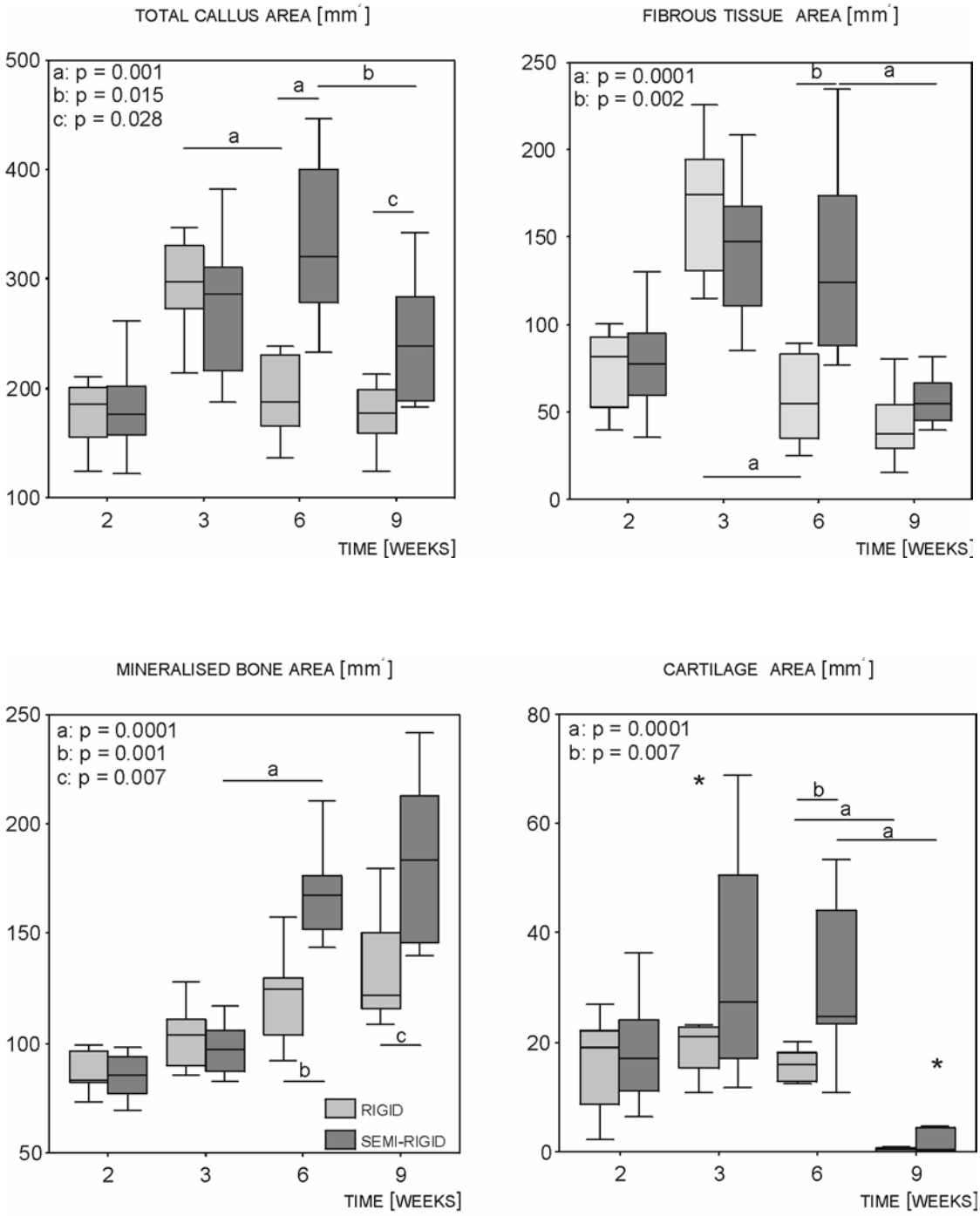


**Figure 3-15 Box plots of histomorphometrical results over the course of healing. Total callus area: Shows the decline in callus area in the rigid fixator treated group. Mineralised Bone Area: Increase in the mineralised bone area is seen up until the 9th postoperative week in the semi-rigid fixator group. Fibrous tissue Area: Fibrous tissue declines earlier in the rigid fixator group as endochondral ossification takes place. Cartilage Area: The presence of cartilage is not only greater but also prolonged in the semi-rigidly stabilised group.**

## 3.4 Discussion

Mechanical conditions are known to be important for the fracture healing process and previous studies have shown that initial mechanical conditions in particular, may determine the long-term outcome. In this study, the influence of fixation stability on callus formation at different stages of bone healing in sheep was investigated. Evidence is provided that not only the healing outcome is influenced by the initial fixation stability but also the course of healing. Contrary to the hypothesis, few differences in the tissue distribution were found during the initial phase of healing. However, there were differences in the progression from the inflammatory phase with remnants of the haematoma persisting longer in sheep treated with less stable fixation. Calluses formed under rigid conditions demonstrated superior mechanical properties and at the end of the observed healing period were further advanced through the remodelling process. Furthermore, a level of fixation stability was identified at which healing was observed to be less effective.

A semi-rigid fixator was used so as to provide decreased stability relative to a rigid fixator. Mechanical testing in vitro showed that the semi-rigid fixator had approximately half the bending stiffness of the rigid fixator. Measurement of the actual interfragmentary movement occurring in vivo revealed that the initial mechanical conditions differed in the amount of shear movement, whilst the axial movements were similar. Following the initial healing phase, differences in the mechanical conditions in vivo could no longer be distinguished.

At two weeks there were few differences that could be observed in the healing. The moment of inertia indicated a slightly higher amount of calcified tissue in the sheep treated with rigid fixation but this did not correlate with the callus area or the mineralised bone area. Similarly, no differences in mineralisation were determined at three weeks. However, at this point the callus morphologies began to differ between the rigid and semi-rigid group. During the later stages of healing, the callus of the tibiae treated with a more flexible fixation was larger with a higher proportion of fibrous tissue. After six weeks healing, the distinct callus morphologies were manifested in different mechanical competences. Higher callus stiffness with the standard fixation was determined despite a shrinking callus. However, the decreased callus size was due to a decrease in the fibrous and cartilaginous tissue components, whilst the amount of mineralised tissue peaked, confirmed by increases observed in

the moment of inertia. The tibiae treated with the more flexible fixation lagged behind in terms of callus strength and stiffness. Although the peak callus and fibrous tissue areas were similar for the two fixation stabilities, the author believes that the callus formed under less stable fixation may have been larger with a higher fibrous tissue and cartilage component. The similarity between the values measured at three weeks and at six weeks in the semi-rigid group suggests that the peak in callus size and fibrous tissue content was most likely reached in between these two time points. In both groups the mechanical competence of the callus increased between the sixth and nineth postoperative week, more so in the flexible fixation group, such that by nine weeks differences in the mechanical competence and the fibrous tissue content of the callus were no longer distinguishable. The size of the callus under standard fixation was smaller at six and nine weeks and no further increase in mineralised bone area was observed after six weeks indicating healing to be more advanced in the remodelling phase. These results show that the course of healing differed not only in callus morphology but also in the rate of callus development.

To the author's knowledge, this is the first study to analyse bone healing at multiple time points using radiological, in vitro and in vivo biomechanical methods, and histomorphometrical techniques in a large animal model. Although no differences in the shear stiffness of the fixators were found, it appears that the difference in the bending stiffness resulted in differences in the shear movement measured at the gap. Because of the highly non-linear nature of the fixator and because in vitro shear stiffness as well as the rotation stiffness may contribute to shear movements at the osteotomy gap in vivo, it is difficult to predict in vivo movements based on the in vitro fixator stiffness alone (Kristiansen et al., 1987). However, in vitro stiffness tests still provide an important means of determining differences before commencing animal experiments. Furthermore, mechanical testing of the healing tibiae performed at earlier intervals revealed differences in the mechanical competences between the two healing paths that no longer existed at nine weeks. This implies that it may be important to investigate earlier time points to discriminate subtle differences in healing.

Contrary to expectations, the different initial fixation stabilities were not manifested in histological differences within the first three weeks. The bone formation within the first three weeks appeared the same regardless of the fixation stability, which was

confirmed by quantitative histomorphometry. Bone formation within the first three weeks was determined to be predominantly by intramembranous ossification due to the absence of cartilage in the callus at two weeks. Although some cartilage was present in the callus at the ossification front by three weeks, the cartilage had not begun to mineralize. This suggests that intramembranous ossification, at least initially, may be independent of mechanical factors, which has not previously been demonstrated in a large animal model but is in accordance with previous findings in a small animal model (Mark et al., 2004a).

This is further supported by the observation that initial bone formation differed on the medial and lateral aspects of the tibia, but was the same for both fixation stabilities. In the sheep, the lateral aspect of the tibia has considerably more soft tissue coverage in comparison to the medial aspect (Nickel et al., 1992). Soft tissues are known to influence the biological potential for healing (McKibbin, 1978). Hence, the slightly larger bone formation on the lateral side is likely related to the higher biological potential of the surrounding tissues. In contrast, the endochondral ossification process did appear to be influenced by the fixation stability. Less stable fixation tended to produce greater amounts of cartilage which persisted longer before ossifying. It is not known whether it is the mechanical stability during the initial or the latter stages of healing that prolonged the chondral phase. Investigations of the molecular basis of fracture healing have revealed that mesenchymal cells commit to either a chondrogenic or an osteogenic lineage during the first few days of healing depending on the mechanical conditions (Thompson et al., 2002, Le et al., 2001). The differentiation of these cells may have lasting implications for the development of the callus. Measurement of the interfragmentary movements in sheep treated with similar external fixation devices to those used in the present study (Klein et al., 2003) found that movements differed only initially and by four weeks the movements had decreased and converged. Therefore it would appear that a delayed endochondral ossification may be related back to adverse initial mechanical conditions rather than the very small movements occurring after the fourth week (Klein et al., 2003).

In addition to examining the temporal distribution of the cartilage, the spatial distribution was also investigated. It was noted that the appearance of hyaline cartilage was always found to be on pre-existing surfaces of bone with endochondral ossification progressing from the existing bone surface. Mark and co-workers also

observed the appearance of chondrocyte like cells in contact with pre-existing periosteal woven bone and hypothesized a relationship between the intramembranously formed bone and the endochondral differentiation process (Mark et al., 2004a).

In the present study the main difference between stable and less stable fixation in the initial phase of healing was the increased time taken to remove remnants of the fracture haematoma in animals treated with less stable fixation. This observation is consistent with the previous finding that macrophages appear earlier and in greater numbers in fractures that are rigidly fixed (Hankemeier et al., 2001). Macrophages are believed to accelerate the transition from the inflammatory phase to the proliferative phase of healing and hence may be vital for timely callus formation.

Although the quantity of bone formed initially was not influenced by the mechanical conditions, the tissue structures did not appear to be randomly formed. After two weeks, fibrous tissue in the intercortical region showed an alignment in the transverse direction. This may suggest that fibrous tissue regeneration is from the very beginning under the guidance of the mechanical conditions. The transverse orientation of the fibres may be hypothesised to provide the greatest possible resistance to compression (by maximising the packing density of the fibres), whilst offering maximal resistance to transverse shear interfragmentary movements (stretching of the fibres). Axial compression and interfragmentary shear were determined to be the main movement components for both fixators, with similar amount of axial compression seen for both fixation stabilities.

Additionally, two distinct orientations of the woven bone were seen and were related to the proximity to the gap. Bone distanced from the gap had a longitudinal orientation and the bone adjacent to the gap was aligned in the radial direction. Whilst the growth distanced from the gap resembles an expansion of the cortex as seen during normal bone growth, the bone closer to the gap appeared to be influenced by the local mechanical environment at the fracture (Claes et al., 1998). Further, it was observed that more bone was deposited in regions located closer to the gap. However, as intramembranous bone formation was similar for both groups, mechanical stimulation appears not to be the dominant factor controlling bone growth; rather a higher concentration of growth factors or density of progenitor cells could be responsible for the greater bone growth in regions adjacent to the gap.

## 3.5 Conclusion

The osteotomy treated with less rigid fixation, which initially produced increased interfragmentary shear, was characterised by an increased amount of soft tissue and prolonged bone formation. Despite these differences, the healing observed in this group should still be described as successful, although, it appears that the path of healing taken was less optimal as a larger callus at nine weeks was required to produce the same final callus strength. At the time of the first measurement the callus produced under semi-rigid fixation was weaker, but seemed to have increased capacity such that by 9 weeks no difference in mechanical competence remained. This raises the question as to whether this increased potential can be harnessed for therapeutic treatment, such as application of growth factors to accelerate mineralisation during the latter stages of healing.

This study showed that the course of healing is influenced by the initial fixation stability and in particular by the increased interfragmentary shear. Decreased stability did not in this case result in delayed healing and the upper limit of stability required for successful healing remains unknown. However, it has been possible to identify an upper limit of stability by which healing is less optimal. In the presence of moderate axial movements (~ 0.5 mm) in a 3mm gap, it appears that shear interfragmentary movement below 0.8 mm would allow optimal healing. The movements determined in this study were smaller than those commonly found in the clinical situation (Gardner et al., 1996, Duda et al., 2003), suggesting fixation systems may be more flexible than is necessary. For smaller gap sizes, correspondingly smaller interfragmentary movements would be necessary to produce similar mechanical conditions in the gap.

Less stable fixation resulted in slower healing whereby the chondral phase was prolonged. In contrast intramembranous ossification appeared independent of the fixation stability. Although previous studies have shown that the initial mechanical conditions may determine the healing outcome, in the present study the chondral phase was identified as being sensitive to mechanics but not the initial bone formation. Therefore in future studies it will be important to determine up until what time this process is influenced mechanically, as this may have an impact for correcting and adjusting fixation. Furthermore, it raises the question as to whether and how the endochondral ossification process can be accelerated with an intervention once it is recognized that initial healing has been delayed.

# 4 Mechanical Conditions during Bone Healing

In this chapter, numerical methods are used to estimate the mechanical conditions in a healing callus. Specifically, the influence of various modes of interfragmentary movement and the development of hard callus on the mechanical conditions is examined. In the first part, a biphasic model is used to examine the influence of axial compression, translational shear and axial torsional movements on the local biophysical stimuli in the early callus. In addition, the initial tissue differentiation as predicted by a number of mechano-biological theories is examined. In the second part of the analyses, the influence of hard callus development on the local mechanical conditions produced by axial and shear movements is examined and movements measured in vivo are applied in order to make comparisons with histological observations.

## 4.1 Introduction

Fixation stability has been widely reported to influence the healing of fractures and by optimising the mechanical conditions it is believed that healing may be enhanced (Einhorn, 1995, Chao et al., 1998). Bone healing in the presence of interfragmentary movements occurs with the formation of a bony callus (Willenegger et al., 1971). Callus formation follows an inflammatory response which leads to pooling and rapid proliferation of pluripotent tissue (McKibbin, 1978, Bostrom, 1998). The proliferation and differentiation of pluripotent tissue is believed to be influenced by the local mechanical environment (Pauwels, 1980). Differentiation of mesenchymal cells towards an osteogenic lineage rather than a chondrogenic lineage has been observed in fractures treated with stable fixation (Le et al., 2001, Thompson et al., 2002). New bone, required to stabilise and reunite the fragments, is subsequently formed directly by intramembranous ossification and by way of a cartilage intermediate during endochondral ossification (Cruess and Dumont, 1975, Brighton, 1984, Frost, 1989, Owen, 1970).

Interfragmentary movements (IFM) are a reflection of the fixation stability at the fracture site. In vivo monitoring of mechanical stability over the course of healing in experimental models has shown that interfragmentary movement peaks approximately one week postoperatively and remain high over the first three to four weeks (Klein et al., 2003, Klein et al., 2004, Schell et al., 2005). Thereafter, the movements decrease as the stiffness of the callus tissue increases. The initial movements were found to be composed of significant axial and shear components (Schell et al., 2005). A finding that has been confirmed by measurements in the clinical situation (Gardner et al., 1997, Duda et al., 2002). The magnitude of shear IFM at the fracture gap has been reported to exceed that occurring in the axial direction (Duda et al., 2003) and an examination of osteotomies treated with unreamed nails found the initial IFMs to consist of a significant axial rotational component (Klein et al., 2004). Axial IFMs in the range of 0.2 – 1.0 mm in gap sizes of 3 mm are believed to promote optimal healing in transverse osteotomies (Claes et al., 1998). The influence of shear IFMs on fracture healing remains a subject of controversy. Traditionally shear movements have been considered detrimental to the healing (Yamagishi and Yoshimura, 1955), but recent experimental evidence has been contradictory (Park et al., 1998, Augat et al., 2003, Klein et al., 2003).

Whilst the magnitude of interfragmentary movement remains relatively constant over the first few weeks of healing, the morphology of the callus undergoes considerable change. By two weeks, the first signs of woven bone are visible and at three weeks the periosteal hard callus has increased in size, such that it begins to bridge the gap (Epari et al., 2005). It is thought that mechanical conditions in the callus may become critical at this time.

Recent studies of bone healing, in both small and large animals models, have found early bone formation by intramembranous ossification to be independent of the fixation stability (Mark et al., 2004a, Epari et al., 2005). At three weeks, corresponding to the onset of endochondral ossification in sheep, no differences were seen in the fibrous tissue, cartilage or mineral content of the callus. However, slower healing was observed under less stable fixation and was attributed to a prolonged chondral phase (Epari et al., 2005).

To explain the influence of mechanics on skeletal tissue differentiation Pauwels studied in vivo the differentiation patterns in normal and experimental conditions (Pauwels, 1980). Two strain invariants, octahedral shear (deviatoric) strain and volumetric (hydrostatic) strain, were identified as being important for mechanical signalling. Pauwels concluded that hydrostatic compression is a specific stimulus for cartilage formation and distortional strain stimulates the development of fibrous tissues. No specific stimulus was found for the formation of bone. In contrast, Perren proposed the "Interfragmentary Strain Theory" which states that the fracture gap can only be filled with a tissue capable of sustaining the interfragmentary strain without rupturing (Perren and Cordey, 1980). The ideas of Pauwels have been further developed and applied to fracture healing in subsequent mechanobiological theories (Carter et al., 1998, Claes and Heigele, 1999). As biological tissues consist of a significant fluid component, a contrasting theory has been developed whereby the biophysical stimuli for tissue differentiation is made up of shear strain in the solid and the fluid flow in the interstitial phase (Prendergast et al., 1997). This approach has been used to simulate tissue differentiation during fracture healing (Lacroix et al., 2002).

The mechanical environment of the callus produced by axial and bending loads has been previously investigated (DiGioia et al., 1986, Cheal et al., 1991, Carter et al., 1998) However, the influence of shear and torsional interfragmentary movements on

the mechanical conditions in bone healing has not been investigated. Previous animal experiments have shown that bone healing is sensitive to the initial mechanical conditions (Le et al., 2001, Thompson et al., 2002, Klein et al., 2003). Furthermore, high levels of interfragmentary shear during the initial phase of healing did not appear to be detrimental to healing (Klein et al., 2003). This finding seems to contradict earlier studies and raises the question as to what degree interfragmentary shear influences the mechanical conditions with the early callus tissue.

The purpose of this study was firstly to determine how the initial mechanical conditions produced by shear and torsional interfragmentary movements differ from those produced by axial compressive movements. For this purpose, the finite element method was used to estimate mechanical parameters in an early callus model and mechanobiological theories were used to determine the theoretical differentiation of initial pluripotent tissue under different modes of interfragmentary movement.

Secondly, in an attempt to better understand and optimise the mechanical conditions for healing; this study aims to (1) determine the local hydrostatic stresses and tensile strains in the callus and how they change with hard callus maturation; and (2) correlate the patterns of hydrostatic stress and tensile strain with sites of ossification observed in the histological analyses of Chapter 1.

## 4.2 Methods

### 4.2.1 Influence of Interfragmentary Movement

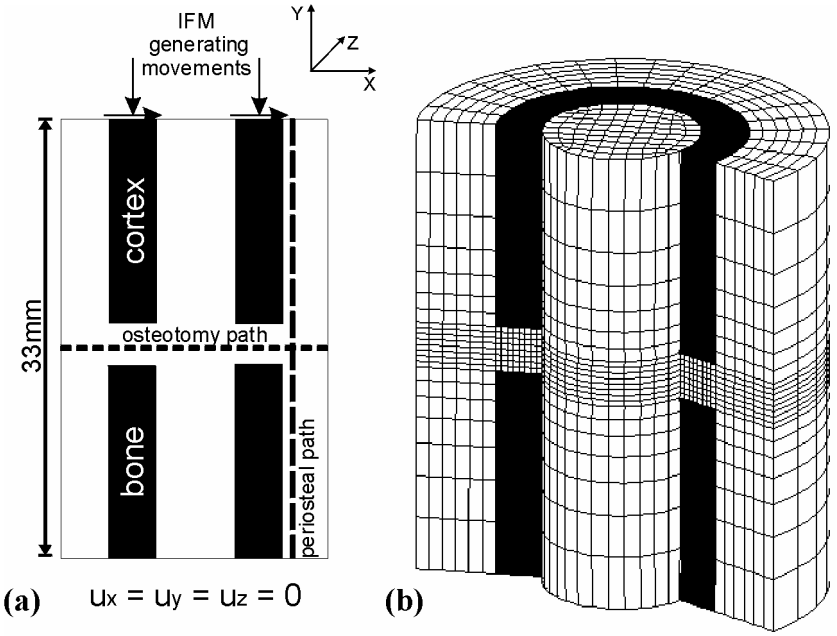


**Figure 4-1 Model schematic showing boundary conditions and the location of node paths are indicated. (b) Section through the FE model showing the mesh. Black regions represent cortical bone, while the remaining elements have been modelled as granulation tissue (white).**

A 3D poro-elastic finite element (FE) model of an experimental fracture was developed and analysed using ABAQUS (ABAQUS v6.3, Hibbit Karlsson & Sorensen, Inc, RI, USA). The geometry of the model was based on histology an osteotomy defect (gap size of 3 mm) in an ovine tibia (Schell et al., 2005). It was assumed that the interfragmentary space (including the endosteal and periosteal spaces) was entirely composed of granulation tissue to represent the initial phase of healing (approx. 7 days post trauma). The cortical bone had an inner and outer diameter of 10 mm and 16 mm respectively. The external diameter of the periosteal space was 26 mm. The cortical bone and granulation tissue were modelled as biphasic poro-elastic mixtures of collagenous and interstitial fluid constituents (Mow et al., 1980). The finite element calculations were performed using ABAQUS's soils consolidation analysis code, which has been demonstrated to adequately simulate the poroelastic properties of biological tissues. Material properties were taken from published sources (Table 4-1).

| | Granulation tissue | Cortical bone |
|---|---|---|
| Young's modulus (MPa) | 0.2[d] | 20000[a] |
| Permeability ($m^4$/Ns) | 1.00E-14[d] | 2.2E-19[e] |
| Poisson's ratio | 0.167[d] | 0.3 |
| Solid compression modulus (MPa) | 2300 | 13920[b] |
| Fluid compression modulus (MPa) | 2300 | 2300 |
| Porosity | 0.8[d] | 0.04[c] |

[a](Claes and Heigele, 1999),[b](Cowin, 1999),[c](Schaffler and Burr, 1988),[d](Lacroix et al., 2002), [e](Smit et al., 2002)

**Table 4-1 Material properties used in the FE analysis.**

Interfragmentary movements, ramped over 0.5 s, were applied as displacements to the nodes of the upper surface of the upper cortical fragment (Figure 4-1). A 0.5 mm axial compression movement, a 1.5 mm transverse shear movement and a $10^o$ axial rotation movement (corresponding to 1.4 mm movement at the periosteal surface of the cortex and 2.3 mm movement at external border of granulation tissue) were simulated in three independent load cases (Table 4-2). The applied movements were derived from IFMs measured experimentally in vivo (Duda et al., 2003, Klein et al., 2003, Klein et al., 2004). Since different movement modes occur simultaneously during gait, the interaction between axial compression and transverse shear was analysed in a fourth load case (axial 0.5 mm, shear 1.0 mm). Nodes on the lower surface of the lower cortical fragment were constrained in all directions. The tissues on the external boundary were modelled as impermeable to fluid flow, while fluid flow was allowed to occur across the upper and lower borders of the model to imitate the continuity of the tibia. The influence of allowing fluid to flow across the periosteal boundary was investigated in preliminary calculations and found to have a negligible effect on the magnitude of fluid flow and strain invariants in the callus.

| | Load cases | Experimental IFMs |
|---|---|---|
| axial (mm) | 0.5 | 0.5 – 1[a] |
| shear (mm) | 1.5 | 1 – 2[a,c] |
| torsion ($^o$) | 10 | 2 – 10[a,b] |
| axial & shear (mm) | 0.5 & 1.0 | 0.6 & 1, 1 & 2[a] |

**Table 4-2 Load cases determined from in vivo measurements and their corresponding interfragmentary movements, as applied to the FE model ([a]Klein et al., 2003; [b]Klein et al., 2004; [c]Duda et al., 2003).**

Convergence of the FE model was tested by doubling the number of elements in the mesh. The summed square of differences between strain path plots obtained from the two models was determined to be less than 5%. The maximum difference was 12%

and occurred at the midway point of the osteotomy path in endosteal region where comparatively small strains were calculated under axial loading conditions. The less refined FE mesh was used and consisted of 11968 twenty-noded brick elements (Figure 4-1).

The mechanical conditions resulting from the different modes of interfragmentary movement were characterised in terms of the components and invariants of the strain tensor, along with the pore pressure and fluid velocity. Path plots (showing the magnitude of a parameter along a specific node path of the FE model) of the mechanical stimuli; strain, pore pressure and fluid velocity, were produced across the osteotomy gap while path plots of strain were determined in the periosteal space parallel to the cortex (Figure 4-1). Contour plots were produced to show the initial stimulus for tissue formation according to three different mechanobiological theories of fracture healing (Perren and Cordey, 1980, Claes and Heigele, 1999, Lacroix et al., 2002). Where more than one stimulus was involved (Claes and Heigele, 1999, Lacroix et al., 2002) the contour plots from the individual stimuli were combined. These three theories were chosen because of distinct differences in the mechanical stimuli used. Furthermore, these theories were readily testable since values for the formation of the various tissues were previously defined (Figure 2-8, Figure 2-10 and Figure 2-11).

### 4.2.2 Influence of Hard Callus Maturation

To estimate the mechanical conditions in the regenerating tissue of the healing callus the finite element (FE) method was used. Finite element models, to represent an initial healing callus and at two and three weeks postoperative, were developed and analysed using ABAQUS (ABAQUS v6.5, Hibbit Karlsson & Sorensen, Inc, RI, USA). The geometry of the model was based on histology of an osteotomy defect (gap size of 3 mm) in an ovine tibia. The experimental model has been extensively described both biomechanically and histologically (Schell et al., 2005, Epari et al., 2005). The inner and outer diameter of the cortical bone was determined to be 12 mm and 16 mm respectively. The external diameter of the periosteal space in all models was 32 mm.

- **Initial Model**

A three-dimensional finite element model of the initial osteotomy situation was created using 59,681 quadratic tetrahedral elements and 1,792 quadratic hexahedral elements (Figure 4-2). The callus was modelled initially as being entirely composed of multipotent mesenchymal (granulation) tissue, which was assumed to be homogeneous, isotropic and nearly incompressible, and was modelled as a linear elastic material with an elastic modulus (E) of 0.05 MPa (Perren and Cordey, 1980) and Poisson's ratio (ν) of 0.49 (Carter et al., 1998). Cortical bone was assumed to be homogeneous and isotropic and was also modelled as a linear elastic material with E = 14,250 MPa and ν = 0.39 (Loboa et al., 2005).

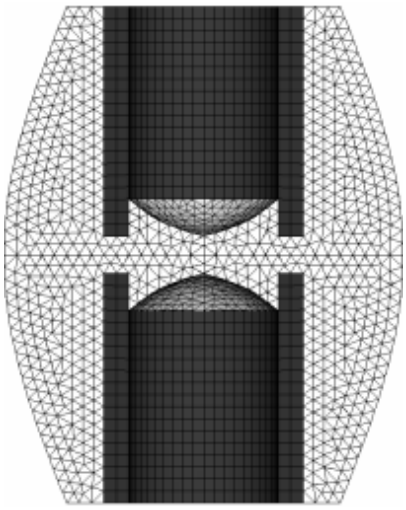

**Figure 4-2 shows the mesh of the initial healing model. Cortical bone is shaded in black and the surrounding granulation tissue is white.**

- **Two Week Model**

A three-dimensional finite element model of the 2-week osteotomy situation was created using 131,769 quadratic tetrahedral elements and 3,344 quadratic hexahedral elements (Figure 4-3). The callus structure was based on histology descriptions at two weeks (Epari et al., 2005). Material properties were the same as in the initial model, with the exception that bone comprising the periosteal hard callus at two weeks was modelled as linear elastic with E = 1250 MPa and a Poisson's ratio of 0.49 (Loboa et al., 2005).

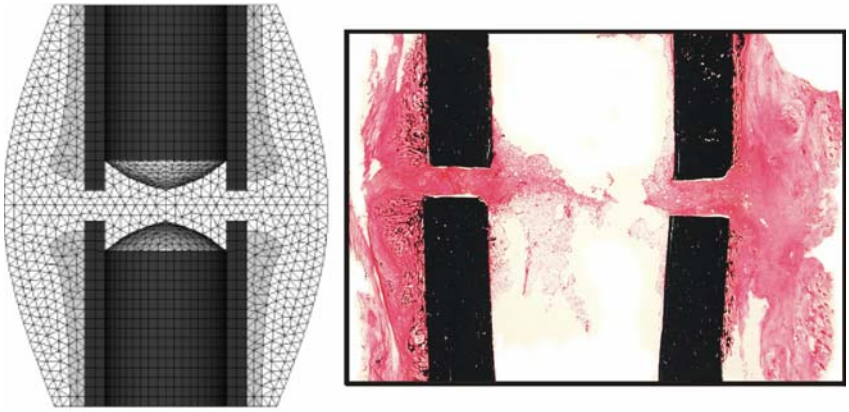

**Figure 4-3 shows the mesh of the two week healing model and histology from a corresponding time point (Safranin Orange /von Kossa stain, Chapter 4). Cortical bone is shaded in black, periosteal woven bone is grey and the surrounding granulation tissue is white.**

- **Three Week Model**

A three-dimensional finite element model of the 3-week osteotomy situation was created using 84,264 quadratic tetrahedral elements and 2,464 quadratic hexahedral elements (Figure 4-4). The callus structure was based on histology descriptions at three weeks (Epari et al., 2005). Material properties were the same as in the initial model, with the exception that bone comprising the periosteal hard callus at three weeks was modelled as linear elastic with E = 1250 MPa and a Poisson's ratio of 0.49 (Loboa et al., 2005).

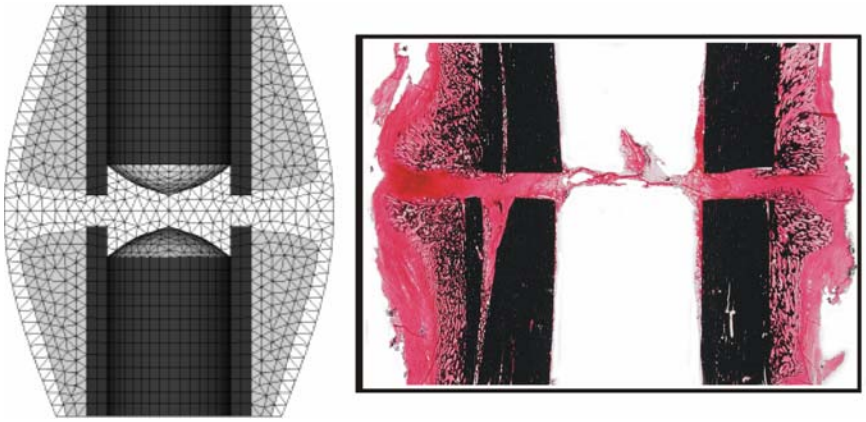

**Figure 4-4 shows the mesh of the three week healing model and corresponding histology at three weeks (Safranin Orange /von Kossa stain, Chapter 4). Cortical bone is shaded in black, periosteal woven bone is grey and the surrounding granulation tissue is white.**

- **Analysis**

Interfragmentary movements, ramped over 0.5 s, were applied as displacements to the nodes of the upper surface of the upper cortical fragment. Nodes on the lower surface of the lower cortical fragment were constrained in all directions to prevent rigid body motion. To investigate the influence of the different components of interfragmentary movement, a 0.5 mm axial compressive movement and a 1.5 mm transverse shear movement were simulated in two independent load cases. For comparison with healing from an experimental model (Schell et al., 2005, Epari et al., 2005), in vivo measured movements were applied to determine the influence of stability (rigid vs. semi-rigid) on the mechanical conditions (Table 4-3). Hydrostatic stresses and tensile strains within the mesenchymal tissue of the distraction gap were calculated using a linear solver.

| Time (days) | Axial compression (mm) | | Interfragmentary shear (mm) | |
|---|---|---|---|---|
| | rigid | semi-rigid | rigid | semi-rigid |
| 3 | 0.36 | 0.50 | 0.53 | 0.84 |
| 14 | 0.51 | 0.69 | 0.63 | 0.85 |
| 21 | 0.40 | 0.65 | 0.62 | 0.90 |

**Table 4-3 Interfragmentary movements measured in vivo over first three weeks of healing in animals treated with rigid and semi-rigid fixation (Schell et al., 2005).**

## 4.3 Results

### 4.3.1 Influence of Interfragmentary Movement

- **Strain**

In the osteotomy gap region, the strains from axial IFMs were characterised by two dominant normal strain components, $\varepsilon_{xx}$ (max. 22%) and $\varepsilon_{yy}$ (max. -28%), having similar magnitudes but opposite profiles (Figure 4-5a). In contrast, shear and torsional movements resulted in relatively large shear strain components, $\varepsilon_{xy}$ (max. 0.42%) and $\varepsilon_{yz}$ (max. ±37%) respectively (Figure 4-5c, Figure 4-5e). The maximum and minimum principal strains from shear (max. 22%, -21%) and torsional (max. 19%, -19%) IFMs were symmetric in nature and of a similar order of magnitude to those produced by axial IFMs (max. 22%, max. -28%) (Figure 4-5b, Figure 4-5d, Figure 4-5f). Shear IFM differed from axial and torsional IFMs in that the strains remained high in the endosteal gap region (Figure 4-5d). In the periosteal region axial IFMs produced, in addition to normal strains (max. 18%), large shear strains (max. 34%) (Figure 4-6a). The peak principal strains in the periosteal region for all modes of IFM were produced at the level of the bone ends (Figure 4-6b, Figure 4-6d, Figure 4-6f). The strains diminished relatively quickly with distance from the gap, except under torsional movements which showed the slowest rate of decrease with distance from the gap (Figure 4-6f). The deviatoric strain was similar to the maximum principal strain for all modes of IFM (Figure 4-5 to Figure 4-7).

The combined load-case produced normal strains in the osteotomy gap region that were of a similar magnitude to those produced from axial movement alone (Figure 4-7a). The profile of the shear strain component was changed however, such that it no longer peaked between the bone fragments. The resulting principal strains (max. 26%) were similar to those from axial movements alone (max. 23%) with the exception that strain was increased in the endosteal gap region (14% compared to 8% with axial IFM alone) (Figure 4-7b).

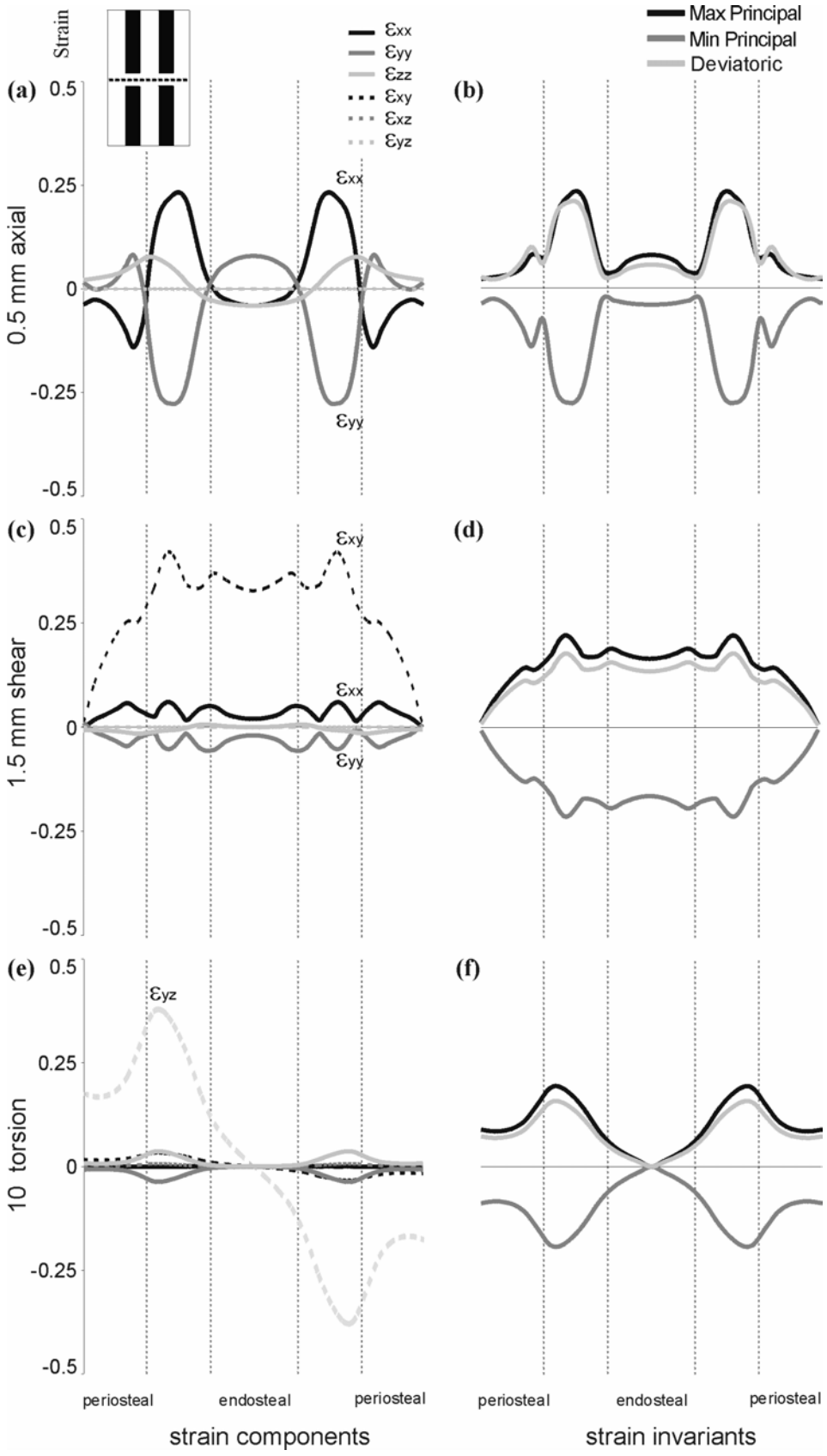


**Figure 4-5 Path plots of strain components (left) and strain invariants (right) in the osteotomy gap for a 0.5 mm axial (top), a 1.5 mm shear (middle), and a 10° torsional (bottom) interfragmentary movement.**

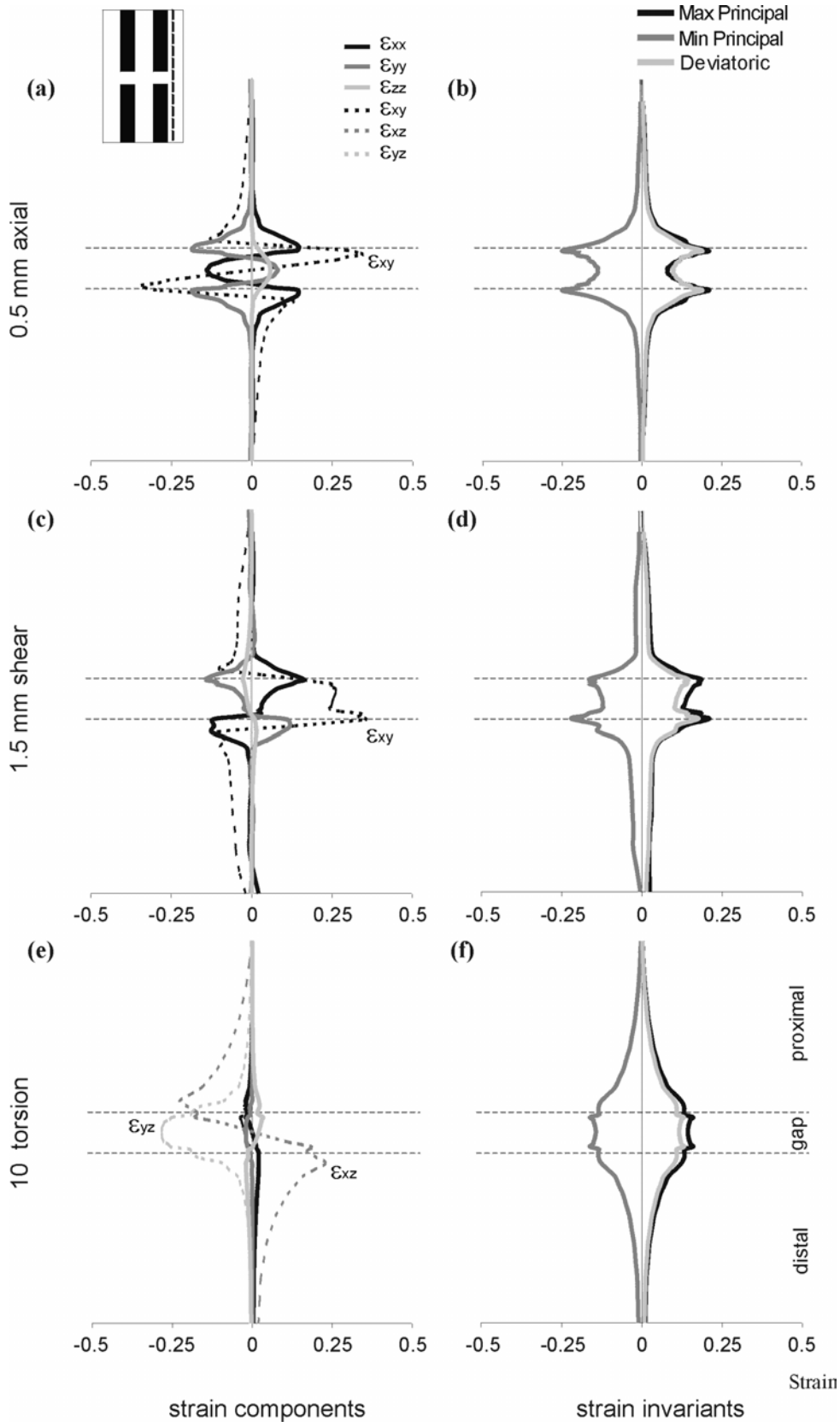


**Figure 4-6 Path plots of strain components (left) and strain invariants (right) in the periosteal region for a 0.5 mm axial (top), a 1.5 mm shear (middle), and a $10^{o}$ torsional (bottom) interfragmentary movement.**

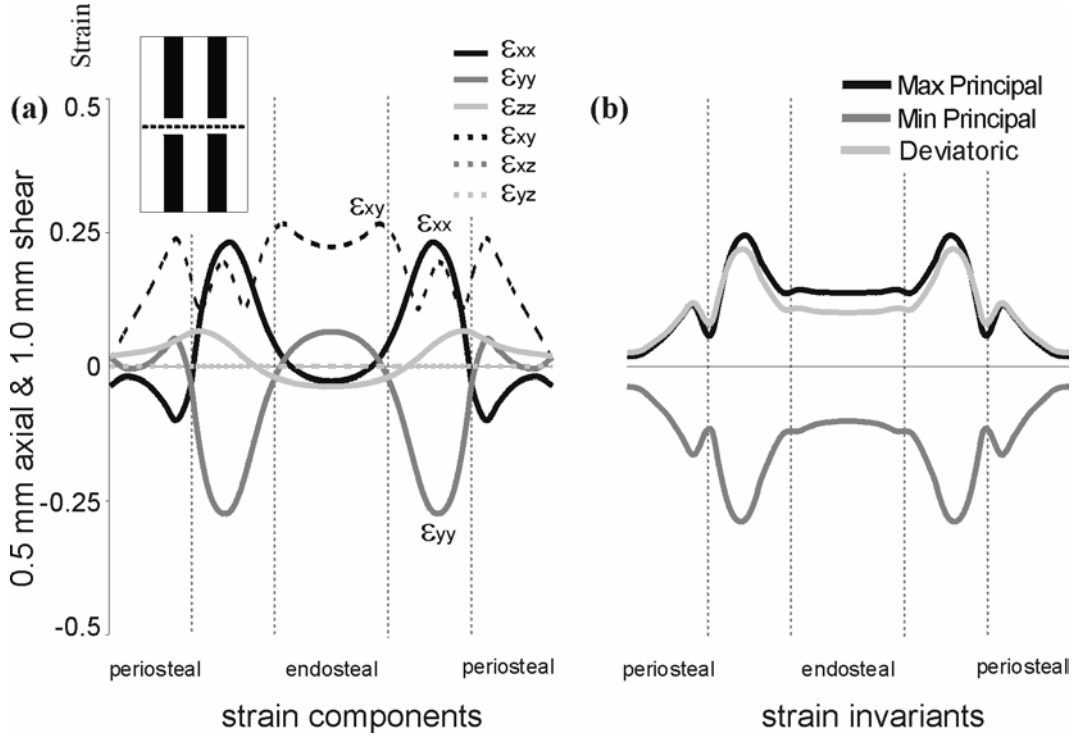


**Figure 4-7 Path plots of strain components (a) and strain invariants (b) in the osteotomy gap for a combined axial (0.5 mm) and shear (1.0 mm) interfragmentary movement.**

- **Pore Pressure and Fluid Flow**

Axial IFMs generated a maximum gap pore pressure of 0.18 MPa. The peak fluid flow (0.54 $\mu ms^{-1}$) occurred between the bone fragments (Figure 4-8). In contrast, shear and torsional IFMs produced relatively small pore pressures and fluid flows (0.015 MPa, 0.13 $\mu ms^{-1}$ and 0.002 MPa, 0.001 $\mu ms^{-1}$ respectively).

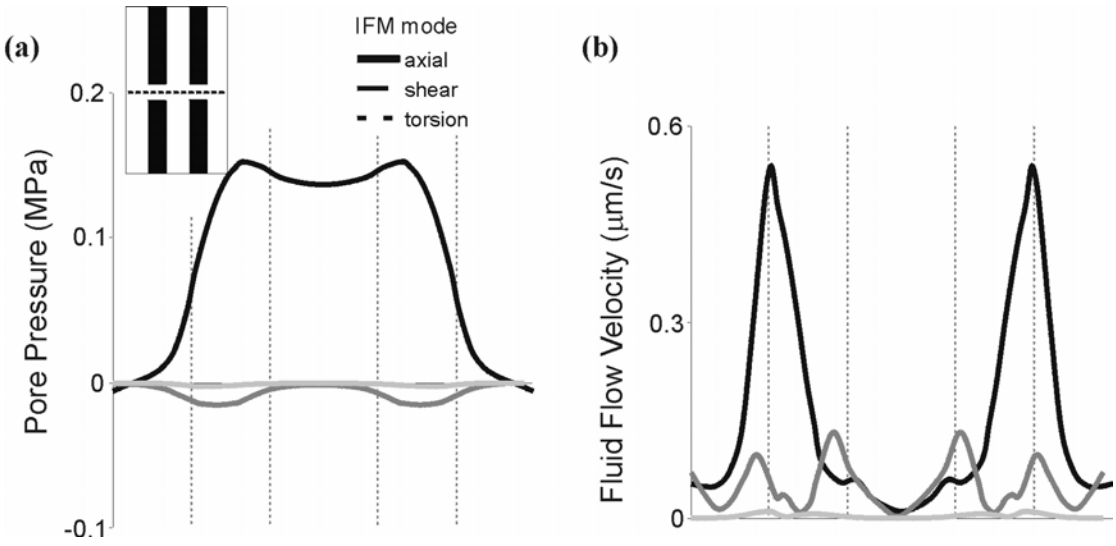


**Figure 4-8 Path plots of pore pressure (a) and fluid flow (b) in the osteotomy gap for axial, shear and torsional interfragmentary movements.**

- **Initial Tissue Differentiation**

The areas in which bone is expected to form when subjected to axial IFMs according to Perren were limited to periosteal regions distanced from the gap and small regions in the marrow cavity (Figure 4-9, Col. 1). Under shear and torsional IFMs, the regions where bone is expected to form were smaller on the periosteal side, while in the marrow cavity, excluding the endosteal gap, bone formation areas were larger. All movement modes produced strains between the bone fragments tolerable only by fibrous tissues. In the case of shear IFM, the area where fibrous tissue is expected to form extended across the entire endosteal fracture gap. On the periosteal side, the regions where cartilage may form were noticeably larger with shear and torsional IFMs.

The biophysical stimuli used by Claes (Claes and Heigele, 1999) and Lacroix (Lacroix et al., 2002) determined areas of expected tissue formation (Figure 4-9, Col. 4 & 7, respectively) qualitatively similar to the application of Perren's IFS theory (Perren and Cordey, 1980), although, the areas where fibrous tissue and cartilage were expected to form were considerably smaller. Only under axial IFMs did the inclusion of hydrostatic pressure change the pattern of biophysical stimuli, adding areas of fibrous tissue formation periosteally and cartilage formation along the endosteal gap (Figure 4-9, Col. 2). The fluid flow stimulus did not modify the regions where bone, cartilage and fibrous tissue formation were expected in the early phase as determined by the deformation stimulus (Figure 4-9, Col. 5).

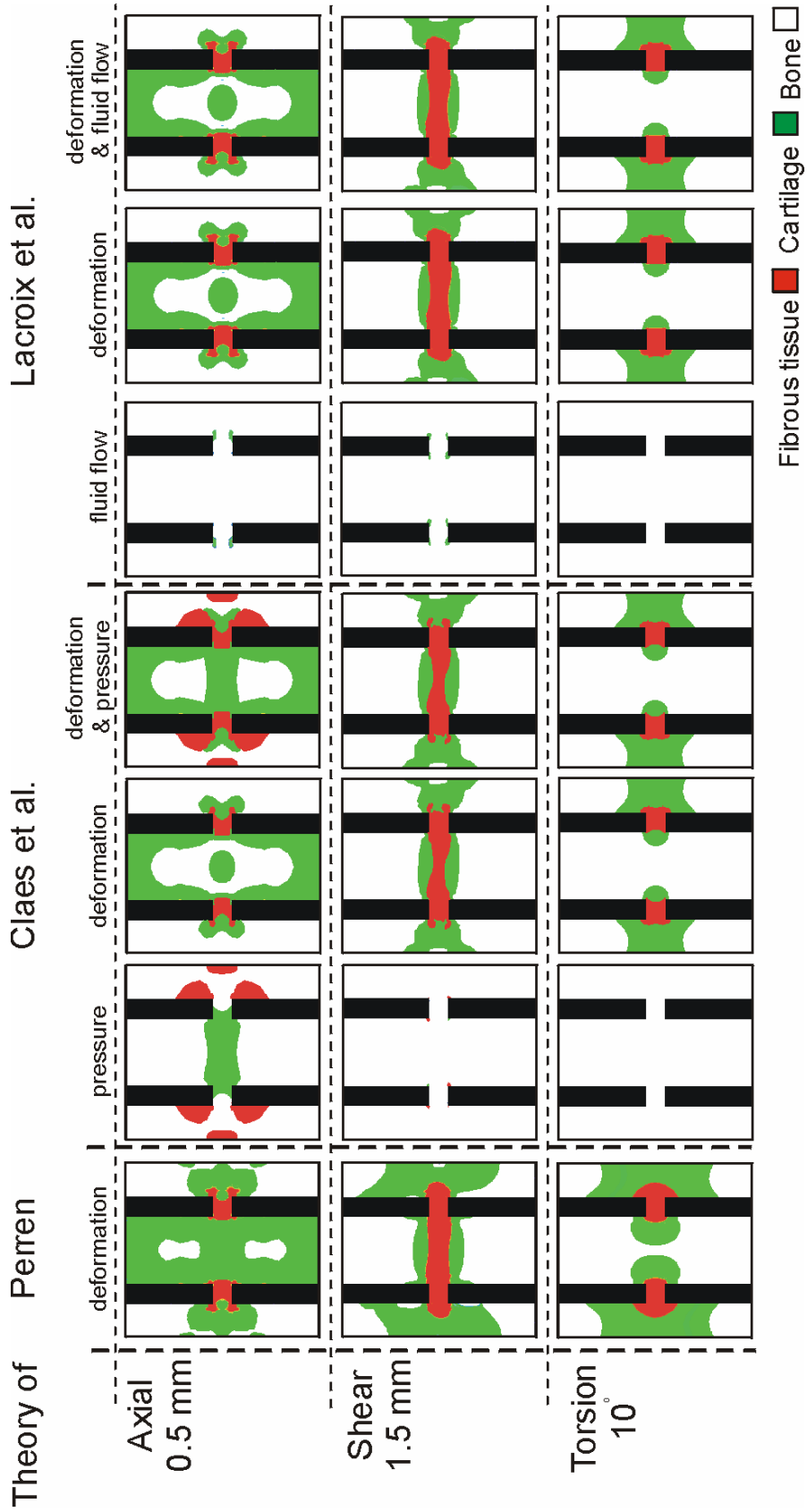


**Figure 4-9 Tissue formation according to three principally different mechanobiological theories of fracture healing (Claes and Heigele, 1999, Lacroix et al., 2002, Perren and Cordey, 1980) in the early callus subjected to axial, shear and torsional interfragmentary movements.**

### 4.3.2 Influence of Hard Callus Maturation

- **Mechanical Conditions Initially**

During the initial phase of healing, the largest strains (Axial: 30%, Shear: ≈ 25%) were located directly in the gap between the cortices (Figure 4-10). In the endosteal region moderate strains were determined. Compared to axial compression, the strains produced by interfragmentary shear were slightly higher endosteally (Axial: ≈ 10%, Shear: 10 - 20%) and at the level of the gap were more widespread in the periosteal region. Along the periosteal surface of the cortex, similarly low magnitudes of strain and negligible hydrostatic pressure were determined for both movement modes (Figure 4-11).

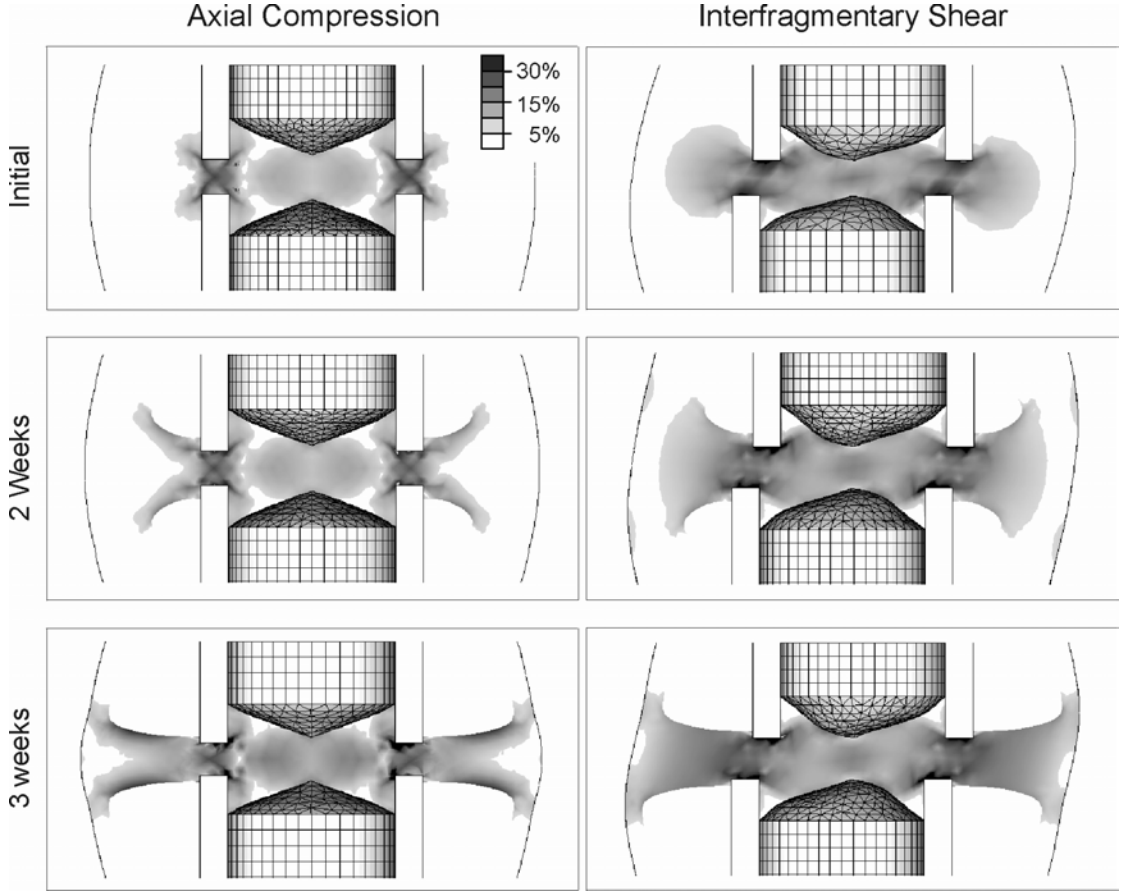


**Figure 4-10 shows the tensile strains initially and two and at three weeks produced by (left) axial and (right) shear interfragmentary movements.**

- **Mechanical Conditions at Two Weeks**

At two weeks, the gap region directly between the cortices remained the location of the largest strains (Axial and Shear: ≈ 25%, Figure 4-10). Along, the surface of the expanding periosteal hard callus moderate to high strains were determined (10 –

15%). Slightly larger strains and pressures were determined as a result of compressive movements (Figure 4-11).

- **Mechanical Conditions at Three Weeks**

The gap region directly between the cortices continued at three weeks to be subjected to the largest strains (Axial: ≈ 30%, Shear: 20-25%). The periosteal (< 10%) and endosteal (< 15%) regions at the level of the gap experienced more moderate strains (Figure 4-10).

At three weeks, the surface of the hard callus, which is beginning to bridge the gap, is subjected to increasing larger strains (Axial: 15 - 25%). The largest strains in this region were located on the most periosteal region (30%). Shear movements produced more uniform but lower strains (18%) along the surface of the hard callus (Figure 4-11). Compressive hydrostatic pressure on the surface of the hard callus also became more pronounced in axially loaded models, the largest pressure was determined on the inner or central region of the hard callus.

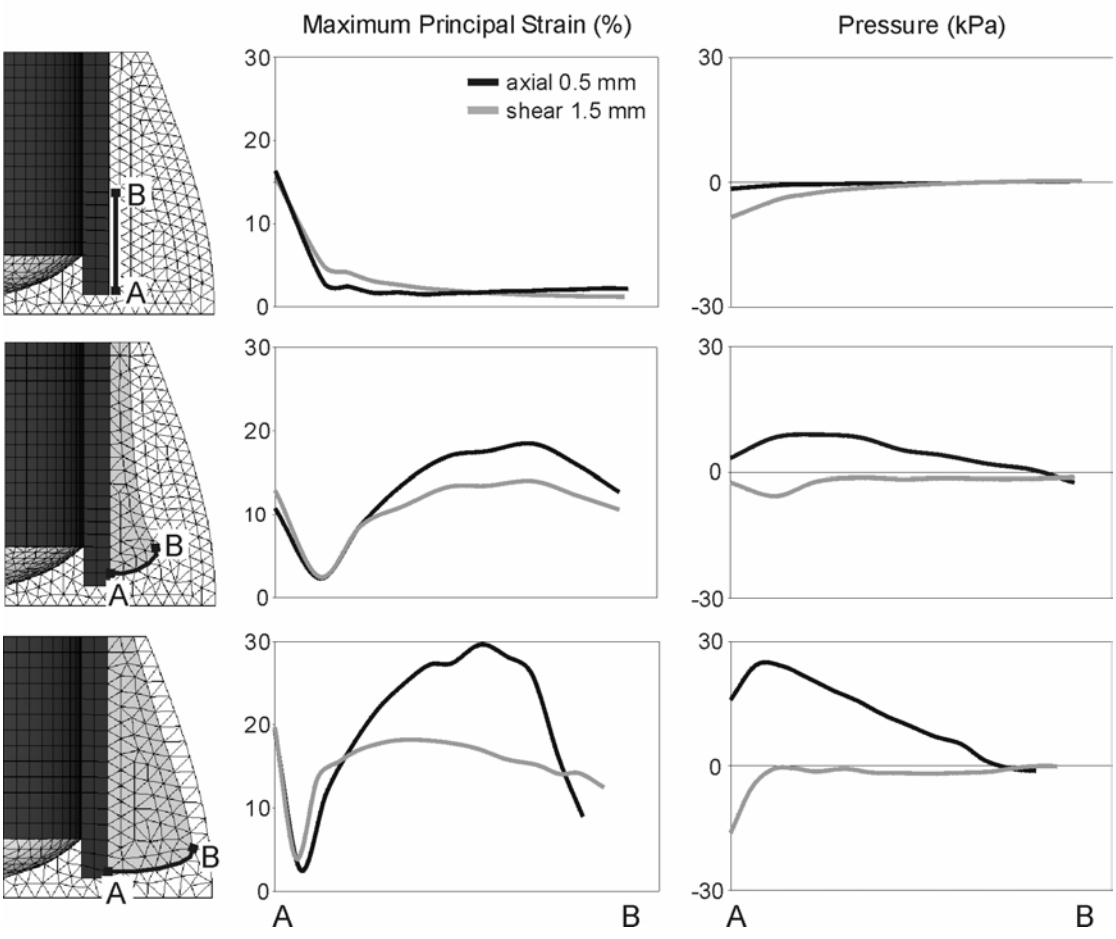


**Figure 4-11 shows the strain and pressure along the ossification front initially and at two and three weeks.**

### 4.3.3 Analysis of In Vivo Experimental Conditions

- **Mechanical Conditions Initially**

Despite interfragmentary movements of almost double the size, the mechanical conditions in the semi-rigid group were initially similar to the rigid group (Figure 4-12). The largest difference was seen directly in the gap (Rigid: ≈ 15% v Semi-rigid: ≈ 25%). However, in the periosteal regions both fixation stabilities resulted in similarly moderate strains and pressures (Figure 4-13).

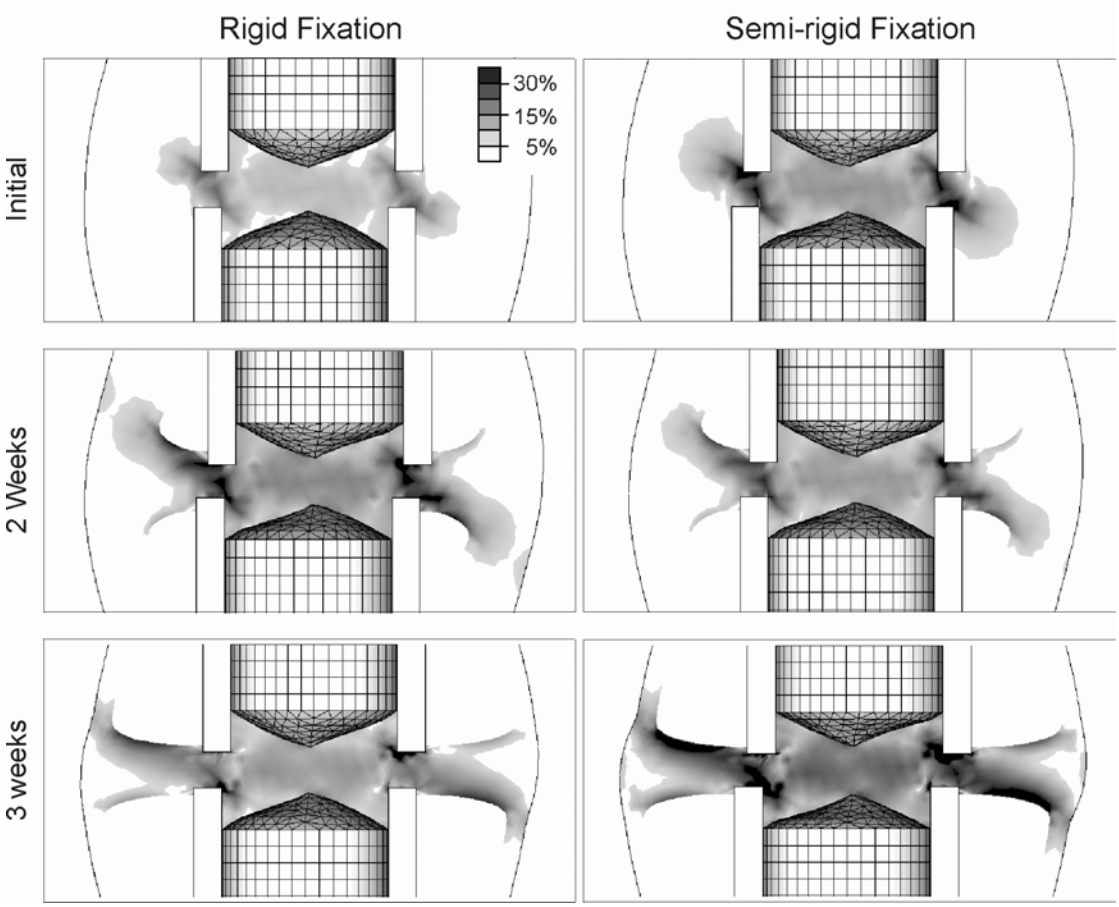


**Figure 4-12 shows the tensile strains initially and two at three weeks produced by (left) rigid and (right) semi-rigid external fixation.**

- **Mechanical Conditions at Two Weeks**

At two weeks (Figure 4-12), the largest maximum principal strains continued to be present in the gap region between the cortices (rigid: 20 % v semi-rigid: 25 %). The maximum principal strains on the surface of the periosteal hard callus became increasingly larger. However, there was still relatively little difference in the strains and pressures along the ossification front (line A-B, Figure 4-13).

- **Mechanical Conditions after Three Weeks**

After three weeks the differences in the mechanical conditions between the two groups had become increasingly distinct. In the rigid group moderate to high strains were present on the surface of the hard callus (≈ 30%). However, in the semi-rigid group the straining (≈ 45%) was considerably larger (Figure 4-12 & Figure 4-13).

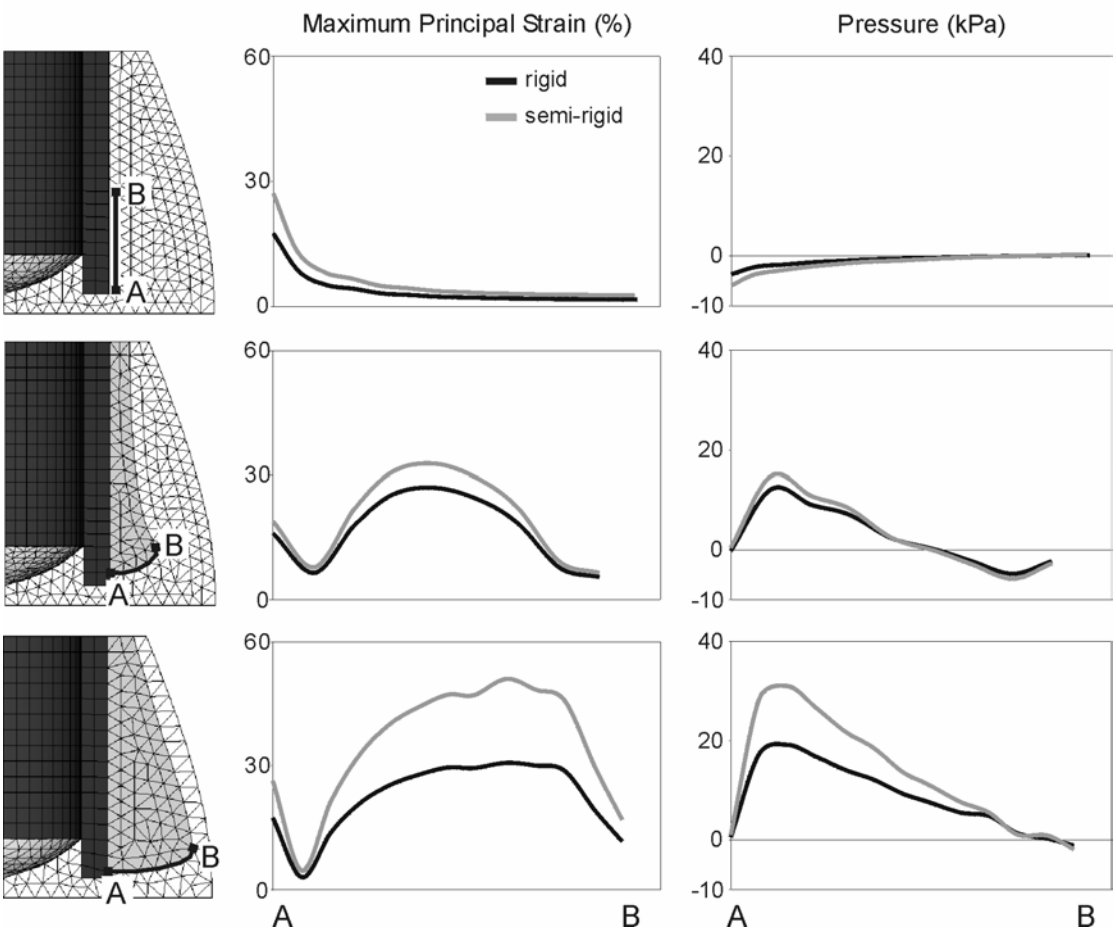


**Figure 4-13 shows the strain and pressure along the ossification front at two and three weeks.**

## 4.4 Discussion

### 4.4.1 Influence of Interfragmentary Movements

Shear interfragmentary movements are thought to be detrimental to healing (Augat et al., 2003), but the mechanical conditions that these movements produce, both alone and in combination with axial movements, have not been evaluated. Previous investigations of healing have shown that the initial phase is important for the healing outcome (Thompson et al., 2002) and that large shear movements during this phase do not appear to be detrimental to healing (Klein et al., 2003). The purpose of this study was to determine how the initial mechanical conditions produced by shear and torsional interfragmentary movements differ from those produced by axial compressive movements. The finite-element model demonstrated that shear and torsional interfragmentary movements on the upper boundary of those observed in vivo (Duda et al., 2002, Klein et al., 2003) produced deviatoric strains comparable to those generated by moderate axial interfragmentary movements that are believed to provide an optimal mechanical environment for healing (Claes et al., 1998). Further, large shear and torsional interfragmentary movements produced significantly less fluid flow and hydrostatic pressure than moderate axial interfragmentary movements. Additionally, when axial and shear movements were applied simultaneously as occurs in vivo (Gardner et al., 1997, Duda et al., 2002), an overall increase in strain was not observed, and with the exception of the endosteal region the strain magnitudes were similar to those produced by axial interfragmentary movements alone.

Regions of compressive hydrostatic pressure have been correlated with the formation of cartilage tissue (Pauwels, 1980) and a less stable fixation has been seen to favour differentiation of mesenchymal cells towards a chondrogenic lineage resulting ultimately in a larger callus and a greater cartilage component in the callus (Thompson et al., 2002). Shear and torsional IFMs were not found to produce volumetric changes, i.e. compressive hydrostatic pressures, which would direct the differentiation of mesenchymal cells towards a chondrogenic path. Therefore increased callus size and an increased component of cartilage in the callus would not appear to be necessarily related to the presence of shear or torsional interfragmentary movements but rather to the level of axial fixation stability.

To explain the delayed healing seen in osteotomies subjected to interfragmentary shear, a mechanism has been suggested by which tensile and shear strains associated

with these movements damage blood vessels and disrupt angiogenesis (Augat et al., 2003). It is known that the blood supply is crucial to the rapidly proliferating tissue in the callus, particularly in the periosteal regions which has been shown to be the main supply during the early stages of healing (Rhinelander, 1968). However, few studies have investigated the influence of mechanical stability on the blood supply during bone healing and they have only considered the influence of axial IFMs (Wallace et al., 1994, Claes et al., 2002). In this study, axial compressive IFMs within an optimal range for healing were also found to produce similarly large tensile and shear strains in the periosteal regions to significantly larger interfragmentary shear movements. Therefore, it seems that in vivo magnitudes of interfragmentary shear are no more likely than axial IFMs to be responsible for disrupting initial healing processes by disrupting blood vessels.

To describe the relationship between mechanics and skeletal regeneration during bone healing, a number of mechanobiological theories based on concepts of deformation, pressure and deformation, and fluid flow and deformation as biophysical stimuli have been proposed (Perren and Cordey, 1980, Claes and Heigele, 1999, Lacroix et al., 2002). As none of these theories have been proven to be true, any patterns of tissue formation predicted by the model used in this study are purely theoretical and for discussion purposes. Whilst distinct in appearance, a high degree of similarity in the initial tissue formations was predicted by the various theories. There are two reasons for the observed similarities. Firstly, although the maximum principal strain and the deviatoric strain, which represent the largest tensile strain and the shape change respectively, are different interpretations of the strain environment, their magnitude and pattern were very similar in all regions of the callus and under all IFM modes (Figure 4-5 to Figure 4-7). Secondly, as the deformations produced by shear and torsional IFMs did not result in a volume change (hydrostatic stress/strain); negligible hydrostatic pressures and fluid flows were associated with these movements. Consequently, the initial tissue formation predicted using the theories of both Claes and Lacroix were hardly influenced by their respective non distortional components (Figure 4-9). Only the axial component of IFM resulted in a hydrostatic pressure that influenced the pattern of tissue prediction. The subtle variance in the tissue formations between the various theories can be explained by the different magnitudes of the limits for when a tissue differentiates according to each theory (Figure 2-8, Figure

2-10 and Figure 2-11). Therefore, although the different mechanobiological theories appear quite different, they have much in common.

In this study the interaction between axial and shear interfragmentary movements was also investigated. When axial and shear IFMs were applied together, in some regions of the callus no increase in strains were observed and in others even a reduction in strain occurred. This would appear to be explained by a cancelling out that occurs through the combination of compressive strains in the longitudinal direction generated by axial IFMs with the tensile strains produced by the interfragmentary shear. Thus, the principal and deviatoric strains produced from combined loading were, with the exception of the endosteal region, similar to those produced by axial IFMs alone. Although the strains in the endosteal region from combined loading were larger than those produced by axial IFMs alone, it is uncertain if this would adversely affect healing as ossification in the endosteal callus has been reported to be driven predominantly by biological factors (McKibbin, 1978).

The fluid flow velocity determined in this study was relatively small and as a biophysical stimulus, little influence was seen on the initial tissue formation prediction. Comparison with the results of Lacroix et al. (2002) confirmed that a similar fluid flow velocity in the intra-cortical gap (0.6 $\mu ms^{-1}$) was also determined in the initial phase of their healing simulation. It was not until the late phase of healing, when the mineralized component of callus had increased, did the magnitude of fluid flow velocity increase to level such that it began to influence tissue differentiation and remodelling. In the present study the role of fluid flow as a biophysical stimulus in the early phase was minimal and suggests, as previously reported, that strain provides the dominant stimulus during bone healing (Kuiper et al., 2000).

The present findings give an explanation for the contradictory observation of seemingly improved healing in the presence of increased interfragmentary shear. In the study of Klein et al. (2003), axial and shear interfragmentary movements were monitored over the course of healing. Despite the presence of higher interfragmentary shear movements initially, healing in the group was not impeded. In this study, the axial and shear movement components partially cancelled one another out with the result being that the combined movement did not lead to an overall increase in the periosteal deviatoric strains. Therefore, contrary to expectations the strains in the callus were not dramatically increased by the addition of interfragmentary shear. The

improved healing may then have been related to stimulation from a slightly higher axial compressive movement accompanying the interfragmentary shear.

In the first part of this analysis, the focus was on the initial phase of bone healing, as a number of investigators have suggested that the initial mechanical conditions may be particularly important for the healing outcome (Le et al., 2001, Thompson et al., 2002, Klein et al., 2003). However, since bone healing consists of a complex sequence of biological events that can be potentially interrupted at any stage, the success or failure of healing can not be exclusively determined by the examination of the initial conditions alone.

Estimates of the mechanical conditions in the early callus obtained using this model must be understood in context of its limitations. The geometry of the initial callus of the sheep (i.e. at 7 days) was unknown. For simplicity, the early callus was modelled as being entirely composed of granulation tissue with a straight edged periosteal border. Other studies investigating the mechanical conditions over the entire healing period have typically prescribed a bell shape geometry which is typical seen once a bony callus has formed periosteally. On comparison with the results of Carter et al. (1998), it was found that both callus forms led to similar patterns of strain and it was concluded that the geometry of the external boundary of the callus had little influence on the initial mechanical conditions in the gap, endosteally and on the periosteal surface of the bone cortices.

A further limitation was the lack of empirical data for the material properties of granulation tissue. As no experimentally determined values were available, values determined by parametric analysis in a previous finite element model were chosen. However, because the loading is applied as a displacement of the fragments in this study, i.e. the interfragmentary movements, and because the rigidity of the cortical bone is many orders of magnitude larger than that of the granulation tissue, the strains calculated in model were found during preliminary analysis to be insensitive to the elastic properties of the granulation tissue.

Whilst the code used to perform the calculations has been verified against experimental results and the values estimated are comparable to those from similar models in the literature, the finite element model presented has not been validated. For this reason, it is important to note that the values given in this study are not to be

taken as absolute values; rather they are estimations presented to allow a relative comparison. The model used in this study is representative of well controlled tibial osteotomy and therefore the findings of this study are not directly transferable to more complex fractures or those with irregular geometries. However, this simple model is sufficient to aid in the understanding of straightforward healing situations, such as those created for experimental purposes.

In summary, this study found that the initial mechanical stimuli generated by shear and torsional interfragmentary movements did differ from those produced by axial interfragmentary movements. In contrast to axial IFMs, interfragmentary shear and torsion did not produce a volumetric stimulus, which according to Pauwels (1980) would favour differentiation of pluripotent tissue towards a cartilage intermediate. Prediction of the initial tissue formation using the different mechanobiological theories established the dominance of the deformation parameter and a high degree of similarity amongst these theories.

### 4.4.2 Influence of Hard Callus Maturation

Callus size and strength are known to be related to the fixation stability (Goodship et al., 1993). However, the influence of local mechanical conditions on the individual processes of callus development is unclear. In this study, the local hydrostatic stresses and tensile strains in the callus, and how they change with hard callus maturation were determined. Furthermore, these patterns of hydrostatic stress and tensile strain were correlated with sites of ossification observed previously in histological analyses.

Finite element analyses to determine the mechanical conditions in the initial callus demonstrated that, regardless of the component of interfragmentary movement and the level of fixation stability, moderate to large strains were confined to the gap region directly between the cortices. In the regions where bone formation is initially observed, i.e. along the periosteal surface of the cortex adjacent to the gap, low strains and pressures were determined and very little difference was determined between the modes of interfragmentary movement and the stabilities simulated. A number of experimental studies have reported that the amount of hard callus formed by intramembranous ossification appears independent of the fixation stability (Mark et al., 2004a, Epari et al., 2005). McKibbin suggested from his observations that hard callus formation is part of the initial inflammatory response to fracture or osteotomy

and is predominantly driven by biological factors (McKibbin, 1978). The results of this study provide a biomechanical explanation for experimental observations of hard callus formation. Since, regardless of the mode of interfragmentary movement and the degree of fixation stability, the magnitudes of tensile strain and hydrostatic stress were similar in the regions of initial bone formation, no differences in bone formation on hand the fixation stability would be expected if intramembranous ossification was mechanically stimulated. The insensitivity of local mechanical conditions to the fixation stability and the low magnitudes of mechanical stimuli in regions of initial bone formations support previous observations that intramembranous ossification is predominantly biologically driven.

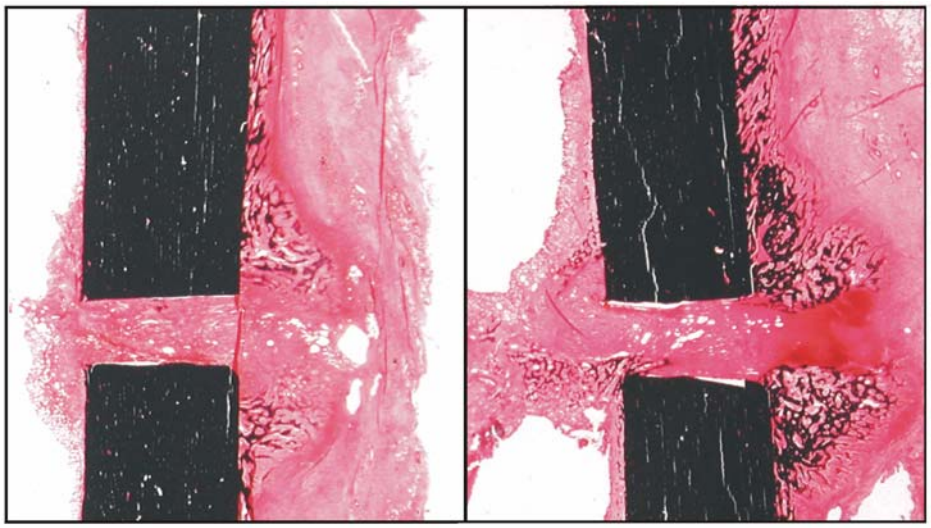

**Figure 4-14 shows histologically the development of periosteal hard callus by intramembranous ossification at two weeks (left) and three weeks (right) (Epari et al., 2005).**

As the periosteal hard callus increased in size, the strains along the ossification front were also seen to increase; reaching up to 30% strain by the time the callus began to bridge the gap. Endochondral ossification has been observed to begin on the surface of the hard callus, once the hard callus starts to bridge the gap, approximately three weeks postoperatively in sheep (Figure 4-14) (Epari et al., 2005). Furthermore, in sheep treated with less rigid fixation, the phase of endochondral ossification appeared to be prolonged (Epari et al., 2005). In this study, the three week finite element model demonstrated that the surface of the periosteal hard callus, the site of endochondral ossification, was subjected to large tensile strains. Tensile strains have been suggested to disrupt vessels and neo-angiogenesis which may lead to oxygen deficient regions (Claes et al., 2002). Such regions may then preferentially ossify by a cartilage intermediate that is known to have lower oxygen requirements (Basset and Hermann,

1961). Cartilage has also been suggested to form in regions of high hydrostatic stress (Pauwels, 1980). However, no correlation could be found between regions experiencing a hydrostatic stress determined in this study and regions of cartilage formation seen histologically (Figure 4-15). At three weeks the largest hydrostatic stress on the ossification front was determined close to the gap while cartilage formation and hypertrophy was first observed on the outermost regions of the hard callus. These results suggest that large tensile strains occurring around three weeks may stimulate the onset of endochondral ossification on the surface of the hard callus. However, if strains are too high, as predicted for semi-rigid fixation, mineralisation of the cartilage may be impaired, thus prolonging the chondral phase of healing.

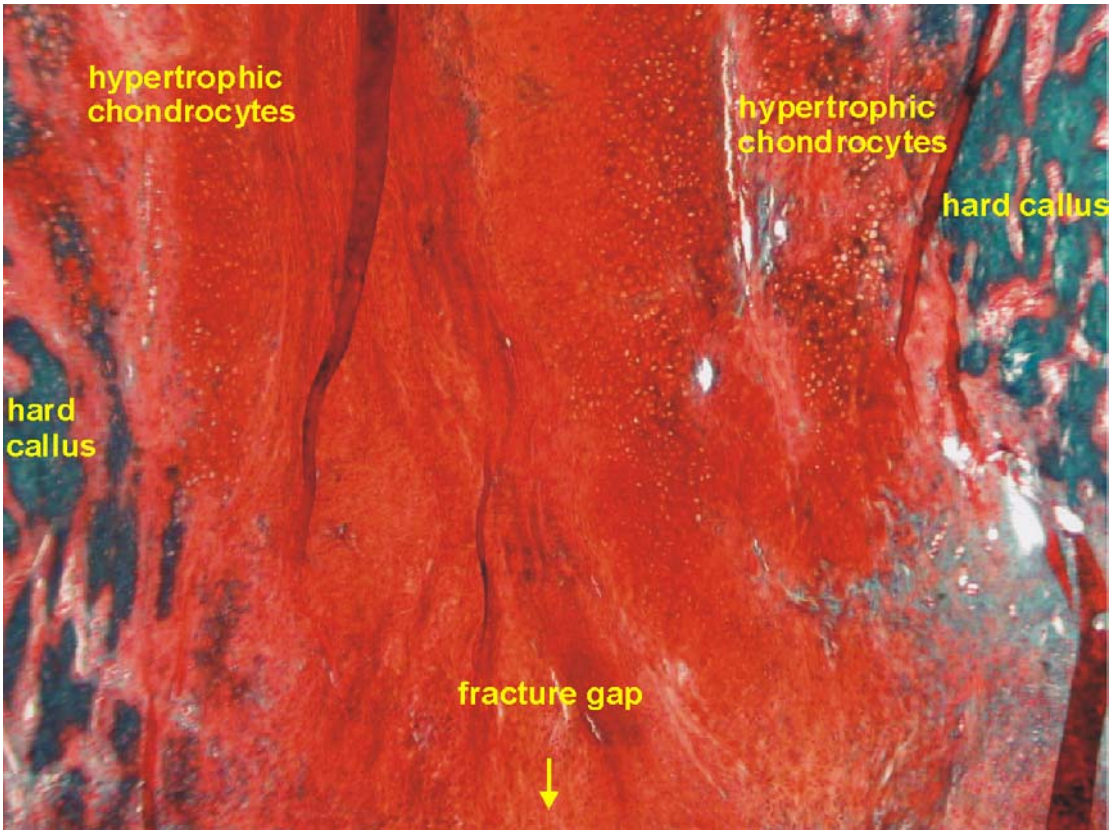


**Figure 4-15 shows the sandwich configuration of fibrocartilage between layers of hypertrophic chondrocytes in hyaline-like cartilage undergoing endochondral ossification (Chapter 3). The regions of hyaline-like cartilage corresponded with regions of high tensile strain, but not of significant hydrostatic pressure.**

The presence of large tensile strains on the surface of the hard callus coinciding with the onset of endochondral ossification was surprising and prompted closer examination of the mechanical conditions in the callus produced by the individual components of interfragmentary movement. Interestingly, the pattern seen when simulating the experimental conditions was exhibited only when applying the axial

compression component but not the shear component (Figure 4-10). This suggests that the large tensile strains on the surface of the hard callus appear to be associated with the axial component of interfragmentary movement and implies that the axial component of fixation stability may be most critical for timely healing.

In a previous study, differences were observed in the rate of breakdown of the callus haematoma (Epari et al., 2005). At the first observation time point of two weeks remnants of the haematoma could only be found in the gap directly between the cortices but nowhere else in the callus. In the semi-rigid fixation group, haematoma remnants remained present longer in the callus, also being observed at three weeks. Macrophages have been previously reported to appear earlier and in greater numbers in rigidly fixed fractures (Hankemeier et al., 2001). Macrophages are believed to accelerate the transition from the inflammatory phase to the proliferative phase. In the present study, the mechanical conditions directly in the gap between the cortices were subject to the highest load and were the most sensitive to the fixation stability. Therefore, differences in stability would result in different mechanical conditions in the gap, which could explain differences in macrophage activity and the observed differences in haematoma breakdown.

A potential limitation of our FE models is that all tissues were modelled as linearly elastic, single phase materials. This simplification requires only the input of the elastic modulus and the Poisson's ratio. This modelling approach was considered appropriate, however, since the initial mesenchymal tissue stress and strain response to the interfragmentary movement was of primary interest, i.e. the time period immediately following heal strike when the fragment movement reaches its maximum value. After this initial response, the tissue exhibits a nonlinear stress relaxation response. If the behaviour of the tissue during its relaxation period, or at slower loading rates were of interest, a poroelastic, biphasic or viscoelastic model would likely be more appropriate (Loboa et al., 2005).

The numerical model developed in this study was based on a well characterised experimental animal model used to examine the influence of fixation stability on bone healing. The geometry of the finite element models was simplified, but done according to previous histological observations (Schell et al., 2005, Epari et al., 2005). The interfragmentary movements applied to the models were measured in vivo in the same experimental model (Schell et al., 2005). This enabled for the first time a

correlation between the results of the finite element model and the corresponding spatial and temporal distribution of tissues comprising the callus seen histologically for two different fixation stabilities.

## 4.5 Conclusion

This study has provided biomechanical explanations for the influence of fixation stability on the ossification processes during bone healing. Regardless of the mode of interfragmentary movement or degree of fixation stability similarly low strains and pressures were estimated in regions of initial bone formation by intramembranous ossification. This explains the similarly sized hard calluses seen in experimental models of bone healing examining the influence of fixation stability. The chondral phase has been previously reported to be prolonged in delayed healing. In this study, changes in the callus morphology due to hard callus maturation increased the sensitivity of periosteal gap regions to fixation stability. Tensile strains were correlated with regions undergoing endochondral ossification implying a role for these strains in stimulating cartilage formation, but in cases of less stable fixation mineralisation may be impaired. The findings of this study imply that appropriate fixation stability during the chondral phase of healing is critical to ensuring timely healing.

# 5 Mechano-biology of Bone Healing

---

This project focused on the interaction between the mechanics and the biology of bone healing. Histologic and histomorphometric techniques were used to document the biology of healing in a well characterised experimental model of bone healing. Numerical analysis was then performed to estimate the mechanical conditions in the healing callus in the initial inflammatory phase and subsequent phase of callus formation. In the first part of this section the main findings to come out of the individual analyses, chapter 1 and 4, are summarised. In the second part, the consequences for the mechano-biology of secondary bone healing are discussed and a revised view of the mechano-biology is introduced.

---

## 5.1 Summary of Findings

In Chapter 1, an in vivo experimental model of ovine bone healing is presented. The mechanical boundary conditions were determined for healing under rigid and semi-rigid fixation stabilities. The mechanical competence of the healing callus was determined post-mortem at 6 and 9 weeks. Calculation of the moment of inertia from reconstructions of computer tomography scans at 2, 3, 6 and 9 weeks provided an assessment of the quantity and quality of the mineralised tissue in the callus. Using these methods, the differences in healing of bones stabilised with rigid and semi-rigid external fixation were characterised. In comparison to rigid fixation, osteotomies treated with semi-rigid fixation showed higher shear interfragmentary movements, inferior stiffness at 6 weeks, similar stiffness at 9 weeks and higher moments of inertia at 6 and 9 weeks. Based on these results, it was concluded that healing under semi-rigid conditions was less efficient producing a larger callus, yet achieving only the same mechanical stability. In addition, an upper limit of interfragmentary shear was defined by which healing was suboptimal.

Analysis of the callus morphology at two and three weeks found that differences in stability produced no identifiable differences in the composition of the callus, i.e. amounts of fibrous tissue, cartilage, and mineralised tissue. However, after three weeks differences became more apparent with the fibrous tissue disappearing from the calluses rigidly fixed, while cartilage persisted longer in the calluses of the semi-rigid group. These findings led to the conclusion that the initial bone formation by intramembranous ossification appeared to be independent of the mechanical stability, while a prolonged endochondral ossification seems to be related to the observed healing delay.

In Chapter 4, numerical analyses were performed to estimate the mechanical conditions in the initial callus, produced by the different modes of interfragmentary movement. Additionally, predictions of initial tissue formation from various mechano-biological theories were examined. Results from the three-dimensional finite element model showed that axial movements produced in addition to compressive and tensile strains, regions of moderate hydrostatic pressure. In contrast, shear and torsional movements were only associated with deviatoric strains. The analysis also showed that significantly larger shear and torsional interfragmentary movements were

required to produce the same level of strain as moderate axial movements. Examination of the different theories of mechano-biology for healing, determined a high degree of similarity in their prediction, despite being based on seemingly different biophysical stimuli. The reason for this was found to be the similarity between the maximum principal strain and the deviatoric strain and the comparatively weak role of stimuli in the fluid phase, i.e. hydrostatic pressure or fluid flow. Additionally, Chapter 4 includes numerical analyses to estimate the mechanical conditions up until the third week of healing. It is thought that this period before bridging of the callus may be critical for healing. Measurements of the in vivo interfragmentary movements have shown that the movements remain relatively constant over the first few weeks of healing. However, dramatic changes in the callus geometry occur during this period. Therefore, mechanical conditions in the callus were evaluated with reference to these callus changes. In addition to investigating the influence of axial and shear movements on the mechanical conditions during this phase of healing, the mechanical conditions during early healing arising from the movements determined in the in vivo model were estimated and compared to the corresponding healing results. It was found that in the areas of highest activity in the initial callus that the mechanical conditions were not so dissimilar. However, by three weeks, changes in the geometry and differences in mechanical stability led to very different mechanical conditions, indicating that the three week time point, corresponding to the onset of endochondral ossification, may be a critical point in bone healing.

## 5.2 Consequences for Mechano-biology

In Chapter 1, a review of the development of mechano-biology and a description of the various theories of mechano-biology of bone healing was given. In this section, elements of these theories are discussed in light of current findings and a refined notion of the mechano-biology of secondary bone healing is introduced.

### 5.2.1 Intramembranous Ossification

Bone healing begins with an inflammatory phase which results in the production of growth factors and the pooling of multi-potent mesenchymal cells (Einhorn, 1998). Whether these cells differentiate predominantly to become bone or cartilage cells has been shown to be related to the fixation stability (Thompson et al., 2002). However, in

this study, the initial tissue composition did not appear to be greatly influenced by the mechanical stability of fixation (Chapter 1).

In the experimental model presented in Chapter 1, fixation stability did not influence the amount of bone formed over the first three weeks (Figure 3-15). Histological observation confirmed that bone formation during this time occurred via the intramembranous path. Examination of the mechanical conditions (Chapter 4) revealed that regardless of the mode of interfragmentary movement, very low strains occur in the regions of initial bone formation (Figure 4-11). Furthermore, the magnitudes of the strains in these regions were relative insensitive to mechanical stability of fixation (Figure 4-13).

Pauwels (1980) stated that a low strain environment is a requirement for bone formation. This requisite has been prevalent in all subsequent mechano-biological theories (Carter et al., 1998, Claes and Heigele, 1999, Prendergast et al., 1997). But how low is low enough and can strains be too small for bone formation. In other words, is bone formation inhibited over a certain threshold or is a certain level of strain necessary to stimulate bone formation.

The strain experienced by healthy intact cortical bone is typically of the order of 1000 - 2000 με (Lanyon et al., 1975), which in percentage terms, corresponds to a strain of 0.1 – 0.2 %. The proliferation of osteoblasts in cell culture has been shown to increase with strains of up to 5% but not larger (Claes et al., 1998). The strains estimated near the periosteal surface of the bone cortex were always below 10% (Chapter 4). Strains on the surface of the bone itself were orders of magnitude lower due to the very high stiffness of the bone. As intramembranous ossification was only observed on existing surfaces of bone, it can be expected that the strains are smaller than 5%. However, estimating the strains seen by bone-lining cells or osteoblasts involved in intramembranous ossification is beyond the scope of the model in this study, as continuum level strains are not necessary those seen by cells (Brand et al., 2001).

A number of authors (McKibbin, 1978, Mark et al., 2004a) have suggested that biological conditions are perhaps the most important factor determining intramembranous ossification, which is supported by the observations in Chapter 1 and the analytical findings of Chapter 4. Claes et al (1999) alluded to the role of existing bone surfaces. In this study, intramembranous ossification was observed only

on existing surfaces of bone, which are known to be covered with bone lining cells (Jee, 2001) capable of producing bone (Miller and Jee, 1987). The recruitment of bone lining cells to produce bone or osteoclasts to resorb bone is believed to be coordinated by osteocytes which are sensitive to mechanical stimuli (Burger et al., 1995). Interestingly, generous bone formation was observed only on the periosteal side of bone fragments dislodged from the cortex in this study (Chapter 1). It is to be expected, in such cases, that the osteocytes are either dead or experiencing lower strains than normal and would react by recruiting osteoclasts (Bakker et al., 2004). Therefore, the bone formation must be explained by signals other than those coming from the osteocytes, such as growth factors released during the inflammatory phase of healing, activating the bone lining cells and inhibiting the recruitment of osteoclasts (Bostrom, 1998). This situation is analogous to the ends of the cortices adjacent to the gap that are also experiencing lower than normal strains due to a shift in the load path through the external fixator. Although, internally increased porosity can be seen as a result of osteoclastic activity, on the periosteal surface of the bone, new bone formation can be seen. This suggests that the signals for bone formation are originating external to the cortical bone.

The surrounding soft tissues are known to be important for the biology of healing (McKibbin, 1978). As the soft tissues are a source of cells as well as blood supply, it could be reasoned that the concentration of growth factors in the healing callus may be related to the adjacent soft tissue mass. Healing of tibia subjected to uniform mechanical conditions, i.e. axial compression or interfragmentary torsion, show typically significantly more bone formation on the lateral aspects of the tibia compared to the medial side (Augat et al., 2003). In the sheep, the lateral side of the tibia has greater soft tissue coverage than the medial side (Nickel et al., 1992).

Finally, intramembranous ossification and hard callus formation is observed in cases of periosteal injury without fracture (McKibbin, 1978). Compared to the fracture or osteotomy situation, where interfragmentary movement is usually seen to occur (Klein et al., 2003, Klein et al., 2004, Schell et al., 2005), intact bone would not be expected to experience higher than normal strains. This last observation would appear to suggest that mechanical stimulation is not absolutely necessary as a stimulus for intramembranous ossification. The question then that remains: is there an upper threshold in strain above which intramembranous ossification is inhibited? Till now,

there has been no evidence showing that intramembranous ossification does not take place in unstable conditions. Therefore it would appear that intramembranous ossification is relatively insensitive to the mechanical conditions and is most strongly driven by the local biological conditions.

The factors most important for intramembranous ossification appear to be

- Bone surfaces covered with bone lining cells, osteoblast precursors, or mesenchymal cells from the cambrium layer of the periosteum
- Concentration of growth factors released during the inflammatory phase by platelets in the haematoma and the fracture fragments

### 5.2.2 Endochondral Ossification

Morphological investigation of healing under different mechanical stability in the present study revealed that cartilage persisted longer in the callus of the tibia treated with semi-rigid fixation (Chapter 1). Since intramembranous ossification was not noticeably influence by the stability, it seems that a disruption of endochondral ossification is responsible for the delay seen in healing.

The first signs of cartilage in the callus become apparent after three weeks of healing. However, the signals which are responsible for initiating endochondral ossification are unknown. It appears that the onset of endochondral ossification may have more to do with the size of the periosteal hard callus, rather than biological timing, i.e. the number of weeks healing. In the healing model of the present study, endochondral ossification always appeared first on the lateral size, where the hard callus was typically larger and more developed than on the medial size, which as previously argued (Section 5.2.1) is most likely due to the ample soft tissue coverage on the lateral side of the tibia. What is not clear, is whether, intramembranous ossification stops and endochondral ossification takes over or whether both processes occur concurrently. Anecdotal evidence in the literature, suggests that intramembranous ossification has a limited response or capacity (McKibbin, 1978). Intramembranous ossification does not continue indefinitely until bridging occurs, but rather if bridging does not occur with a certain time frame the hard callus recedes (McKibbin, 1978). In any case, by the time the hard callus reaches a certain size and begins to bridge the gap, regions of cartilage at the ossification front on both sides of the fracture (proximal and distal) begin to appear (Chapter 1). These islands of cartilage (hyaline)

are separated by what appears to be fibrocartilage (Figure 3-14). Chondrocytes closest to the bone surface hypertrophy first giving rise to ossification of the cartilage which would appear to proceed in a step wise manner until the gap is bridged. It is not clear what causes the cartilage to form and then to ossify. In this study the length of the chondral phase was shown to be dependant on the mechanical stability. The numerical analyses demonstrated that large tensile strains appear on the surface of the periosteal hard callus around three weeks (Figure 4-13) as the hard callus matures and begins to bridge the gap. It is not yet clear if these high strains are responsible for the emergence of cartilage tissue or whether they play some role in delaying its ossification. Till now, various theories have been postulated to explain the necessity for bone formation via a cartilage intermediate. One theory is that high shear or tensile strains impair angiogenesis creating regions with low oxygen partial pressures which are favoured by cartilage tissues which have low oxygen requirements (Basset and Hermann, 1961).

Other authors have cited hydrostatic stress as being the stimulus for cartilage formation (Carter et al., 1998, Claes and Heigele, 1999). However, in the analyses of the present study (Chapter 4), regions of higher hydrostatic stress did not appear to correlate with sites of cartilage formation (Chapter 1). In fact it was only once the hard callus had partially bridged the gap did the maximum hydrostatic pressure shift from between the cortices to between the ossification front and the sites where cartilage was observed to form. If hydrostatic pressure alone stimulated the differentiation to cartilage then it would be expected that cartilage would also be seen between the cortices, but this is rarely the case in regular bone healing and only occurs in non-unions and critical healing. Instead, endochondral ossification was only observed on existing bone surfaces. Mark and co-workers (2004) suggested that existing bone may serve an important biological role in mediating endochondral ossification. Given that the mechanical conditions in this region appear to become critical as endochondral ossification begins, it appears to be of great importance that more emphasis is placed on the interactions and signalling occurring at this interface under various levels of stability.

## 5.3 Revised Theory of Bone Healing Mechano-biology

### 5.3.1 Inflammatory Stage

In this study, the only difference observed initially was in the rate of breakdown of the haematoma (Chapter 1). In both fixation groups remnants of the haematoma were observed in the gap directly between the cortices but nowhere else in the callus. In the semi-rigid fixation group, haematoma remnants were found more often and remained present longer in the callus being observed also at three weeks. Macrophages have been previously reported to appear earlier and in greater numbers in rigidly fixed fractures (Hankemeier et al., 2001). Macrophages are believed to accelerate the transition from the inflammatory phase to the proliferative phase. Since the mechanical conditions directly in the gap between the cortices are most sensitive to the initial fixation stability (Chapter 4), this suggests a relationship between the mechanics and the biology.

Assuming that the conversion of haematoma to granulation tissue is achieved by macrophages and their activity is related to the local mechanical strain, a mathematical relationship can be assigned for the rate of breakdown of haematoma and conversion to granulation tissue. As the exact mechanism is not known, it would be reasonable to assume that in stable conditions macrophage activity and hence haematoma breakdown and conversion is optimal. With decreasing stability, macrophage activity is negatively affected giving an inverse relationship (Figure 5-1).

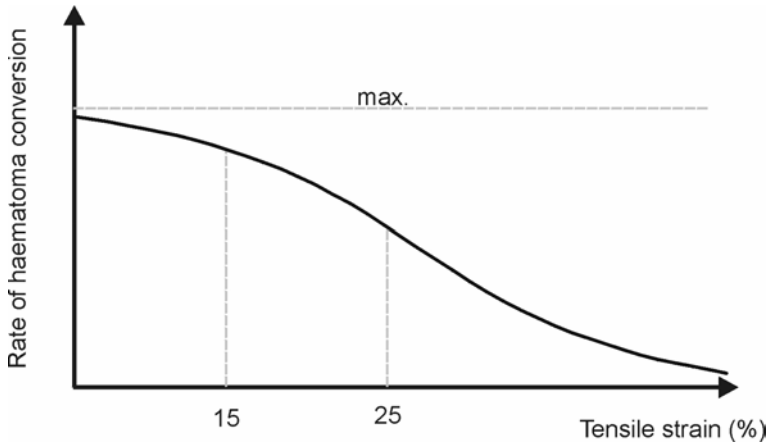


**Figure 5-1 illustrates an assumed relationship between the rate at which haematoma is broken down and converted to granulation tissue and the local mechanical strain.**

Whilst not rigid in the absolute sense, the rigid fixator resulted in timely healing. After two weeks, remnants of the haematoma could not longer be seen (Chapter 1). In Section 4.3.3, tensile strains of 15% were estimated in the gap region of calluses treated with rigid fixation. In the semi-rigid group, were remnants of the haematoma were still visible at three weeks, tensile strains of approximately 25% were determined.

Once haematoma has been converted to granulation tissue, the inherent pluripotent cells may proliferate and differentiate which is necessary for the development of the hard and soft callus components and ultimately bridging of the fracture. Others have suggested relationships governing the mechanical regulation of pluripotent cell differentiation (Carter et al., 1988, Prendergast et al., 1997).

### 5.3.2 Hard Callus Stage

In the experimental model of Chapter 1 the initial bone formation by intramembranous ossification was seen to be independent of the fixation stability. It was reasoned that biological factors and in particular the surrounding concentration of growth factors released during the inflammatory and early stages of healing are mostly likely responsible for the rate of intramembranous bone formation. Within the first three weeks of healing, bone was formed almost exclusively via the intramembranous path. Due to the limited number of investigative time points, it was not possible to determine whether intramembranous ossification ended with the onset of endochondral ossification or whether these two processes occurred simultaneously.

Given that intramembranous ossification is controlled by biological factors, a relationship could be prescribed between the rate of bone formation and the local concentration of growth factors (Figure 5-2) with the limitation that bone formation is restricted to existing bone surfaces covered with bone-lining cells. Bone formation would be at a maximum for a particular concentration of growth factor and then decreases with decreasing growth factor concentration. Above certain saturation levels a continued increase in growth factor concentration may not further increase the rate of bone formation due to other inherent limiting factors e.g. number of osteoblasts or availability of mineral calcium phosphate. At the other end of the scale a certain minimum concentration may be required before bone formation is initiated.

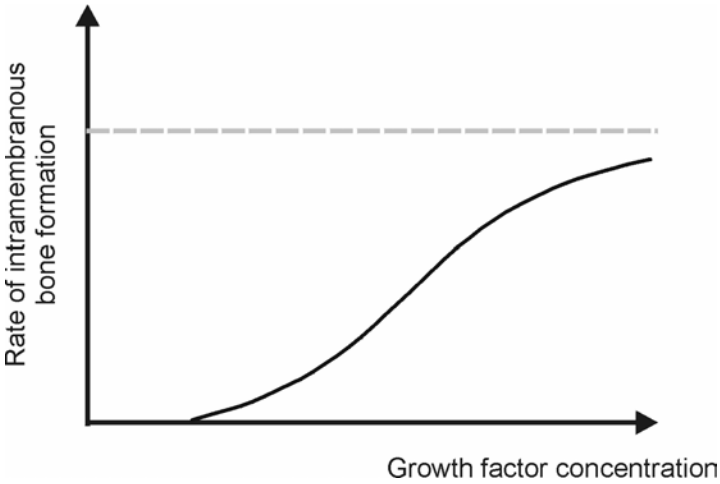


**Figure 5-2 illustrates the relationship between local bone growth factor concentration and the rate of intramembranous bone formation. Bone formation can only occur on existing bone surfaces where viable bone-lining cells are present.**

There is some evidence in the literature to suggest that bone formation by intramembranous ossification has a limited potential and that bone formation may cease prior to complete bridging (McKibbin, 1978). If the production of growth factors in the callus is a function of the initial inflammatory reaction, the concentration may be expected to decrease with time. This could explain the cessation of intramembranous bone formation as growth factor concentration falls. At this stage a mechanism can not be defined, but this may be related to the transition from the inflammatory to proliferative phase described in Section 5.3.1.

### 5.3.3 Soft Callus Stage

Endochondral ossification begins with the accumulation of chondrocytes on the surface of the periosteal hard callus. In Section 5.2.2 it was reasoned that the onset of endochondral ossification is most likely related to the size of the periosteal callus rather than biological timing. Further, in chapter 4 it was observed that when the hard callus reached a certain size, the mechanical conditions on the surface of the periosteal callus became critical with large tensile strains.

It could be assumed that the appearance of chondrocytes is related to the local mechanical strain with a certain level of strain being necessary for differentiation to and proliferation of chondrocytes (>15%, Section 4.3.3). However, if strains are too large (>30%, Section 4.3.3) fibrous tissue proliferation may become preferential and thus explaining the higher fibrous tissue composition in less stable fixation conditions

(Chapter 1). The dependence of cartilage formation on the local mechanical strain may take the form of the mathematical relationship illustrated in Figure 5-3.

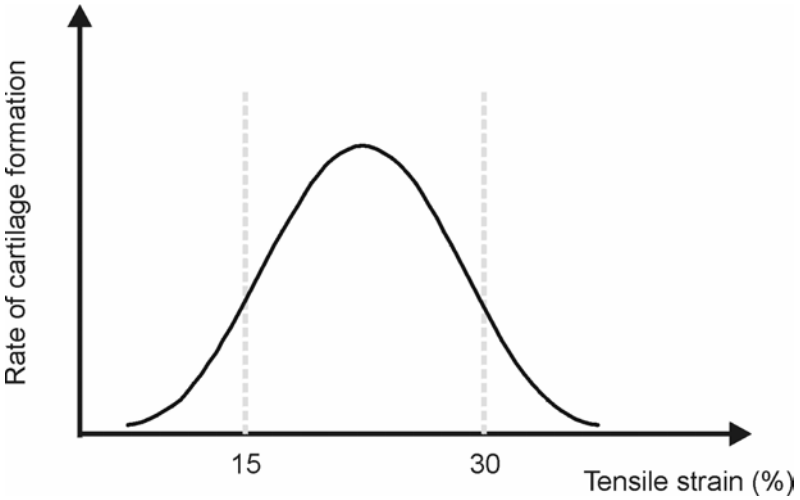


**Figure 5-3 illustrates the relationship between the rate of cartilage formation and the local mechanical tissue strain.**

In chapter 1 it was concluded that the delay in healing observed under less stable conditions was related to a prolonged chondral phase, where continued cartilage formation resulted in a larger callus that required longer to mineralise. Therefore, it may be reasonable assume that there is a relationship between cartilage mineralisation and the local mechanical strain. This relationship has been illustrated in Figure 5-4. It is to be expected that it is necessary for the strain to decrease for mineralisation to occur with mineralisation being hampered at larger strains.

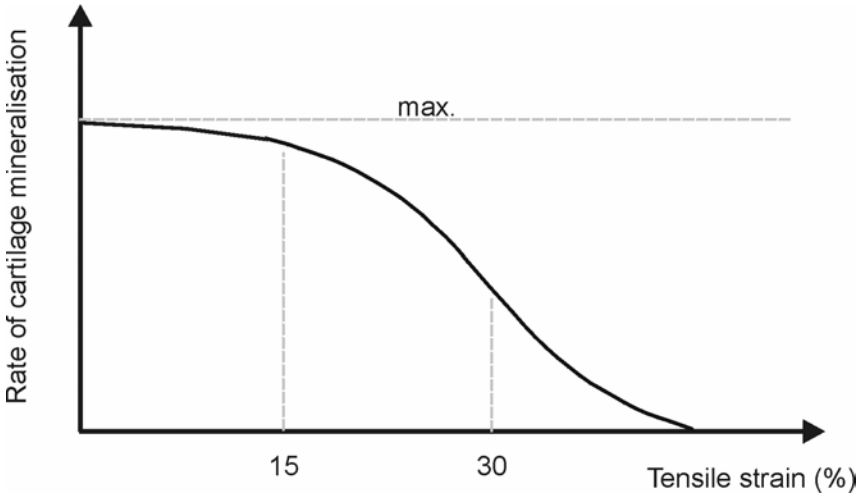


**Figure 5-4 illustrates the relationship between the rate of cartilage mineralisation and the local mechanical tissue strain.**

### 5.3.4 Remodelling and Resorption

Once bridging of the callus occurs and the direct load path through the bone had been restored the external callus becomes excessive to requirements. As the strains in the callus reduce, processes of remodelling and resorption become the dominant activities in the callus. Relationships have already been described governing the remodelling of bone according to the local strain environment (Van Rietbergen et al., 1993) Figure 5-5.

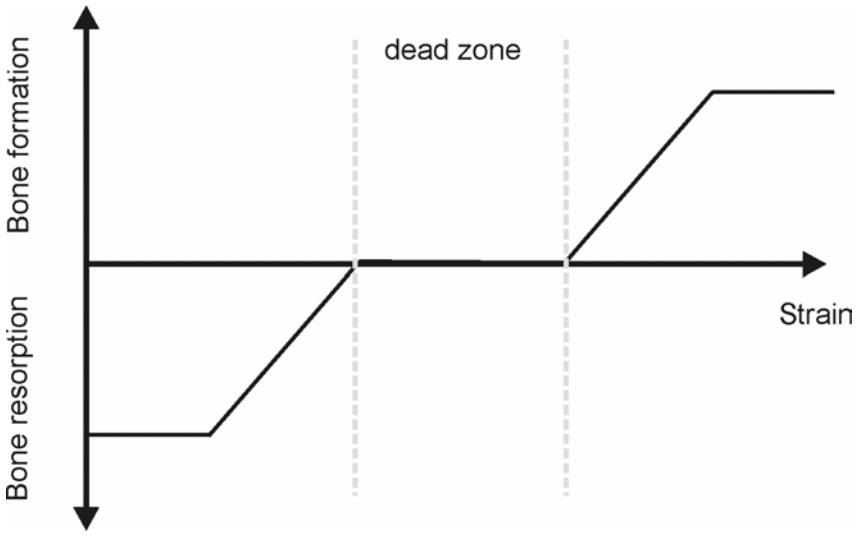


**Figure 5-5 shows the relationship for bone remodelling based on the tri-linear curve theory (Van Rietbergen et al., 1993).**

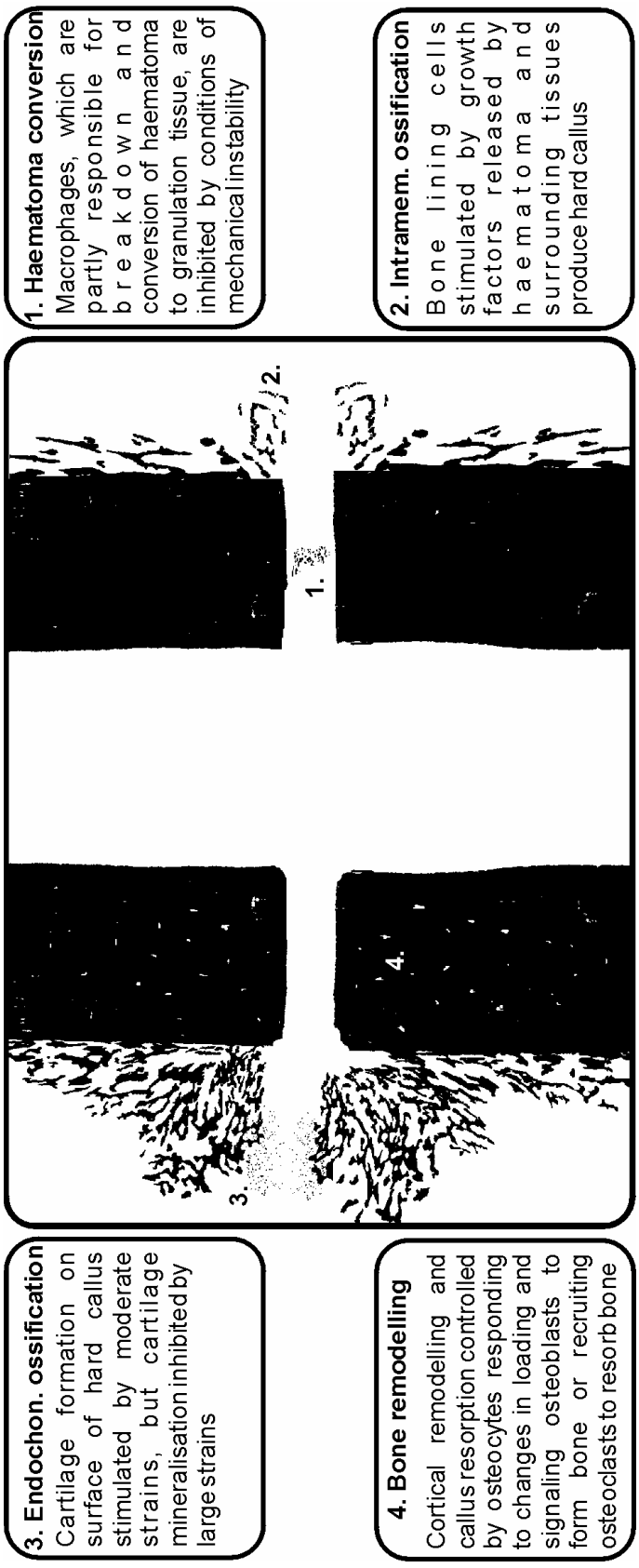


**Figure 5-6 summarises the dominant mechano-biological influences on various processes involved in callus development and maturation.**

## 5.4 Discussion

In this section relationships for a number of aspects of bone healing were theorised in order to describe the interaction between local mechanical conditions and biological processes, summarised in Figure 5-6. The relationships given here are not intended to be exclusive but rather cover the most important findings to come out of the present experimental and numerical analyses. Further research will be necessary to better understand the relationships suggested here and identify others that could not be identified, i.e. the relationship between mechanics and blood supply.

The incorporation of mechano-biological relationships into iterative finite elements models that simulate healing may help to better understand the influence of mechanics on healing and eventually provide a predictive tool for determining the healing outcome under different conditions of fixation stability.

# 6 Conclusion

This study provided the first opportunity to examine the histological conditions at various healing time points in an established large animal of bone healing that could be monitored mechanically. Contrary to hypothesis, not all aspects of callus formation were dependent upon the mechanical stability of fixation.

This healing model clearly demonstrated that differences in healing were attributable to a prolonged endochondral ossification observed in animals treated with semi-rigid fixation. Thereby, a limit of shear stability was determined by which healing was found to be suboptimal.

Numerical analyses of the healing callus demonstrated that shear and torsional interfragmentary movements do not create mechanical stimuli that in themselves can be considered detrimental to healing. The distortional component of the current mechano-biological models of bone healing was seen to be primarily responsible for the initial tissue differentiation patterns predicted. Finally, mechanical conditions were found to become critical in the region of endochondral ossification. At this time, it is not known if these mechanical conditions are responsible for the shift from intramembranous ossification to endochondral ossification, or if they are somehow responsible for prolonging the cartilage phase and delaying cartilage ossification.

Achieving optimal healing thus appears to lie with creating the right conditions for speedy endochondral ossification. In answering the following questions these conditions may be discovered,

- Why does intramembranous ossification stop and endochondral ossification begin? Or do they occur concurrently?
- How is endochondral ossification regulated? What role does blood supply play and what role does the hard callus have?
- Are critical mechanical conditions on the surface of the hard callus responsible for delaying the onset of endochondral ossification or the ossification of cartilage?

The development of surgical or pharmaceutical interventions may need to be more closely tailored to address deficiencies leading to prolonged endochondral ossification. Also, development of methods to detect a potential delay will not be trivial given the initial callus formation appears independent of the stability and therefore provides no evidence to suggest if healing is proceeding normally or not. However, if endochondral ossification is the critical phase, correction of fixation stability several weeks after fracture may be beneficial and prevent cases of non-union and delayed healing.

# 7 References


Anderson, D. E., St Jean, G., 1996. External skeletal fixation in ruminants. Vet Clin North Am Food Anim Pract. 12, 117-52.

Augat, P., Burger, J., Schorlemmer, S., Henke, T., Peraus, M., Claes, L., 2003. Shear movement at the fracture site delays healing in a diaphyseal fracture model. Journal of Orthopaedic Research. 21, 1011-7.

Augat, P., Merk, J., Genant, H. K., Claes, L., 1997. Quantitative assessment of experimental fracture repair by peripheral computed tomography. Calcified Tissue International. 60, 194-9.

Babhulkar, S., Pande, K., 2005. Nonunion of the diaphysis of long bones. Clin Orthop Relat Res. 50-6.

Bailon-Plaza, A., van der Meulen, M. C., 2001. A mathematical framework to study the effects of growth factor influences on fracture healing. J Theor Biol. 212, 191-209.

Bailon-Plaza, A., van der Meulen, M. C., 2003. Beneficial effects of moderate, early loading and adverse effects of delayed or excessive loading on bone healing. J Biomech. 36, 1069-77.

Bakker, A., Klein-Nulend, J., Burger, E., 2004. Shear stress inhibits while disuse promotes osteocyte apoptosis. Biochem Biophys Res Commun. 320, 1163-8.

Basset, C. A., Hermann, I., 1961. Influence of oxygen concentration and mechanical factors on differentiation of connective tissue in vivo. Nature. 190, 460-461.

Blachut, P. A., O'Brien, P. J., Meek, R. N., Broekhuyse, H. M., 1997. Interlocking intramedullary nailing with and without reaming for the treatment of closed fractures of the tibial shaft. A prospective, randomized study. J Bone Joint Surg Am. 79, 640-6.

Bolander, M. E., 1992. Regulation of fracture repair by growth factors. Proc. Soc. Exp. Biol. Med. 200, 165.

Bostrom, M. P., 1998. Expression of bone morphogenetic proteins in fracture healing. Clin Orthop. S116-23.

Brand, R. A., Stanford, C. M., Nicolella, D. P., 2001. Primary adult human bone cells do not respond to tissue (continuum) level strains. J Orthop Sci. 6, 295-301.

Brighton, C. T., 1984. The biology of fracture repair. Instructional Course Lectures. 33, 60-82.

Brighton, C. T., Hunt, R. M., 1991. Early histological and ultra-structural changes in medullary fracture callus. Journal of Bone and Joint Surgery. 73, 832-847.

Burger, E. H., Klein-Nulend, J., van der Plas, A., Nijweide, P. J., 1995. Function of osteocytes in bone--their role in mechanotransduction. Journal of Nutrition. 125, 2020S-2023S.

Carter, D. R., Beaupre, G. S., Giori, N. J., Helms, J. A., 1998. Mechanobiology of skeletal regeneration. Clinical Orthopaedics and Related Research. 355 Suppl, S41-55.

Carter, D. R., P.R., B., Beaupre, G. S., 1988. Correlations between mechanical stress history and tissue differentiation in intial fracture healing. Journal of Orthopaedic Research. 6, 736-748.

Chao, E. Y., Inoue, N., Elias, J. J., Aro, H., 1998. Enhancement of fracture healing by mechanical and surgical intervention. Clinical Orthopaedics and Related Research. 355 Suppl, S163-78.

Cheal, E. J., Mansmann, K. A., DiGioia, A. M., 3rd, Hayes, W. C., Perren, S. M., 1991. Role of interfragmentary strain in fracture healing: ovine model of a healing osteotomy. Journal of Orthopaedic Research. 9, 131-42.

Claes, L., Augat, P., Suger, G., Wilke, H. J., 1997. Influence of size and stability of the osteotomy gap on the success of fracture healing. Journal of Orthopaedic Research. 15, 577-84.

Claes, L., E., 1990. [The biomechanics of osteosynthesis]. Aktuelle Probl Chir Orthop. 34, 32-38.

Claes, L., Eckert-Hubner, K., Augat, P., 2002. The effect of mechanical stability on local vascularization and tissue differentiation in callus healing. Journal of Orthopaedic Research. 20, 1099-1105.

Claes, L. E., Heigele, C. A., 1999. Magnitudes of local stress and strain along bony surfaces predict the course and type of fracture healing. Journal of Biomechanics. 32, 255-66.

Claes, L. E., Heigele, C. A., Neidlinger-Wilke, C., Kaspar, D., Seidl, W., Margevicius, K. J., Augat, P., 1998. Effects of mechanical factors on the

fracture healing process. Clinical Orthopaedics and Related Research. 355 Suppl, S132-47.

Claes, L. E., Ito, K., 2005. Biomechanics of fracture fixation and fracture healing in: Mow, V. C. and Huiskes, R., (Eds), Basic Orthopaedic Biomechanics and Mechano-Biology, Lippincott, Williams and Wilkins, London,

Cowin, S. C., 1999. Bone poroelasticity. Journal of Biomechanics. 32, 217-38.

Cruess, R. L., Dumont, J., 1975. Fracture healing. Canadian Journal of Surgery. 18, 403-13.

DiGioia, A. M., 3rd, Cheal, E. J., Hayes, W. C., 1986. Three-dimensional strain fields in a uniform osteotomy gap. Journal of Biomedical Engineering. 108, 273-80.

Duda, G. N., Eckert-Hubner, K., Sokiranski, R., Kreutner, A., Miller, R., Claes, L., 1998. Analysis of inter-fragmentary movement as a function of musculoskeletal loading conditions in sheep. J Biomech. 31, 201-10.

Duda, G. N., Sollmann, M., Sporrer, S., Hoffmann, J. E., Kassi, J. P., Khodadadyan, C., Raschke, M., 2002. Interfragmentary motion in tibial osteotomies stabilized with ring fixators. Clinical Orthopaedics and Related Research. 396, 163-72.

Duda, G. N., Sporrer, S., Sollmann, M., Hoffmann, J. E., Kassi, J. P., Khodadadyan, C., Raschke, M., 2003. Interfragmentary movements in the early phase of healing in distraction and correction osteotomies stabilized with ring fixators. Langenbeck's Archives of Surgery. 387, 433-40.

Einhorn, T. A., 1995. Enhancement of fracture-healing. Journal of Bone and Joint Surgery. 77, 940-56.

Einhorn, T. A., 1998. The cell and molecular biology of fracture healing. Clinical Orthopaedics and Related Research. 355 Suppl, S7-21.

Epari, D. R., Schell, H., Bail, H., Duda, G. N., 2005. Influence of fixation stability on the morphology of secondary bone healing. Bone. In Press,

Frost, H. M., 1989. The biology of fracture healing. An overview for clinicians. Part I. Clinical Orthopaedics and Related Research. 248, 283-93.

Gardner, T. N., Evans, M., Kenwright, J., 1996. The influence of external fixators on fracture motion during simulated walking. Medical Engineering and Physics. 18, 305-13.

Gardner, T. N., Evans, M., Kenwright, J., 1997. A biomechanical study on five unilateral external fracture fixation devices. Clinical Biomechanics (Bristol, Avon). 12, 87-96.

Gardner, T. N., Evans, M., Simpson, H., 1998. Temporal variation of applied inter fragmentary displacement at a bone fracture in harmony with maturation of the fracture callus. Med Eng Phys. 20, 480-4.

Goodship, A. E., Cunningham, J. L., Kenwright, J., 1998. Strain rate and timing of stimulation in mechanical modulation of fracture healing. Clin Orthop. S105-15.

Goodship, A. E., Watkins, P. E., Rigby, H. S., Kenwright, J., 1993. The role of fixator frame stiffness in the control of fracture healing. An experimental study. Journal of Biomechanics. 26, 1027-35.

Hankemeier, S., Grassel, S., Plenz, G., Spiegel, H. U., Bruckner, P., Probst, A., 2001. Alteration of fracture stability influences chondrogenesis, osteogenesis and immigration of macrophages. Journal of Orthopaedic Research. 19, 531-8.

Hente, R., Fuchtmeier, B., Schlegel, U., Ernstberger, A., Perren, S. M., 2004. The influence of cyclic compression and distraction on the healing of experimental tibial fractures. Journal of Orthopaedic Research. 22, 709-15.

Höntzsch, D., 1997. Fixateur-externe-Montagen mit dem AO-Rohrsystem. OP-Journal. 13, 18-21.

Hulth, A., 1989. Current concepts of fracture healing. Clin. Orthop. 265-84.

Jee, W. S. S., 2001. Integrated Bone Tissue Physiology: Anatomy and Physiology in: Cowin, S. C., (Eds), Bone Mechanics Handbook, CRC, New York,

Kassi, J. P., Hoffmann, J. E., Heller, M., Raschke, M., Duda, G. N., 2001. [Evaluating the stability of fracture fixation systems: mechanical device for evaluation of 3-D stiffness in vitro]. Biomed Tech (Berl). 46, 247-52.

Klein, P., Opitz, M., Schell, H., Taylor, W. R., Heller, M. O., Kassi, J. P., Kandziora, F., Duda, G. N., 2004. Comparison of unreamed nailing and external fixation of tibial diastases--mechanical conditions during healing and biological outcome. Journal of Orthopaedic Research. 22, 1072-8.

Klein, P., Schell, H., Streitparth, F., Heller, M., Kassi, J. P., Kandziora, F., Bragulla, H., Haas, N. P., Duda, G. N., 2003. The initial phase of fracture healing is

specifically sensitive to mechanical conditions. Journal of Orthopaedic Research. 21, 662-9.

Krettek, C., Schandelmaier, P., Rudolf, J., Tscherne, H., 1994. Current status of surgical technique for unreamed nailing of tibial shaft fractures with the UTN (unreamed tibia nail). Unfallchirurg. 97, 575-99.

Krischak, G. D., Janousek, A., Wolf, S., Augat, P., Kinzl, L., Claes, L. E., 2002. Effects of one-plane and two-plane external fixation on sheep osteotomy healing and complications. Clin Biomech (Bristol, Avon). 17, 470-6.

Kristiansen, T., Flemming, B., Neale, G., Reinecke, S., Pope, M. H., 1987. Comparative study of fracture gap motion in external fixation. Clinical Biomechanics. 2, 191-195.

Kuiper, J. H., Ashton, B. A., Richardson, J. B., 2000. Computer simuluation of fracture callus formation and stiffness restoration. Proceedings of the 12th Conference of European Society of Biomechanics. 61.

Lacroix, D., Prendergast, P. J., Li, G., Marsh, D., 2002. Biomechanical model to simulate tissue differentiation and bone regeneration: application to fracture healing. Medical and Biological Engineering and Computing. 40, 14-21.

Lanyon, L. E., Hampson, W. G. J., Goodship, A. E., Shah, J. S., 1975. Bone deformation recorded in vivo from strain gauges attached to the human tibial shaft. Acta Orthopaedica Scandinavica. 46, 256-268.

Le, A. X., Miclau, T., Hu, D., Helms, J. A., 2001. Molecular aspects of healing in stabilized and non-stabilized fractures. Journal of Orthopaedic Research. 19, 78-84.

Li, J., Ahmad, T., Spetea, M., Ahmed, M., Kreicbergs, A., 2001. Bone reinnervation after fracture: a study in the rat. J Bone Miner Res. 16, 1505-10.

Lill, C. A., Hesseln, J., Schlegel, U., Eckhardt, C., Goldhahn, J., Schneider, E., 2003. Biomechanical evaluation of healing in a non-critical defect in a large animal model of osteoporosis. Journal of Orthopaedic Research. 21, 836-42.

Loboa, E. G., Fang, T. D., Parker, D. W., Warren, S. M., Fong, K. D., Longaker, M. T., Carter, D. R., 2005. Mechanobiology of mandibular distraction osteogenesis: finite element analyses with a rat model. J Orthop Res. 23, 663-70. Epub 2005 Jan 18.

Mark, H., Nilsson, A., Nannmark, U., Rydevik, B., 2004a. Effects of fracture fixation stability on ossification in healing fractures. Clinical Orthopaedics and Related Research. 419, 245-50.

Mark, H., Penington, A., Nannmark, U., Morrison, W., Messina, A., 2004b. Microvascular invasion during endochondral ossification in experimental fractures in rats. Bone. 35, 535-42.

Marsh, D. R., Li, G., 1999. The biology of fracture healing: optimising outcome. Br Med Bull. 55, 856-869.

McKibbin, B., 1978. The biology of fracture healing in long bones. Journal of Bone and Joint Surgery. British Volume. 60-B, 150-62.

Miller, S. C., Jee, W. S. S., 1987. The bone lining cell: a distinct phenotype? Calcified Tissue International. 41, 1-5.

Mow, V. C., Kuei, S. C., Lai, W. M., Armstrong, C. G., 1980. Biphasic creep and stress relaxation of articular cartilage in compression? Theory and experiments. Journal of Biomechanical Engineering. 102, 73-84.

Nickel, R., Schummer, A., Seiferle, E., 1992. The locomotor system of the domestic mammals, Verlag Paul Parey, Berlin.

Owen, M., 1970. The origin of bone cells. International Review of Cytology. 28, 213-38.

Palmer, R. H., Hulse, D. A., Hyman, W. A., Palmer, D. R., 1992. Principles of bone healing and biomechanics of external skeletal fixation. Vet Clin North Am Small Anim Pract. 22, 45-68.

Parfitt, A. M., 1988a. Bone histomorphometry: proposed system for standardization of nomenclature, symbols, and units. Calcified Tissue International. 42, 284-6.

Parfitt, A. M., 1988b. Bone histomorphometry: standardization of nomenclature, symbols and units. Summary of proposed system. Bone and Mineral. 4, 1-5.

Park, S. H., O'Connor, K., McKellop, H., Sarmiento, A., 1998. The influence of active shear or compressive motion on fracture-healing. Journal of Bone and Joint Surgery. 80, 868-78.

Pauwels, F., 1980. Biomechanics of the Locomotor Apparatus, Springer-Verlag, Berlin.

Perren, S. M., 2002. Evolution of the internal fixation of long bone fractures. The scientific basis of biological internal fixation: choosing a new balance between stability and biology. Journal of Bone and Joint Surgery. British Volume. 84, 1093-110.

Perren, S. M., Cordey, J., 1980. The concept of interfragmentary strain in: Uhthoff, H. K., (Eds), Current Concepts of Internal Fixation of Fractures, Springer-Verlag, Berlin, 63-77

Prendergast, P. J., Huiskes, R., Soballe, K., 1997. ESB Research Award 1996. Biophysical stimuli on cells during tissue differentiation at implant interfaces. journal of Biomechanics. 30, 539-48.

Rhinelander, F. W., 1968. The normal microcirculation of diaphyseal cortex and its response to fracture. J Bone Joint Surg Am. 50, 784-800.

Rosenbaum, D., Becker, H. P., 1997. Plantar pressure distribution measurements. Technical background and clinical applications. Foot and Ankle Surgery. 3, 1-14.

Roux, W., 1895. Gesammelte Abhandlungen über Entwicklungsmechanik der Organismen, Wilhem Engelmann, Leipzig.

Rüedi, T., Murphy, W., 2000. AO principles of fracture management, Thieme, Stuttgart.

Runkel, M., Klepsch, M., 1999. Wandel bei der Behandlung der Unterschenkelschaftfraktur. Trauma Berufskrankh. 1, 229-239.

Sarmiento, A., McKellop, H. A., Llinas, A., Park, S. H., Lu, B., Stetson, W., Rao, R., 1996. Effect of loading and fracture motions on diaphyseal tibial fractures. Journal of Orthopaedic Research. 14, 80-4.

Schaffler, M. B., Burr, D. B., 1988. Stiffness of compact bone: effects of porosity and density. Journal of Biomechanics. 21, 13-16.

Schell, H., Epari, D. R., Kassi, J. P., Bragulla, H., Bail, H. J., Duda, G. N., 2005. The course of bone healing is influenced by the initial shear fixation stability. Journal of Orthopaedic Research. 23, 1022-28.

Simmons, D. J., 1985. Fracture healing perspectives. Clin Orthop. 100-13.

Smit, T. H., Huyghe, J. M., Cowin, S. C., 2002. Estimation of the poroelastic parameters of cortical bone. J Biomech. 35, 829-35.

Stürmer, K. M., 1988. Histologie und Biomechanik der Frakturheilung unter den Bedingungen des Fixateur externe. Hefte Unfallheilkd. 200, 233-242.

Stürmer, K. M., 1996. [Elastic plate osteosynthesis, biomechanics, indications and technique in comparison with rigid osteosynthesis]. Unfallchirurg. 99, 816-29.

Stürmer, K. M., Schuchardt, W., 1980. [New aspects of closed intramedullary nailing and marrow cavity reaming in animal experiments. III. Bone-healing, revascularisation and remodelling (author's transl)]. Unfallheilkunde. 83, 1980.

Tarr, R. R., Wiss, D. A., 1986. The mechanics and biology of intramedullary fracture fixation. Clin Orthop. 10-7.

Thompson, Z., Miclau, T., Hu, D., Helms, J., 2002. A model for intramembranous ossification during fracture healing. Journal of Orthopaedic Research. 20, 1091-1098.

Van Rietbergen, B., Huiskes, R., Weinans, H., Sumner, D. R., Turner, T. M., Galante, J. O., 1993. ESB Research Award 1992. The mechanism of bone remodeling and resorption around press-fitted THA stems. J Biomech. 26, 369-82.

Vecsei, V., Hertz, H., 1977. [Experience with the locking nail (author's transl)]. Arch Orthop Unfallchir. 89, 191-8.

Wallace, A. L., Draper, E. R., Strachan, R. K., McCarthy, I. D., Hughes, S. P., 1991. The effect of devascularisation upon early bone healing in dynamic external fixation. Journal of Bone and Joint Surgery. British Volume. 73, 819-25.

Wallace, A. L., Draper, E. R., Strachan, R. K., McCarthy, I. D., Hughes, S. P., 1994. The vascular response to fracture micromovement. Clinical Orthopaedics and Related Research. 281-90.

Webb, J. C. J., Tricker, J., 2000. Bone biology- A review of fracture healing. Current Orthopaedics. 14, 457-463.

Wentzensen, A., 1999. Tibiaschaftfraktur. Trauma Berufskrankh. 1, 227-228.

Willenegger, H., Perren, S. M., Schenk, R., 1971. Primary and secondary healing of bone fractures. Chirurg. 42, 241-52.

Wolf, S., Janousek, A., Pfeil, J., Veith, W., Haas, F., Duda, G., N., Claes, L., E., 1998. The effects of external mechanical stimulation on the healing of diaphyseal

osteotomies fixed by flexible external fixation. Clinical Biomechanics. 13, 359-364.

Wu, J. J., Shyr, H. S., Chao, E. Y., Kelly, P. J., 1984. Comparison of osteotomy healing under external fixation devices with different stiffness characteristics. Journal of Bone and Joint Surgery. 66, 1258-64.

Yamagishi, M., Yoshimura, Y., 1955. The biomechanics of fracture healing. Journal of Bone and Joint Surgery. 37-A, 1035-68.

# 8 Appendix

## 8.1 Biomechanical Testing of Healed Tibia

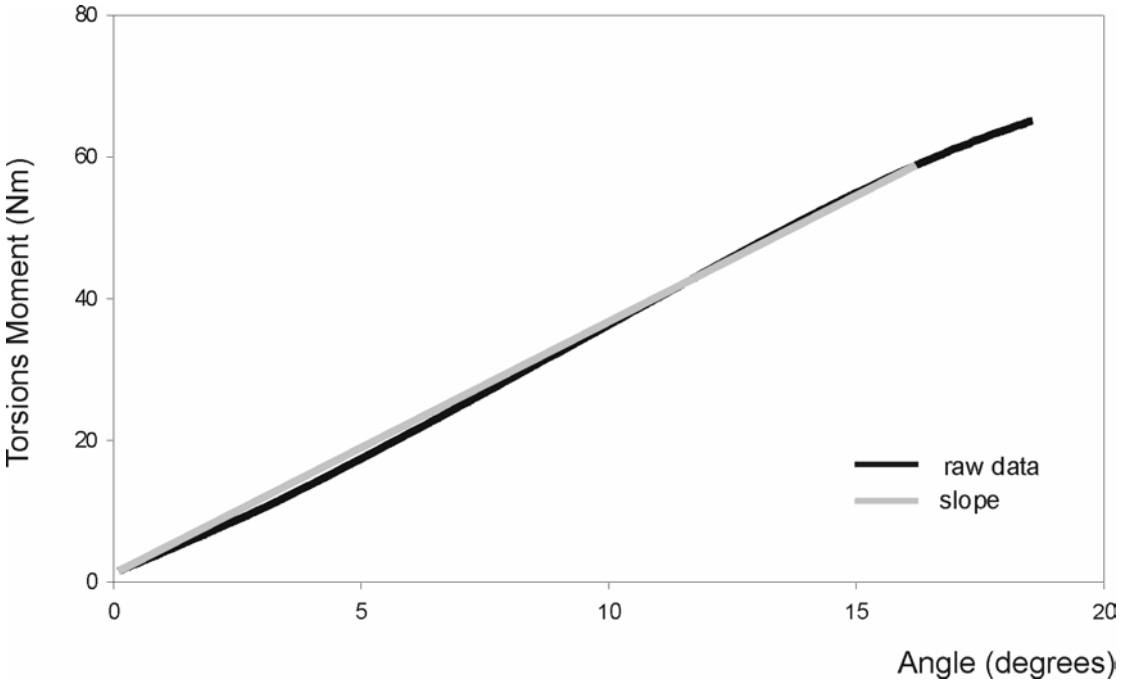


**Figure 8-1 shows the calculated slope against a plot of raw data captured on a mechanical testing machine. The slope of the linear portion of the plot gives the torsional stiffness and the maximum torsions moment corresponds to the torsional moment at failure.**

| 6 weeks | sheep | Intact | | Fractured | | Normalised | |
|---|---|---|---|---|---|---|---|
| | | moment [Nm] | stiffness [Nm/°] | moment [Nm] | stiffness [Nm/°] | moment [%] | stiffness [%] |
| rigid | 9 | 66.2 | 3.7 | 20.7 | 2.5 | 31.3 | 68.4 |
| | 21 | 71.0 | 4.0 | 34.9 | 2.9 | 49.1 | 72.2 |
| | 23 | 85.2 | 3.7 | 30.9 | 2.7 | 36.2 | 72.4 |
| | 25 | 89.3 | 5.1 | 32.0 | 3.4 | 35.8 | 67.0 |
| | 26 | 75.3 | 3.0 | 41.0 | 3.1 | 54.4 | 103.3 |
| | 27 | 74.9 | 3.7 | 27.3 | 2.7 | 36.4 | 74.1 |
| | 28 | 68.8 | 3.3 | 49.4 | 3.7 | 71.8 | 110.7 |
| | mean | 75.8 | 3.8 | 33.7 | 3.0 | 45.0 | 81.2 |
| | st.dev | 8.5 | 0.7 | 9.3 | 0.4 | 14.4 | 17.9 |
| semi-rigid | 32 | 61.6 | 2.2 | 27.8 | 2.0 | 45.1 | 90.3 |
| | 33 | 64.2 | 3.6 | 24.4 | 2.1 | 37.9 | 58.1 |
| | 34 | 65.4 | 3.6 | 26.2 | 3.0 | 40.1 | 82.6 |
| | 35 | 57.3 | 2.0 | 27.9 | 2.3 | 48.7 | 112.5 |
| | 36 | 77.8 | 3.2 | 19.5 | 1.9 | 25.0 | 58.6 |
| | 44 | 74.5 | 3.9 | 16.7 | 1.8 | 22.4 | 46.7 |
| | 37 | 69.6 | 3.5 | 15.6 | 2.1 | 22.5 | 60.0 |
| | 49 | 71.7 | 3.9 | 23.7 | 2.7 | 33.1 | 70.1 |
| | mean | 67.8 | 3.2 | 22.7 | 2.2 | 34.4 | 72.4 |
| | st.dev | 6.9 | 0.7 | 4.9 | 0.4 | 10.3 | 21.5 |

**Table 8-1 contains data from mechanical testing of intact and fractured tibia after 6 weeks healing of healing. Fractured tibias were treated with either rigid or semi-rigid external fixation. Normalised values are given in the finals columns, i.e. percent of contralateral intact tibia.**

| 9 weeks | sheep | Intact | | Fractured | | Normalised | |
|---|---|---|---|---|---|---|---|
| | | moment [Nm] | stiffness [Nm/°] | moment [Nm] | stiffness [Nm/°] | moment [%] | stiffness [%] |
| rigid | 2 | 74.3 | 4.2 | 49.2 | 3.2 | 66.2 | 75.1 |
| | 3 | 69.8 | 4.1 | 55.6 | 3.8 | 79.6 | 92.7 |
| | 5 | 57.8 | 3.3 | 26.1 | 2.3 | 45.1 | 71.1 |
| | 6 | 66.1 | 3.8 | 64.6 | 3.5 | 97.7 | 93.8 |
| | 12 | 62.1 | 3.5 | 51.9 | 3.8 | 83.6 | 110.0 |
| | 13 | 68.7 | 3.3 | 36.3 | 2.6 | 52.9 | 79.0 |
| | 16 | 56.0 | 2.5 | 38.2 | 2.6 | 68.2 | 104.0 |
| | 17 | 57.7 | 2.9 | 32.9 | 3.4 | 57.0 | 115.1 |
| | 61 | 63.3 | 3.5 | 45.0 | 3.4 | 71.1 | 98.3 |
| | mean | 64.0 | 3.4 | 44.4 | 3.2 | 69.0 | 93.2 |
| | st.dev | 6.2 | 0.5 | 12.2 | 0.5 | 16.3 | 15.5 |
| semi-rigid | 20 | 63.1 | 3.5 | 41.8 | 1.9 | 66.3 | 53.4 |
| | 43 | 72.3 | 4.2 | 36.7 | 3.9 | 50.7 | 92.9 |
| | 46 | 72.9 | 4.0 | 50.4 | 3.3 | 69.2 | 81.6 |
| | 48 | 63.6 | 3.5 | 38.8 | 3.2 | 61.0 | 91.1 |
| | 54 | 63.6 | 3.8 | 48.2 | 4.2 | 75.8 | 112.1 |
| | 59 | 62.8 | 3.9 | 37.2 | 3.5 | 59.2 | 90.2 |
| | 63 | 47.1 | 3.3 | 49.5 | 3.1 | 105.0 | 95.3 |
| | mean | 63.6 | 3.7 | 43.2 | 3.3 | 69.6 | 88.1 |
| | st.dev | 8.5 | 0.3 | 6.0 | 0.7 | 17.5 | 17.9 |

**Table 8-2 contains data from mechanical testing of intact and fractured tibia after 9 weeks healing of healing. Fractured tibias were treated with either rigid or semi-rigid external fixation. Normalised values are given in the finals columns, i.e. percent of contralateral intact tibia.**

## 8.2 Moment of Inertia

| 2 weeks | sheep | Intact | | | Fractured | | | Normalised | | |
|---|---|---|---|---|---|---|---|---|---|---|
| | | Max | Mid | Min | Max | Mid | Min | Max | Mid | Min |
| rigid | 60 | 213029 | 195117 | 167774 | 231343 | 212597 | 145312 | 109 | 109 | 87 |
| | 67 | 243204 | 212985 | 190628 | 230324 | 191402 | 169180 | 95 | 90 | 89 |
| | 71 | 223828 | 197537 | 145737 | 232450 | 209470 | 132181 | 104 | 106 | 91 |
| | 74 | 281862 | 237110 | 155153 | 289235 | 254600 | 164827 | 103 | 107 | 106 |
| | 76 | 339354 | 312727 | 234346 | 288840 | 256445 | 195277 | 85 | 82 | 83 |
| | 85 | 331389 | 278388 | 230184 | 285666 | 243248 | 186031 | 86 | 87 | 81 |
| | 86 | 283844 | 238243 | 181298 | 262370 | 223121 | 157266 | 92 | 94 | 87 |
| | 90 | 328871 | 284922 | 223105 | 252126 | 215000 | 155529 | 77 | 75 | 70 |
| | mean | 280673 | 244629 | 191028 | 259044 | 225735 | 163200 | 94 | 94 | 87 |
| | st.dev | 50087 | 43373 | 34667 | 26367 | 23364 | 20580 | 11 | 13 | 10 |
| semi-rigid | 68 | 344919 | 311675 | 230890 | 280029 | 248755 | 166586 | 81 | 80 | 72 |
| | 70 | 283203 | 247470 | 182367 | 259186 | 224859 | 138323 | 92 | 91 | 76 |
| | 75 | 339821 | 301429 | 202872 | 222651 | 178846 | 126747 | 66 | 59 | 62 |
| | 77 | 314956 | 284118 | 213599 | 239555 | 210745 | 148893 | 76 | 74 | 70 |
| | 81 | 298365 | 253875 | 225889 | 270530 | 230007 | 176797 | 91 | 91 | 78 |
| | 83 | 322912 | 283932 | 201968 | 278540 | 228313 | 160077 | 86 | 80 | 79 |
| | 84 | 374737 | 318898 | 255780 | 314719 | 273636 | 181302 | 84 | 86 | 71 |
| | 88 | 291786 | 259659 | 211078 | 231453 | 192534 | 144576 | 79 | 74 | 68 |
| | mean | 321337 | 282632 | 215555 | 262083 | 223462 | 155413 | 82 | 79 | 72 |
| | st.dev | 30817 | 27011 | 22138 | 30340 | 30082 | 19078 | 8 | 10 | 6 |

**Table 8-3 contains raw data from measurement of the moment of inertia about the principal axes after 2 weeks healing of healing. Fractured tibias were treated with either rigid or semi-rigid external fixation. Normalised values are given in the final columns, i.e. percent of contralateral intact tibia.**

| 3 weeks | sheep | Intact | | | Fractured | | | Normalised | | |
|---|---|---|---|---|---|---|---|---|---|---|
| | | Max | Mid | Min | Max | Mid | Min | Max | Mid | Min |
| rigid | 8 | 373960 | 330422 | 232152 | 348556 | 317023 | 196761 | 93 | 96 | 85 |
| | 10 | 298778 | 256148 | 192606 | 333955 | 289987 | 188732 | 112 | 113 | 98 |
| | 18 | 407856 | 335074 | 273186 | 385185 | 337611 | 225420 | 94 | 101 | 83 |
| | 19 | 325474 | 286039 | 208875 | 346165 | 312055 | 206246 | 106 | 109 | 99 |
| | 29 | 340287 | 292180 | 220468 | 355005 | 310850 | 206906 | 104 | 106 | 94 |
| | 30 | 349354 | 305733 | 208653 | 364149 | 318853 | 207554 | 104 | 104 | 99 |
| | 42 | 451846 | 403465 | 248145 | 430366 | 391132 | 231056 | 95 | 97 | 93 |
| | mean | 363936 | 315580 | 226298 | 366197 | 325359 | 208954 | 101 | 104 | 93 |
| | st.dev | 52049 | 47211 | 27368 | 32557 | 32215 | 14892 | 7 | 6 | 7 |
| semi-rigid | 41 | 348771 | 319557 | 211835 | 354865 | 326677 | 181434 | 102 | 102 | 86 |
| | 47 | 455728 | 420382 | 249151 | 349278 | 310343 | 201321 | 77 | 74 | 81 |
| | 51 | 383654 | 326038 | 242381 | 402142 | 355569 | 230544 | 105 | 109 | 95 |
| | 52 | 323732 | 283830 | 214309 | 342146 | 305702 | 185717 | 106 | 108 | 87 |
| | 53 | 317042 | 289379 | 189593 | 366350 | 332252 | 193970 | 116 | 115 | 102 |
| | 55 | 336808 | 309542 | 191912 | 317057 | 297837 | 169658 | 94 | 96 | 88 |
| | 50 | 353205 | 304778 | 210933 | 344254 | 304440 | 194905 | 97 | 100 | 92 |
| | 58 | 440998 | 372830 | 283105 | 375882 | 321785 | 236843 | 85 | 86 | 84 |
| | mean | 369992 | 328292 | 224152 | 356497 | 319326 | 199299 | 98 | 99 | 89 |
| | st.dev | 52585 | 46200 | 31825 | 25418 | 18862 | 23360 | 12 | 13 | 7 |

**Table 8-4 contains raw data from measurement of the moment of inertia about the principal axes after 3 weeks healing of healing. Fractured tibias were treated with either rigid or semi-rigid external fixation. Normalised values are given in the final columns, i.e. percent of contralateral intact tibia.**

| 6 weeks | sheep | Intact | | | Fractured | | | Normalised | | |
|---|---|---|---|---|---|---|---|---|---|---|
| | | Max | Mid | Min | Max | Mid | Min | Max | Mid | Min |
| rigid | 9 | 311327 | 262188 | 204235 | 345032 | 293934 | 232788 | 111 | 112 | 114 |
| | 21 | 405409 | 339623 | 244528 | 408840 | 358738 | 253623 | 101 | 106 | 104 |
| | 23 | 372614 | 301670 | 282858 | 374731 | 317726 | 275843 | 101 | 105 | 98 |
| | 24 | 444675 | 401262 | 298074 | 595767 | 537351 | 361589 | 134 | 134 | 121 |
| | 25 | 505651 | 416044 | 365227 | 654844 | 569949 | 402157 | 130 | 137 | 110 |
| | 26 | 349600 | 313455 | 213780 | 391288 | 361997 | 257882 | 112 | 115 | 121 |
| | 27 | 317930 | 266386 | 219608 | 479063 | 424305 | 282687 | 151 | 159 | 129 |
| | 28 | 387956 | 315836 | 247434 | 432797 | 373492 | 257452 | 112 | 118 | 104 |
| | mean | 386895 | 327058 | 259468 | 460295 | 404687 | 290503 | 119 | 123 | 113 |
| | st.dev | 65298 | 56603 | 53875 | 110406 | 100022 | 59334 | 18 | 19 | 11 |
| semi-rigid | 32 | 367202 | 317401 | 205313 | 453571 | 370947 | 265245 | 124 | 117 | 129 |
| | 33 | 302612 | 270108 | 206464 | 413134 | 394859 | 235425 | 137 | 146 | 114 |
| | 34 | 319739 | 278748 | 179044 | 427429 | 379177 | 203417 | 134 | 136 | 114 |
| | 35 | 292057 | 254384 | 215636 | 409101 | 356897 | 230951 | 140 | 140 | 107 |
| | 37 | 389270 | 349993 | 205668 | 518710 | 449966 | 278341 | 133 | 129 | 135 |
| | 44 | 494027 | 439848 | 300243 | 536056 | 478709 | 304926 | 109 | 109 | 102 |
| | 49 | 311211 | 268988 | 208107 | 347263 | 287235 | 224305 | 112 | 107 | 108 |
| | mean | 353731 | 311353 | 217211 | 443609 | 388256 | 248944 | 127 | 126 | 116 |
| | st.dev | 71306 | 65632 | 38355 | 65764 | 62722 | 35238 | 12 | 16 | 12 |

**Table 8-5 contains raw data from measurement of the moment of inertia about the principal axes after 6 weeks healing of healing. Fractured tibias were treated with either rigid or semi-rigid external fixation. Normalised values are given in the final columns, i.e. percent of contralateral intact tibia.**

| 9 weeks | sheep | Intact | | | Fractured | | | Normalised | | |
|---|---|---|---|---|---|---|---|---|---|---|
| | | Max | Mid | Min | Max | Mid | Min | Max | Mid | Min |
| rigid | 2 | 423068 | 353689 | 244248 | 710151 | 612897 | 525271 | 168 | 173 | 215 |
| | 3 | 378089 | 321002 | 232132 | 602909 | 542190 | 441907 | 159 | 169 | 190 |
| | 5 | 295966 | 262708 | 169109 | 344532 | 298778 | 195515 | 116 | 114 | 116 |
| | 6 | 477032 | 410873 | 277012 | 1001472 | 900149 | 723513 | 210 | 219 | 261 |
| | 12 | 316098 | 288711 | 207558 | 526263 | 495971 | 389746 | 166 | 172 | 188 |
| | 13 | 355031 | 320026 | 185820 | 553376 | 505061 | 363349 | 156 | 158 | 196 |
| | 16 | 238792 | 206645 | 158019 | 456230 | 374186 | 347148 | 191 | 181 | 220 |
| | 17 | 318089 | 269531 | 197345 | 490055 | 403720 | 323927 | 154 | 150 | 164 |
| | 61 | 351906 | 299378 | 215089 | 537326 | 462420 | 361999 | 153 | 154 | 168 |
| | mean | 350452 | 303618 | 209592 | 580257 | 510597 | 408042 | 164 | 166 | 191 |
| | st.dev | 70486 | 58161 | 37588 | 186874 | 173449 | 147824 | 26 | 28 | 41 |
| semi-rigid | 20 | 354918 | 314432 | 244821 | 635940 | 559174 | 471480 | 179 | 178 | 193 |
| | 43 | 446677 | 405053 | 285728 | 856873 | 754688 | 605785 | 192 | 186 | 212 |
| | 46 | 332406 | 299722 | 212597 | 712325 | 614759 | 459738 | 214 | 205 | 216 |
| | 48 | 343140 | 299611 | 202160 | 611273 | 512582 | 398079 | 178 | 171 | 197 |
| | 54 | 417627 | 388113 | 243021 | 970740 | 853877 | 614790 | 232 | 220 | 253 |
| | 59 | 343140 | 299611 | 202160 | 611273 | 512582 | 398079 | 178 | 171 | 197 |
| | 66 | 419634 | 377677 | 246162 | 538977 | 479476 | 327601 | 128 | 127 | 133 |
| | mean | 379649 | 340603 | 233807 | 705343 | 612448 | 467936 | 186 | 180 | 200 |
| | st.dev | 46625 | 47438 | 30297 | 154725 | 140826 | 108091 | 33 | 30 | 36 |

**Table 8-6 contains raw data from measurement of the moment of inertia about the principal axes after 9 weeks healing of healing. Fractured tibias were treated with either rigid or semi-rigid external fixation. Normalised values are given in the final columns, i.e. percent of contralateral intact tibia.**

## 8.3 Histomorphometry

| Weeks | Sheep | Total Callus | Min bone | Fibrous Tissue | Cartilage |
|---|---|---|---|---|---|
| 2 | 60 | 175.74 | 73.47 | 81.19 | 21.09 |
| 2 | 67 | 200.80 | 96.13 | 87.68 | 16.99 |
| 2 | 71 | 194.75 | 81.73 | 98.48 | 14.54 |
| 2 | 74 | 211.26 | 83.80 | 100.34 | 27.11 |
| 2 | 76 | 201.53 | 96.47 | 81.65 | 23.41 |
| 2 | 85 | 134.15 | 82.83 | 49.10 | 2.21 |
| 2 | 86 | 124.53 | 82.44 | 39.31 | 2.77 |
| 2 | 90 | 176.08 | 99.53 | 55.60 | 20.95 |
| 3 | 8 | 338.80 | 102.42 | 225.59 | 10.80 |
| 3 | 10 | 213.62 | 85.39 | 114.90 | 13.32 |
| 3 | 18 | 347.36 | 110.54 | 168.14 | 68.68 |
| 3 | 19 | 292.88 | 88.07 | 181.53 | 23.29 |
| 3 | 29 | 302.16 | 91.80 | 193.05 | 17.30 |
| 3 | 30 | 321.29 | 105.40 | 195.60 | 20.29 |
| 3 | 31 | 267.93 | 111.17 | 134.80 | 21.97 |
| 3 | 42 | 277.25 | 127.94 | 127.11 | 22.20 |
| 6 | 9 | 222.94 | 129.01 | 81.54 | 12.38 |
| 6 | 21 | 170.05 | 125.20 | 24.66 | 20.19 |
| 6 | 23 | 180.54 | 124.04 | 38.97 | 17.53 |
| 6 | 24 | 161.03 | 114.61 | 30.82 | 15.60 |
| 6 | 25 | 238.80 | 157.35 | 68.14 | 13.31 |
| 6 | 26 | 136.54 | 92.20 | 41.32 | 3.02 |
| 6 | 27 | 238.56 | 130.45 | 89.18 | 18.92 |
| 6 | 28 | 194.90 | 93.41 | 85.06 | 16.43 |
| 9 | 2 | 213.14 | 164.87 | 47.46 | 0.81 |
| 9 | 3 | 124.50 | 108.98 | 15.33 | 0.19 |
| 9 | 6 | 201.98 | 179.80 | 22.15 | 0.03 |
| 9 | 12 | 180.75 | 118.92 | 61.18 | 0.65 |
| 9 | 13 | 194.27 | 113.38 | 80.66 | 0.22 |
| 9 | 16 | 174.95 | 136.02 | 38.23 | 0.70 |
| 9 | 17 | 156.75 | 120.27 | 35.90 | 0.59 |
| 9 | 61 | 160.21 | 124.29 | 35.92 | 0.00 |

**Table 8-7 contains raw data from measurement of histomorphometric parameters in callus at 2, 3, 6 and 9 weeks for animals treated with rigid external fixation (averaged for two observers).**

| Weeks | Sheep | Total Callus | Min bone | Fibrous Tissue | Cartilage |
|---|---|---|---|---|---|
| 2 | 68 | 200.61 | 76.63 | 107.34 | 16.64 |
| 2 | 70 | 261.25 | 94.66 | 130.25 | 36.34 |
| 2 | 75 | 159.98 | 98.09 | 44.34 | 17.56 |
| 2 | 77 | 155.42 | 69.12 | 75.37 | 10.93 |
| 2 | 81 | 180.96 | 89.97 | 79.72 | 11.27 |
| 2 | 83 | 171.82 | 77.40 | 74.56 | 19.87 |
| 2 | 84 | 203.77 | 92.74 | 82.81 | 28.22 |
| 2 | 88 | 122.67 | 81.09 | 35.14 | 6.44 |
| 3 | 41 | 284.67 | 94.07 | 162.75 | 27.85 |
| 3 | 47 | 293.05 | 90.91 | 139.83 | 62.31 |
| 3 | 50 | 288.33 | 106.36 | 155.03 | 26.94 |
| 3 | 51 | 382.82 | 105.52 | 208.44 | 68.86 |
| 3 | 52 | 226.93 | 99.74 | 115.44 | 11.75 |
| 3 | 53 | 328.00 | 116.95 | 172.50 | 38.56 |
| 3 | 55 | 186.99 | 82.54 | 84.97 | 19.48 |
| 3 | 58 | 204.69 | 83.60 | 106.51 | 14.58 |
| 6 | 32 | 233.20 | 145.26 | 77.19 | 10.76 |
| 6 | 33 | 350.31 | 170.52 | 144.77 | 35.02 |
| 6 | 34 | 289.63 | 177.31 | 90.04 | 22.27 |
| 6 | 35 | 270.84 | 143.59 | 102.69 | 24.56 |
| 6 | 36 | 447.08 | 158.83 | 234.94 | 53.31 |
| 6 | 37 | 388.19 | 210.48 | 152.45 | 25.26 |
| 6 | 44 | 412.75 | 164.35 | 195.43 | 52.97 |
| 6 | 49 | 285.28 | 175.29 | 85.44 | 24.55 |
| 9 | 20 | 228.47 | 171.13 | 56.86 | 0.49 |
| 9 | 43 | 342.14 | 241.82 | 81.71 | 18.61 |
| 9 | 46 | 273.67 | 205.31 | 64.22 | 4.13 |
| 9 | 48 | 294.09 | 220.92 | 68.58 | 4.59 |
| 9 | 54 | 248.53 | 196.46 | 52.07 | 0.00 |
| 9 | 59 | 191.39 | 144.00 | 47.04 | 0.35 |
| 9 | 63 | 186.95 | 147.61 | 39.18 | 0.16 |
| 9 | 66 | 183.38 | 139.64 | 43.53 | 0.21 |

**Table 8-8 contains raw data from measurement of histomorphometric parameters in callus at 2, 3, 6 and 9 weeks for animals treated with semi-rigid external fixation (averaged for two observers).**

# Curriculum Vitae

Devakara Rao Epari

Born in Hobart, Australia on April 20th, 1977

*Education*

1980 – 1994, The Hutchins School, Sandy Bay, Tasmania

Tasmanian Certificate of Education
Graduated with Distinction

1995-1999 University of New South Wales, Kensington, NSW

Bachelor of Mechanical Engineering (1st Class Honours)
Masters in Biomedical Engineering

*Professional Experience*

1998 - 1999 Orthopaedic Research Laboratory, Prince of Wales Hospital, Australia
Research Assistant

2001 – 2006, Centre for Musculoskeletal Surgery, Charité Universitätsmedizin Berlin
Research Engineer

*Awards*

2003, Young Investigator's Travel Award, German Society for Biomechanics, Germany

*Publications*

D.R. Epari, F Kandziora, G.N. Duda, Stress shielding in box and cylinder cervical interbody fusion cage designs, Spine, 2004, 30:908 – 14

D.R. Epari, H. Schell, H.J. Bail, G.N. Duda, Instability prolongs the chondral phase during bone healing in sheep, Bone, 2006, 38(6):864-70

D.R. Epari, W.R. Taylor, M.O. Heller, G.N. Duda, Mechanical conditions in the early phase of bone healing, Clinical Biomechanics, 2006, 21(6):646-55

H. Schell, D.R. Epari, P. Seebeck, H. Bail, G.N. Duda, Course of healing is influenced by early fixation stability, Journal of Orthopaedic Research, 2005, 23:1022 – 1028